

# Structural Chemistry of Peptides Containing Backbone Expanded Amino Acid Residues: Conformational Features of $\beta$ , $\gamma$ , and Hybrid Peptides

Prema. G. Vasudev,<sup>†</sup> Sunanda Chatterjee,<sup>‡</sup> Narayanaswamy Shamala,<sup>\*,†</sup> and Padmanabhan Balaram<sup>\*,‡</sup>

*Department of Physics and Molecular Biophysics Unit, Indian Institute of Science, Bangalore 560012, India*

Received March 25, 2010

## Contents

1. Introduction	657
2. Nomenclature and Substitution Patterns	660
3. Conformationally Constrained Residues	661
3.1. Gem-Dialkyl Substitution	661
3.2. Side Chain–Backbone Cyclization	661
4. Intramolecularly Hydrogen Bonded Rings in Peptides	662
4.1. Single Residue Hydrogen Bonds ( $3 \rightarrow 1, 1 \rightarrow 1$ )	663
4.2. Hydrogen-Bonded Ribbons	664
4.3. Two Residue Hydrogen Bonds ( $4 \rightarrow 1, 1 \rightarrow 2$ )	666
4.4. $3_{10}$ Helix Expanded Analogs	667
4.5. Three-Residue Hydrogen-Bonded Turns ( $5 \rightarrow 1, 1 \rightarrow 3$ )	669
4.6. $\alpha$ Helix Expanded Analogs	669
4.7. Helices with Reverse Directionality Hydrogen Bonds	670
5. Helices with Alternate Hydrogen Bond Directionalities	671
6. $\omega$ Amino Acids in Hairpins	672
6.1. Insertion into Turn Segments	672
6.2. Extended Strands	673
7. Conformational Representations	673
7.1. Conformationally Constrained Residues	675
8. Conformational Variability and Biological Activity	677
8.1. Conformational Variability in Solution	677
8.2. Biological Activity of Synthetic Peptides	678
9. Revisiting Hydrogen-Bonded Rings and Polypeptide Helices	678
10. Conclusions	682
11. Acknowledgments	684
12. Supporting Information Available	684
13. References	684



Prema G. Vasudev received a Masters degree in organic chemistry from the Mahatma Gandhi University in 2001. She received PhD in X-ray crystallography from the Indian Institute of Science in 2009 and now continues as a post doctoral researcher there.



Sunanda Chatterjee received her post graduate degree from the University of Burdwan in 2003 and her Ph.D degree from the Indian Institute of Science in 2009 on the conformational analysis of synthetic peptides containing gamma amino acid residue gabapentin. She is presently working as a postdoctoral researcher in the University Paris Descartes, France.

## 1. Introduction

The remarkable complexity of globular protein structures was first revealed about half a century ago, when the crystal structure of myoglobin was determined at 2.4 Å.<sup>1</sup> In the decades since, the diversity of protein structures has been extensively catalogued, establishing that the polypeptide backbone can be induced to adopt a very large range of compact folded conformations.<sup>2–5</sup> In natural proteins, struc-

tural diversity arises due to patterning of 20 chemically distinct, genetically coded,  $\alpha$  amino acids along the length of the polypeptide chains. Local folding patterns are determined by backbone conformational preferences of individual residues, which depend principally on short-range interactions, involving forces between nonbonded atoms and hydrogen bonding between donor NH and acceptor CO groups on the polypeptide backbone.<sup>6–10</sup> Globular protein structures effectively consist of short pieces of regular secondary structures like helices and  $\beta$ -strands, connected by irregular segments generally denoted as loops. The association of extended strands by interstrand hydrogen

\* To whom correspondence should be addressed. Fax: (+91) 80-2360-2602. E-mail: shamala@physics.iisc.ernet.in. Fax: (+91) 80-2360-0535. E-mail: pb@mbu.iisc.ernet.in.

<sup>†</sup> Department of Physics.

<sup>‡</sup> Molecular Biophysics Unit.



N. Shamala is a professor of Biocrystallography in the Department of Physics at the Indian Institute of Science. After obtaining a Masters degree from the University of Mysore and PhD from the University of Madras, she joined as post doctoral researcher with G. N. Ramachandran at the Molecular Biophysics Unit, IISc and worked on the X-ray diffraction studies of peptides. Subsequently, she went to Washington University Medical School at St. Louis and worked with F. Scott Mathews towards determining the crystal structure of several proteins. She joined the faculty of the Indian Institute of Science in 1990. Her research interests are the X-ray crystallographic studies of peptides and proteins, and the identification of novel secondary structures.



P. Balaram is a professor of Molecular Biophysics at the Indian Institute of Science, Bangalore. He obtained a Masters degree from the Indian Institute of Technology, Kanpur, and PhD from Carnegie Mellon University. After his post doctoral research with R. B. Woodward at Harvard University he joined the faculty of the Indian Institute of Science in 1973. His research interests are on the design, synthesis, conformation, and folding of peptides and proteins.

bonding results in the formation of sheets. Tertiary interactions, between projecting side chains held on the secondary structure scaffold, result in compact packing into well-defined globular structures. Since protein backbones are composed exclusively of  $\alpha$  amino acids linked by peptide bonds, folded structures in polypeptides are conveniently defined using backbone torsion angles  $\phi$  and  $\psi$ , as backbone descriptors of local conformations.<sup>11,12</sup> Each  $\alpha$  amino acid residue in a protein possesses two degrees of torsional freedom about the N-C $^{\alpha}$  ( $\phi$ ) and C $^{\alpha}$ -CO ( $\psi$ ) bonds, with the peptide unit largely restricted to a trans, planar ( $\omega \sim 180^\circ$ ) conformation. The Ramachandran map that outlines the stereochemically allowed regions of conformational space in a two-dimensional plane with  $\phi$  and  $\psi$  as variables, provides a convenient means of analyzing and representing the observed backbone conformations of  $\alpha$  amino acid residues in peptides and proteins.<sup>13–16</sup> A very large range of noncoded amino acids, both synthetic and natural, have been used in generation of analogues of

biologically and structurally interesting compounds.<sup>17,18</sup> There has also been considerable effort in developing methodologies for the introduction of noncoded amino acids into proteins using the methods of molecular biology.<sup>19,20</sup> A new dimension to the field of biomimetic structures has been introduced, by Seebach and co-workers, through the recognition that the repertoire of polypeptide conformations can be greatly expanded by the creation of structures that incorporate backbone homologated amino acids, synthetically accessible from the proteinogenic amino acids (Figure 1).<sup>21–25</sup> Studies of model peptides containing covalently constrained  $\beta$  amino acids, by Gellman and co-workers, led to the realization that new classes of folded polyamide structures (foldamers) could be generated in sequences containing backbone expanded amino acids.<sup>26,27</sup> Omega ( $\omega$ ) amino acids may be defined as residues in which a variable number of backbone atoms are introduced between the terminal amino and carboxylic acid groups involved in amide bond formation. The insertion of additional atoms in between the flanking peptide units enhances the number of degrees of torsional freedom, resulting in an expansion of energetically accessible conformational space. For example, in the  $\beta$  amino acid residue, local backbone conformations are determined by values of three torsional variables ( $\phi$ ,  $\theta$ ,  $\psi$ ) while for the  $\gamma$ -residue, the number of torsional variables is four ( $\phi$ ,  $\theta_1$ ,  $\theta_2$ ,  $\psi$ ) (Figure 1). In this review, peptides formed by linkages involving  $\alpha$  amino and  $\alpha$  carboxyl groups are referred to as  $\alpha$  peptides, while linkages involving homologated residues are termed as  $\beta$ ,  $\gamma$ ... $\omega$  peptides.

The finding by Hanby and Rydon in 1946 that the capsular substance of *Bacillus anthracis* was “a long chain molecule made up of  $\alpha$  peptide chains of 50–100 D-glutamic residues joined together by  $\gamma$  peptide chains of D-glutamic acid residues” constitutes the first report of a polymer containing  $\omega$  peptide bonds.<sup>28</sup> Subsequent studies of the poly- $\gamma$ -D-glutamate produced by *Bacillus* species using optical rotatory methods suggested the possibility of structural states that depended upon the state of ionization of the  $\alpha$  carboxylic acid group, which projects out from a  $\gamma$  peptide backbone.<sup>29,30</sup> In his 1964 study,<sup>30</sup> Rydon did consider folded, intramolecularly hydrogen bonded helical structures for this  $\gamma$  polypeptide, basing his proposals on the models that had been considered in the literature by Bragg, Kendrew, and Perutz<sup>31</sup> and Pauling, Corey, and Branson.<sup>32</sup> The development of the pentachlorophenyl active ester approach for the synthesis of optically pure higher molecular weight polypeptides led to the study of poly  $\beta$ -L-aspartic acid using optical rotatory dispersion. In a 1965 report, Kovacs et al.<sup>33</sup> concludes that “A number of poly- $\beta$ -amino acid helices have been constructed with Courtauld stereomodels. One helix that appears to be particularly favorable... is formed by hydrogen bonding each carbonyl to the third amide group removed toward the N-terminus. This model has 3.4 residues/turn and an axial translation of 1.58 Å/ residue. It is necessarily right-handed for the  $\beta$ -amino acids with the L-configuration at the  $\alpha$ -carbon.” In a subsequent study using NMR methods, Glickson and Applequist concluded that poly  $\beta$  peptide helix would be unstable because of “the entropic effect of one additional single bond in the residue backbone”. These authors also advanced the generally accepted view that gauche conformations necessary for helix formation would tend to be energetically unfavorable relative to the extended trans form.<sup>34</sup> Much of the early structural investigations in the 1980s on polyamides focused on the nylons.<sup>35–43</sup> These

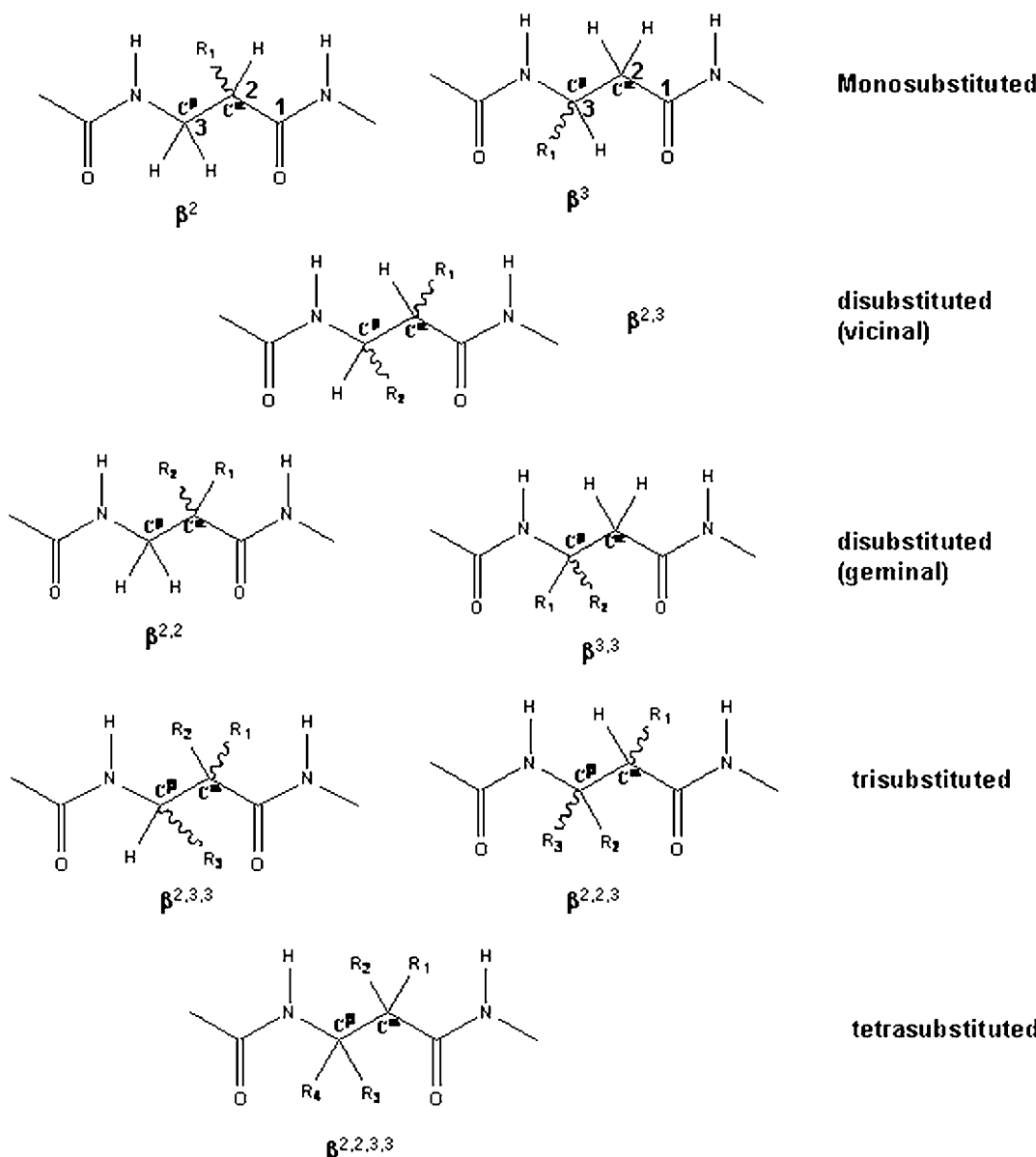


**Figure 1.** Substitution patterns for a  $\beta$  amino acid residue. Numbering of C atoms from the C-terminus is indicated. For monosubstituted residues, the substitution can be on C2 ( $\beta^2$ ) or C3 ( $\beta^3$ ) and in each case, depending on the configuration at the C2 or C3 atoms, two different possibilities (2S and 2R or 3S and 3R) arise. Disubstituted residues are of two kinds, depending on whether the substituents are on adjacent C atoms (vicinal) or on the same C atom (geminal). Within the two types, configuration at each C atom leads to four different possibilities of substitution. Similar situations can be considered for tri- and tetrasubstituted residues.

extensive investigations by Muñoz-Guerra, Subirana, and co-workers, used fiber X-ray diffraction and infrared spectroscopy.

Recent interest in the chemistry and biology of peptides containing backbone expanded amino acid residues stems from the studies reported in the mid 1990s that novel polypeptide helices could be formed in oligo  $\beta$ -peptides<sup>44–52</sup> and the characterization of hybrid structures<sup>53,54</sup> that demonstrated that the  $\beta$  and  $\gamma$  residues can be accommodated into canonical helical folds, with an expansion of the intramolecular hydrogen bonded rings. At first glance, these findings appear surprising since folded helical structures require gauche conformation about the additional C–C bonds in  $\beta$  and  $\gamma$  residues. Subsequent structural studies have established ready accessibility of folded structures in  $\beta$  and  $\gamma$  peptides. This review summarizes the available structural information on the molecular conformation of peptides obtained principally from X-ray diffraction studies. We

attempt to integrate available information in the light of extensive knowledge available in  $\alpha$  peptide structures, in order to stimulate the design of new folding patterns in synthetic molecules. The creation of hybrid structures that pattern backbone homologated amino acids in specific fashion may provide an entry to a novel class of synthetic protein mimics. The recent literature in the field of  $\beta$  and  $\gamma$  residues has been the subject of several reviews and overviews.<sup>21–27,55–62</sup> To avoid overlap with these accounts we will restrict our focus primarily to the structural chemistry of peptides containing backbone expanded amino acid residues. Complete list of currently available crystal structures of peptides containing  $\omega$  amino acid residues, together with relevant backbone dihedral angles and literature citations, used for discussions in this review is provided as Supporting Information, Table S1.

## 2. Nomenclature and Substitution Patterns

The current literature on peptides containing homologated residues describe the extensive use of a variety of substituted  $\omega$  amino acid residues. Figure 1 illustrates the substitution pattern for a  $\beta$  amino acid residue. The most commonly used monosubstituted ( $\beta^3$ ) residues are those derived by Arndt-Eistert homologation of the readily available  $\alpha$  amino acid residues that occur in protein structures.<sup>63–66</sup> Synthetic routes to  $\beta^2$ -monosubstituted and multiply substituted  $\beta$  residues<sup>67–84</sup> and  $\gamma$  residues<sup>85–91</sup> have also been the subject of several investigations. Substitution at backbone carbon atom in the  $\omega$  amino acids can result in the creation of new chiral centers which can then influence the handedness of folded backbone conformations. Methodologies for homologation of the C-terminal residue in synthetic  $\alpha$  peptides have also been studied.<sup>92</sup> In substituted  $\omega$  amino acids, the presence of one or more chiral centers along the backbone of the residue results in the need for careful consideration of nomenclature issues. The reviews by Seebach<sup>21,22</sup> provides a comprehensive description. For the present overview of folded conformations, simplified abbreviations for the substituted residues are used and defined at appropriate points in the text. Representative examples of substituted  $\beta$  and  $\gamma$  residues

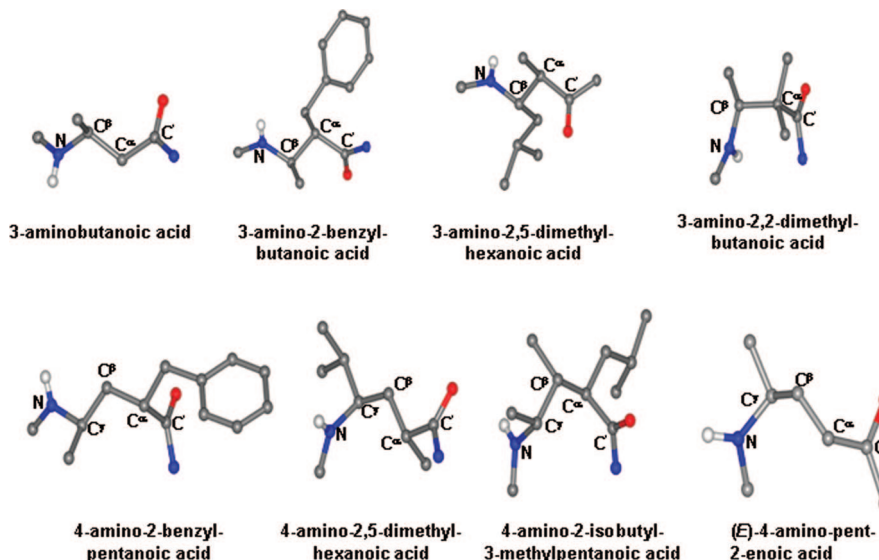


**Figure 2.** Representative examples of crystallographically characterized substituted  $\beta$  (top panel) and  $\gamma$  (bottom panel) residues.

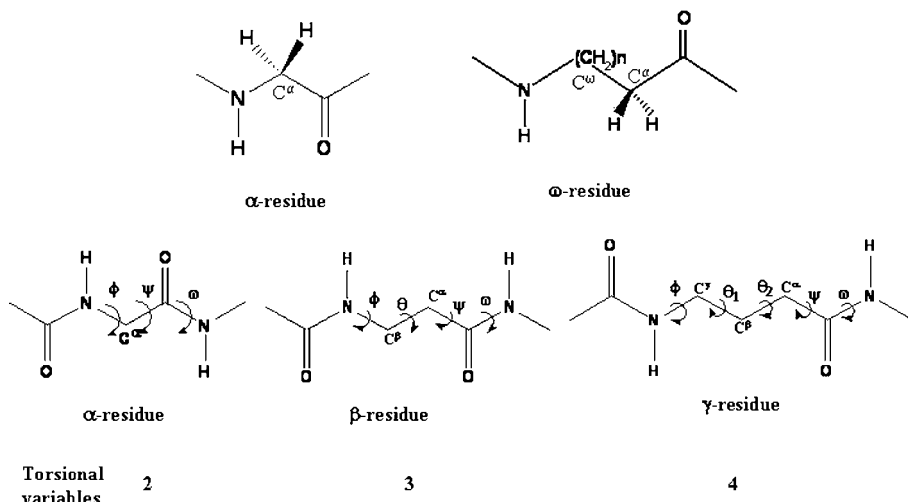


**Figure 3.** Chemical structures of  $\alpha$  and  $\omega$  amino acid residues (top) and definition of backbone torsion angles of  $\alpha$ ,  $\beta$ , and  $\gamma$  residues (bottom). The number of torsional variables is also indicated.

present in the crystallographically characterized peptides are illustrated in Figure 2.

Figure 3 illustrates the definition of the backbone torsion angles used throughout this review. Designation of the  $N-C^\omega$  bond as  $\phi$ , and the  $C^\alpha-CO$  bond as  $\psi$ , permits analogies to be drawn between  $\alpha$  residues and their higher homologues. The numbering scheme for the remaining backbone torsion angles  $\theta_n$ , is in increasing order of  $n$  from the amino terminus. The use of a numeral subscript avoids excessive use of multiple Greek letters as the number of torsional variables increases.<sup>62</sup>

Unsubstituted  $\omega$  amino acids are expected to be able to sample a much larger extent of conformational space than their substituted counterparts. In the case of  $\alpha$  amino acid residues, the sterically allowed regions of  $\phi$ ,  $\psi$  (Ramachandran) space diminishes dramatically on going from the  $C^\alpha$  unsubstituted residue Gly, to the monosubstituted residue Ala, to the disubstituted residue  $\alpha$ -aminoisobutyric acid, Aib.<sup>93–96</sup> Accessible conformational space can also be restricted by side-chain backbone cyclization as in the case of the  $\alpha$  amino acid Pro, where the torsion angle  $\phi$  is limited by the constraint of pyrrolidine ring formation.<sup>93</sup>

### 3. Conformationally Constrained Residues

In the case of  $\beta$  and  $\gamma$  amino acid residues, the conformational space available for  $\alpha$  peptide backbone may be restricted by the introduction of substituents. Indeed, first hints for folded structures in oligo  $\beta$  peptides were derived from the work of Seebach and co-workers, in which they established folded intramolecularly hydrogen bonded structures in solution for short sequences containing monosubstituted  $\beta$  residues ( $\beta^3$ ).<sup>44</sup> The sampling of conformational space can be further restricted by introducing additional substituents or by the use of cyclic  $\omega$  amino acids.

#### 3.1. Gem-Dialkyl Substitution

In the case of  $\alpha$  amino acid residues, the introduction of gem-dialkyl groups at the  $C^\alpha$  atom, dramatically reduces sterically allowed conformational space. The  $\alpha$ -amino isobutyryl residue Aib, the most extensively studied member of this class has been shown to promote helical conformations, resulting in its use in the design of a large number of peptides with folded structures.<sup>93–96</sup> Geminally disubstituted  $\beta$  amino acids were first introduced into synthetic peptides by the group of Seebach.<sup>70,97,98</sup> Figure 4a depicts  $\beta$  and  $\gamma$  residues which have been used in the design of peptides, where a gem-dialkyl substitution pattern is present.

In our hands the  $\beta,\beta'$ -disubstituted  $\gamma$ -amino acid residue, 1-(aminomethyl) cyclohexaneacetic acid, gabapentin (Gpn, Figure 4a), has proved extremely valuable in revealing the features of novel folding patterns in hybrid sequences.<sup>99–107</sup> The presence of geminal substituents at the  $C^\beta$  carbon atom restricts the torsion angles  $\theta_1$  and  $\theta_2$  primarily to gauche conformations, a feature that will be considered subsequently.<sup>105–107</sup>

#### 3.2. Side Chain–Backbone Cyclization

Restricting torsional freedom using cyclic amino acids is an attractive possibility as illustrated in the examples in Figure 4b. The first crystallographic characterization of novel helices in oligo- $\beta$  peptides by Gellman was based on the use of the amino acids *trans*-2-aminocyclopentanecarboxylic acid (ACPC) and *trans*-2-aminocyclohexanecarboxylic acid (AHC) in which the dihedral angle  $\theta$  is constrained to conformations close to the gauche form, necessary for the helical folding in the backbone.<sup>46–49</sup> Nipecotic acid provides an interesting example of a  $\beta$ -residue in which the torsion angles  $\phi$  and  $\theta$  are constrained by cyclization.<sup>108,109</sup> A recent report describes the synthesis of a  $\gamma^{2,3,4}$ -trisubstituted residue, in which the torsional freedom is constrained by side chain–backbone cyclization.<sup>90,110</sup>

Folding of the polypeptide backbone in peptides containing backbone homologated residues is facilitated when gauche conformations are adopted at the new C–C bonds in the backbone. In the initial studies of oligo- $\beta$ -peptides, using  $\beta^3$ -substituted residues, the observation of folded structures was considered surprising.<sup>44,45</sup> Extended backbone conformations with  $\theta=180^\circ$  might have been anticipated for the  $\beta$  residues. The growing body of structural data in peptides containing  $\beta$  and  $\gamma$  residues however suggests that this expectation was misplaced. Figure 5 summarizes the backbone conformations observed about the C–C bonds in peptides containing  $\beta$  and  $\gamma$  amino acid residues. It is evident that an appreciable number of examples of  $\beta$  residues adopt gauche conformations in the case of the unsubstituted amino acid  $\beta$ Gly and also mono substituted residues.<sup>53,111–117</sup> Similarly, several examples of  $\gamma$ Abu in gg conformations have been reported.<sup>118,119</sup>

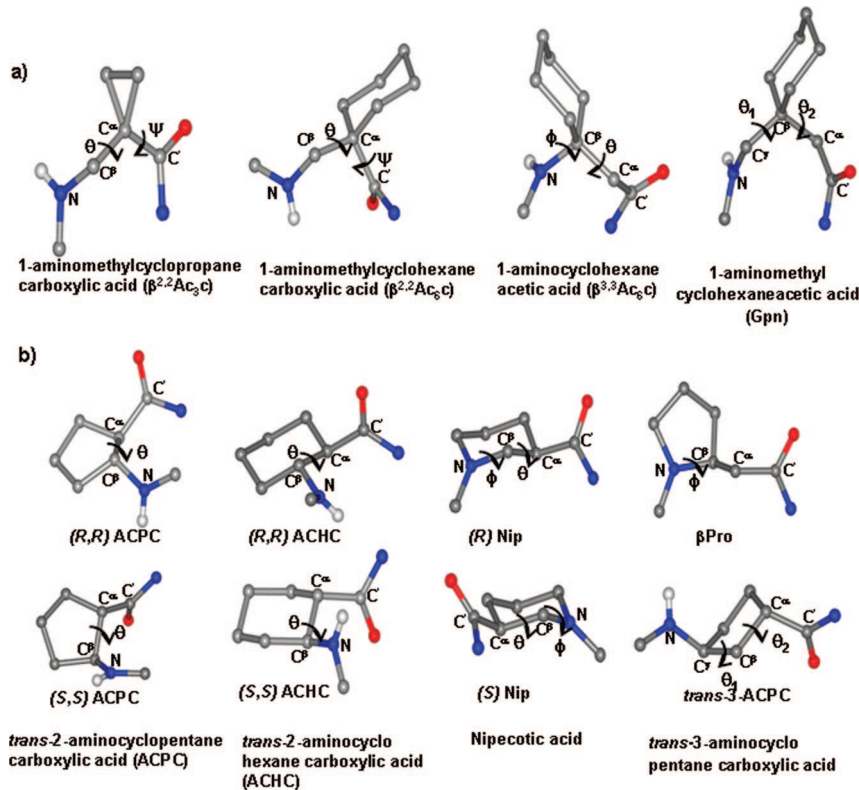


**Figure 4.** Examples of  $\beta$  and  $\gamma$  amino acid residues in which torsional freedom has been restricted using (a) geminal dialkyl substitution and (b) side chain–backbone cyclization.

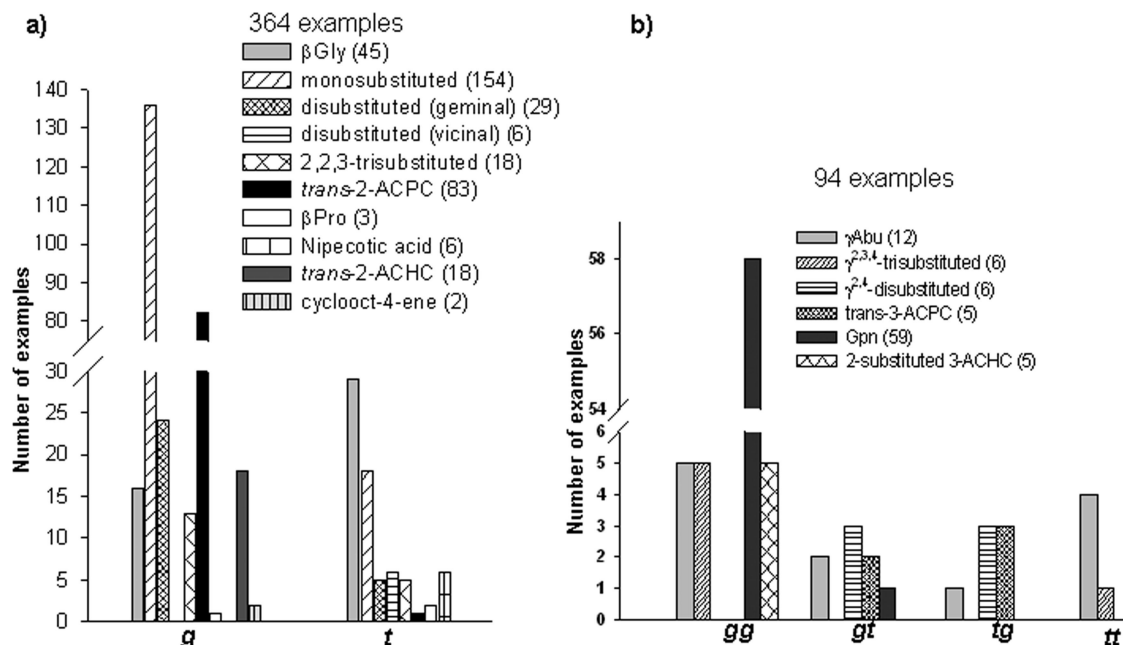


**Figure 5.** Distribution of the dihedral angle  $\theta$  (about C–C bonds) for (a)  $\beta$ -residues and (b)  $\gamma$ -residues in crystal structures. The number of examples in each case are indicated in parentheses. In the case of  $\beta$ -residues, the maximum number of examples are for  $\beta^3$ -residues, followed by the cyclic residue ACPC. The average value of  $\theta$  for the ACPC residue is approximately  $85^\circ$ , while for all other examples the average values of  $\theta$  are close to  $60^\circ$ .

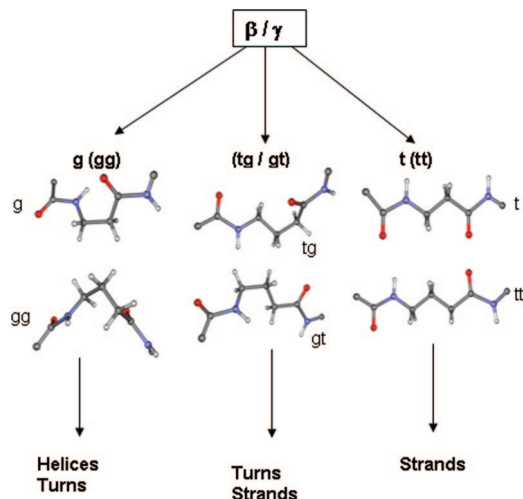


**Figure 6.** Conformational possibilities about the C–C bonds in  $\beta$  and  $\gamma$  residues. The gauche conformations about the additional C–C bonds in these cases are observed in helical structures and turns, while the trans conformation is observed in extended strands or  $\beta$ -hairpins (The sole exception is the (R)Nip-(S)Nip C<sub>12</sub> turn in  $\beta$ -peptides, in which Nip residues are constrained to  $\theta \approx 180^\circ$ ).<sup>108,109</sup> See Figure 15, and Table S1). In the case of  $\gamma$ -residues, hydrogen bonded turns can also result with one of the C–C single bond in a gauche conformation (tg/gt).<sup>103</sup> (See Figure 23)

Figure 6 summarizes the conformational possibilities about the C–C bonds in  $\beta$  and  $\gamma$  residues. The *Gauche* conformations are generally observed for residues in helices and turns, while the extended trans conformation is readily accommodated into  $\beta$ -strand structures. Figure 7 provides examples of unsubstituted  $\beta$ ,  $\gamma$ , and  $\delta$  residues that have been characterized in peptide sequences that adopt helical and hairpin conformations in the crystalline state. Inspection of the molecular conformations of the hairpin peptides Boc-Leu-Val- $\gamma$ Abu-Val-<sup>D</sup>Pro-Gly-Leu- $\gamma$ Abu-Val-Val-OMe<sup>120</sup> and Boc-Leu-Val-Val-<sup>D</sup>Pro- $\delta$ Ava-Leu-Val-Val-OMe<sup>121</sup> reveals example of the  $\gamma$ Abu ( $\gamma$ -aminobutyric acid) in the extended

strand and  $\delta$ Ava ( $\delta$ -aminovaleric acid) in the ( $i + 2$ ) position of a  $\beta$ -hairpin facilitating turn. Clearly, these two examples illustrate the structural plasticity of the unsubstituted  $\omega$  amino acid residues, with conformational choices likely to be influenced by the nature of the cooperative hydrogen bond interactions formed in the folded conformation of the peptides. The possibility that the folding transitions of short  $\beta$  and  $\gamma$  peptides is noncooperative in nature has been considered.<sup>122–125</sup> Figure 8 provides examples of  $\beta^3$  amino acid residues in both peptide helices and hairpins. Backbone homologation can therefore be accomplished within the framework of canonical peptide structures like helices and hairpins.

#### 4. Intramolecularly Hydrogen Bonded Rings in Peptides

The importance of hydrogen bonded rings in stabilizing the regular structures of fibrous proteins was first recognized by Maurice Huggins, whose major reviews in the early 1940s contain the fore-runners of many of the structures that have become commonplace today.<sup>126,127</sup> In a paper published in 1950, Bragg, Kendrew, and Perutz extended the ideas of Huggins in understanding the structural features that emerged in the early analysis of crystalline hemoglobin and myoglobin.<sup>31</sup>

Pauling's insights into the secondary structures formed by polypeptide chains were based principally on the assumption that the intramolecular hydrogen bonding is a dominant force in determining folded conformations of polypeptide chains.<sup>32,128</sup> Helices and  $\beta$ -sheets constitute a most dramatic illustration of the importance of hydrogen bond formation in promoting the folding of the polypeptide backbone in protein structures. The  $\beta$ -turns, which facilitate the reversal of polypeptide chain direction, are a widespread element in protein structures and were first identified in a theoretical study that examined all the stereochemically accessible conformations for a system of three linked peptide units, in which a 4 → 1 hydrogen

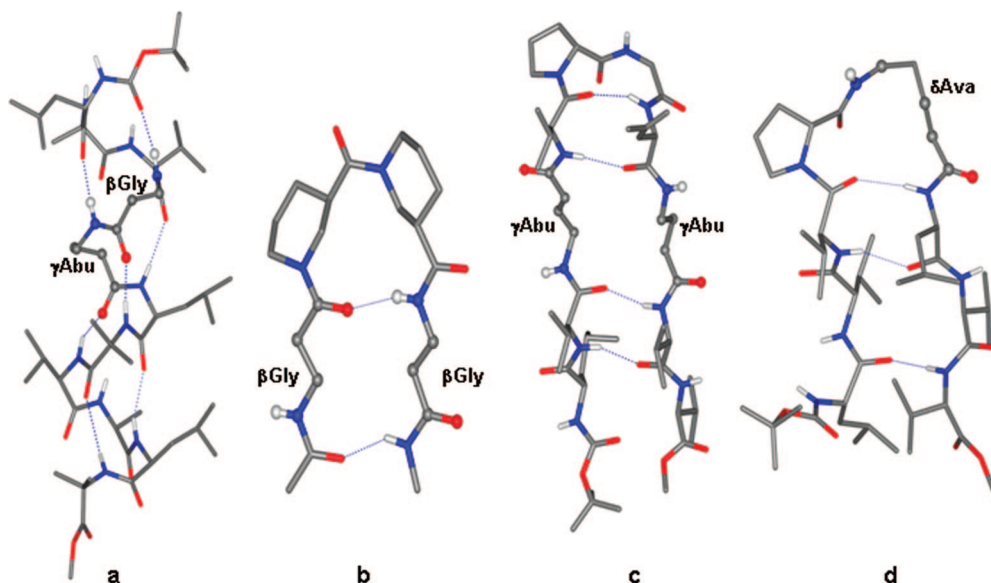


**Figure 7.** Unsubstituted  $\beta$ ,  $\gamma$ , and  $\delta$  residues in helix and hairpin structures. (a) Boc-Leu-Aib-Val- $\beta$ Gly- $\gamma$ Abu-Leu-Aib-Val-Ala-Leu-Aib-OMe,<sup>54</sup> (b) Ac- $\beta$ Gly-Nip-Nip- $\beta$ Gly-NHMe,<sup>109</sup> (c) Boc-Leu-Val- $\gamma$ Abu-Val-<sup>D</sup>Pro-Gly-Leu- $\gamma$ Abu-Val-Val-OMe,<sup>120</sup> and (d) Boc-Leu-Val-Val-<sup>D</sup>Pro- $\delta$ Ava-Leu-Val-Val-OMe.<sup>121</sup>

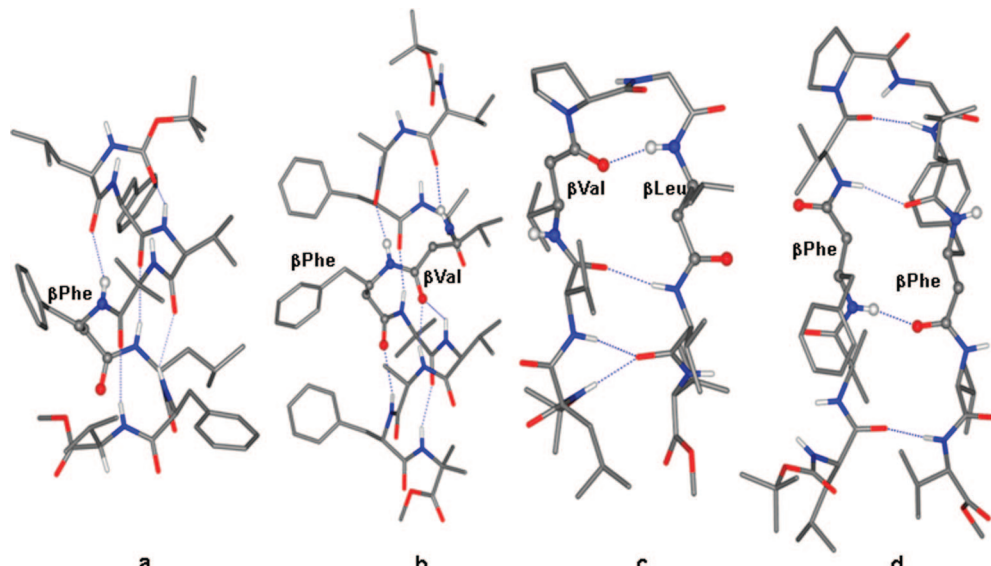


**Figure 8.** Crystallographic examples of  $\beta^3$  amino acid residues in peptide helices and  $\beta$ -hairpins. (a) Boc-Leu-Phe-Val-Aib- $\beta$ Phe-Leu-Phe-Val-OMe,<sup>102</sup> (b) Boc-Val-Ala-Phe-Aib- $\beta$ Val- $\beta$ Phe-Aib-Val-Ala-Phe-Aib-OMe,<sup>190</sup> (c) Boc-Leu-Val- $\beta$ Val-<sup>D</sup>Pro-Gly- $\beta$ Leu-Val-Val-OMe,<sup>209</sup> and (d) Boc-Leu-Val- $\beta$ Phe-Val-<sup>D</sup>Pro-Gly-Leu- $\beta$ Phe-Val-Val-OMe.<sup>209</sup> The backbone atoms of the  $\beta$ -residues are shown in a ball and stick representation.

bond is formed between the CO group of the residue (*i*) and the NH group of the residue (*i* + 3).<sup>129,130</sup> This theoretical study identified specific families of  $\beta$ -turns, which differ in the backbone torsion angles  $\phi$  and  $\psi$  at the (*i* + 1) and (*i* + 2) residues, characterized by the formation of a 10 atom ( $C_{10}$ ) hydrogen bonded ring. In view of the importance of intramolecular hydrogen bonding in determining the local conformations over short peptide segments, we consider the nature of the hydrogen-bonded rings that may be of importance in peptides containing backbone homologated residues. Hydrogen bonds in helical structures of peptides containing  $\alpha$  amino acids have the directionality CO(*i*) $\cdots$ NH(*i* + *n*), where *n* = 3, for a  $\text{3}_{10}$  helix, 4, for an  $\alpha$  helix, and 5, for a  $\pi$  helix. This results in hydrogen bonded ring sizes of 10 atoms ( $C_{10}$ ), 13 atoms ( $C_{13}$ ), and 16 atoms ( $C_{16}$ ). The acceptor CO lies toward the N-terminus of the sequence while the donor NH group lies toward the C-

terminus end. In the case of peptides containing homologated amino acids, for example oligo- $\beta$ -peptides, two types of helical structures with opposing directionality of hydrogen bonds are possible. This feature needs to be borne in mind when exploring the conformations of peptides containing backbone homologated amino acid residues. Hydrogen bonded structures involving  $\omega$  amino acid residues are considered below.

#### 4.1. Single Residue Hydrogen Bonds (3 → 1, 1 → 1)

Figure 9 compares the hydrogen bonded rings that can be obtained by an interaction between the peptide units flanking a single amino acid residue. In the case of an  $\alpha$  amino acid, two structures can be considered. There is the  $C_7$  ( $\gamma$  turn) conformation, which is stabilized by a 3 → 1 hydrogen bond between CO(*i*) $\cdots$ NH(*i* + 2). The Ramachandran  $\phi$ ,  $\psi$  angles

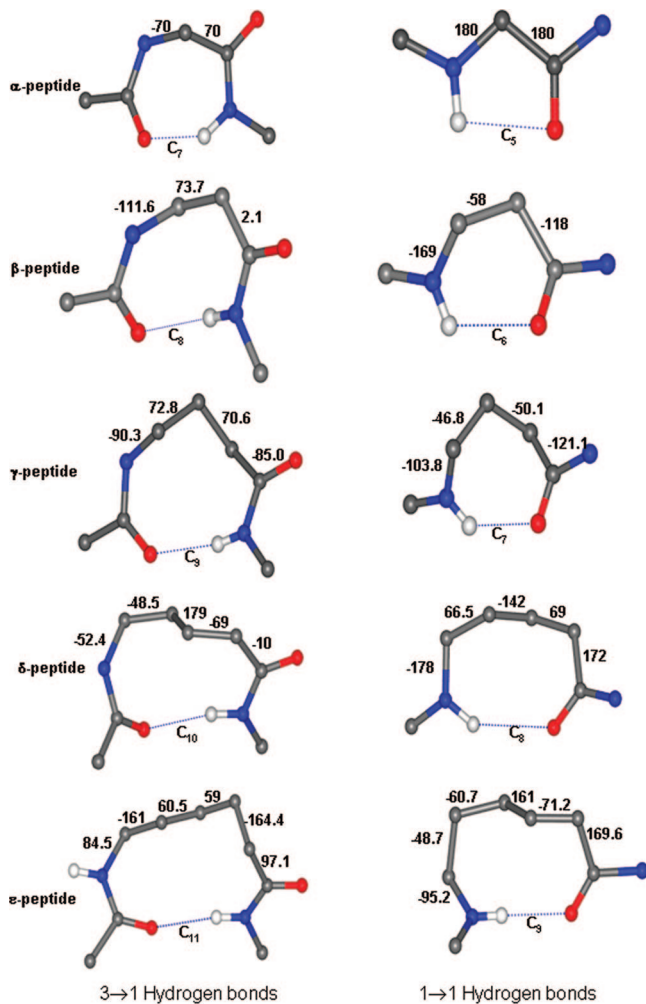


**Figure 9.** Single residue ( $3 \rightarrow 1$  and  $1 \rightarrow 1$ ) hydrogen-bonded rings in peptides. For  $\alpha$  residues, idealized values are shown for structures. For  $\beta$  and  $\gamma$  residues, specific examples are shown from crystal structures:  $C_8$  ( $\beta$ ), Boc- $\beta^{2,2}Ac_3c-\beta^{2,2}Ac_3c-\beta^{2,2}Ac_3c-OH$  (no. 38, Table S1),<sup>97</sup>  $C_6$  ( $\beta$ ), Boc- $\beta^{3,3}Ac_6c-\beta^{3,3}Ac_6c-NHMe$  (no. 50, Table S1),<sup>142</sup>  $C_9$  ( $\gamma$ ), Piv-Pro-Gpn-Val-OMe (no. 158, Table S1),<sup>100</sup> and  $C_7$  ( $\gamma$ ), Boc-Aib-Gpn-Aib-Gpn-NHMe (no. 165, Table S1).<sup>191</sup> For  $\delta$  and  $\epsilon$  peptides, the values are obtained from theoretical studies.<sup>138,139</sup>

have values of  $\pm 70^\circ$ ,  $\pm 70^\circ$ . In the case of L amino acids, the  $-70^\circ$ ,  $+70^\circ$  conformation is energetically favored. The  $3 \rightarrow 1$  hydrogen bond directionality places the acceptor CO groups at the N-terminus and the donor NH group at the C-terminus. The  $\gamma$  turn is widely observed in protein structures and cyclic peptides.<sup>131–135</sup> A second hydrogen bonded ring involving a single residue is the  $C_5$  conformation.<sup>136</sup> This feature is formed by a fully extended polypeptide chain, placing the NH and the CO groups of the  $\alpha$  residue almost parallel to one another resulting in an unfavorable hydrogen bond angle. Such  $C_5$  conformations have been crystallographically characterized for  $C^{\alpha,\alpha}$ -disubstituted residues like diethylglycine (Deg) and di-n-propylglycine (Dpg).<sup>136,137</sup> The insertion of additional backbone atoms in the homologated amino acids expands the hydrogen bond ring size. Figure 9 illustrates the conformations that have been obtained by X-ray crystallography for the case of  $\beta$  and  $\gamma$  residues. For the  $\delta$  and  $\epsilon$  residues, the hydrogen bonded turns indicated in the Figure 9 are modeled. For the  $C_{10}$  and the  $C_8$  hydrogen bonded rings of the  $\delta$  amino acid residue and the  $C_{11}$  and  $C_9$  hydrogen bonded rings of the  $\epsilon$  residue,

the models have been constructed using torsion angle values computed by Hofmann.<sup>138,139</sup> In the case of  $\delta$  amino acid residues, the  $C_{10}$  atom hydrogen bond is equivalent to the  $4 \rightarrow 1$  hydrogen bonded  $\beta$ -turn in an  $\alpha\alpha$  segment with the central  $C^\beta-C^\gamma$  bond in a trans conformation.<sup>138</sup> In the case of  $\epsilon$  amino acid residues, the 11 atom hydrogen bond is equivalent to the  $4 \rightarrow 1$  hydrogen bonded ring in the case of  $\alpha\beta$  hybrid peptides.<sup>139</sup>

## 4.2. Hydrogen-Bonded Ribbons

The regular repetition of hydrogen bonded rings formed by single amino acid residues results in the generation of ribbonlike structures (flattened helices). For  $\alpha_n$  sequences, a  $C_7$  ribbon or  $2.2_7$  helix has not been characterized in a long peptide, although isolated  $C_7$  hydrogen bonded rings ( $\gamma$  turns) are frequently observed in proteins and cyclic peptides.<sup>131–135</sup> Figure 10 illustrates the nature of hydrogen bonded ribbons that can be formed in  $\alpha_n$ ,  $\beta_n$ , and  $\gamma_n$  sequences. Crystalllo-

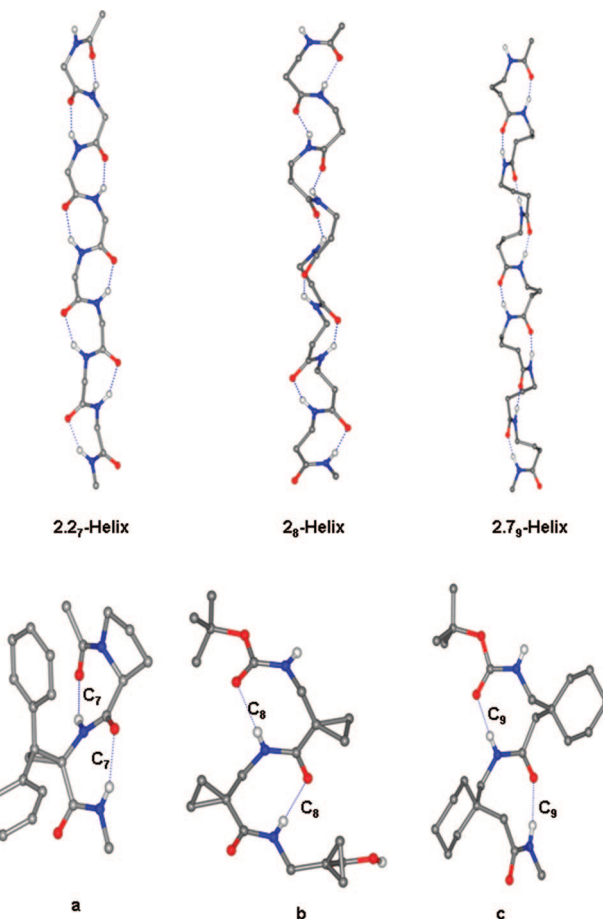


**Figure 10.**  $3 \rightarrow 1$  hydrogen bonded structures. (a) A model  $2.2_7$  helix constructed by using the ideal values for  $\gamma$  turn ( $\phi = -70^\circ$ ,  $\psi = 70^\circ$ ) (top) and the structure of a dipeptide with consecutive  $\gamma$  turns in the crystal structure of  $Ac-L-Pro-D-c3Dip-NHMe$ <sup>140</sup> (bottom). (b)  $C_8$  ( $2_8$ ) Ribbon in  $\beta$ -peptides (top) and the crystal state conformation of a tripeptide Boc- $\beta^{2,2}Ac_3c-\beta^{2,2}Ac_3c-\beta^{2,2}Ac_3c-OH$ <sup>97</sup> (no. 38, Table S1). (c)  $2.7_9$  Helix of  $\gamma$  peptide (Reprinted with permission from ref 141. Copyright 2005 Wiley-VCH Verlag GmbH & Co. KGaA.) and the molecular conformation of the dipeptide Boc-Gpn-Gpn-NHMe<sup>141</sup> (no. 156, Table S1) in crystals. The models for  $\beta$ -peptide and  $\gamma$ -peptide ribbons/helices are constructed using the average values of torsion angles observed in crystals and then minimizing the resulting model in INSIGHT II, to relieve any short contacts. The average values of torsion angles in the minimized models provided in Table 1 are used to build the final models shown in the top panel for  $\beta$  and  $\gamma$  peptides.

**Table 1.** Backbone Dihedral Angles (deg) for Ribbons Stabilized with 3 → 1 Hydrogen Bonds<sup>a</sup>

helix type (n, h)	residue repeat	atoms in hydrogen bond ring	$\phi$	$\psi$	$\phi$	$\theta_1$	$\theta_2$	$\psi$	method <sup>b</sup>
3 → 1									
C <sub>7</sub> (2.2 <sub>7</sub> ) (2.2, 2.7)	$\alpha$	7	-70	70					C
C <sub>8</sub> (2.2 <sub>8</sub> ) (2.2, 3)	$\beta$	8			-112.3 (-111.5)	69.6 (68.6)			C/T
C <sub>9</sub> (2.7 <sub>9</sub> ) (2.7, 3.4)	$\gamma$	9			-100 (-97.4)	70 (69.6)	70 (75.1)	-90 (-97)	C/T

<sup>a</sup> The torsion angles given in parentheses for  $\beta$  and  $\gamma$  peptides correspond to that suggested by theoretical calculation.<sup>144,151</sup> The average values of torsion angles in the minimized models, constructed by using the crystallographically determined values of dihedral angles (See Figure 10). <sup>b</sup> C and T indicate crystallographic and theoretical studies, respectively.

graphically characterized examples of peptides containing successive hydrogen bonded rings are also illustrated. A recent example of two consecutive C<sub>7</sub> hydrogen bonds is seen in the crystal structure of the dipeptide Piv-Pro-c<sub>3</sub>-Dip-NHMe (c<sub>3</sub>-Dip = 2,2-diphenyl-1-aminocyclopropane carboxylic acid).<sup>140</sup> A novel C<sub>8</sub> structure has been established in the tetrapeptide Boc-(1-(aminomethyl)cyclopropanecarboxylic acid)<sub>4</sub>-OMe.<sup>97</sup> The stereochemically constrained  $\gamma$  amino acid residue, gabapentin (Gpn) favors the C<sub>9</sub> conformation and ribbon structures are observed in the dipeptide Boc-Gpn-Gpn-NHMe and the tetrapeptide Boc-(Gpn)<sub>4</sub>-NHMe.<sup>141</sup> In considering hydrogen bonded ribbons, it is pertinent to note that for achiral sequences, the signs of backbone torsion angles need not be correlated between adjacent residues, resulting in a large number of conformational possibilities within the framework of a ribbon scaffold. For the  $\gamma$  amino acid C<sub>9</sub> ribbon, when the handedness of the adjacent residues alternates, a significant curvature of the backbone leads to cyclization after a large number of residues.<sup>141</sup> Table 1 lists the torsional variables for the hydrogen bonded rings that have been characterized experimentally (X-ray crystallography) or theoretically (quantum mechanical calculations). For single-residue rings formed by hydrogen bonds with opposite directionality (1 → 1), repetitive structures have not been observed thus far in peptide crystal structures. However, isolated C<sub>6</sub> hydrogen bonded rings in  $\beta$  residues<sup>92,98,142</sup> and C<sub>7</sub> hydrogen bonded rings in  $\gamma$  residues,<sup>100</sup> specifically Gpn containing peptides, have been observed in the crystal structures (Supporting Information, Table S1).

There has been considerable interest in the theoretical analysis of energetically allowed conformations of  $\beta$ -peptides and their higher homologues.<sup>138,139,143–151</sup> Molecular dynamics simulations using GROMOS have been extensively carried out by van Gunsteren, Seebach, and their colleagues, integrating theoretical studies with experimental investigations. This approach permits analysis of the effect of specific amino acid residues on folding-unfolding equilibrium.<sup>152–158</sup> Hofmann and co-workers have carried out extensive theoretical studies providing a systematic conformational analysis of  $\omega$  amino acid monomers and homooligomers using ab initio MO theory (HF/6-31G\*, B3LYP/6-31G\*, PCM/HF/6-31G\*).<sup>138,139,150,151</sup> These studies provide a framework for assessing the energetics of various intramolecularly hydrogen bonded structures in peptides containing  $\beta$ ,<sup>150</sup>  $\gamma$ ,<sup>151</sup>  $\delta$ ,<sup>138</sup> and  $\epsilon$ <sup>139</sup> amino acid residues. Interestingly, these theoretical studies reveal conformational possibilities which are yet to be experimentally realized. A  $\delta$  amino acid residue may be considered as equivalent to a system of two linked  $\alpha$  amino acids, in which the connecting peptide bond is replaced by a CH<sub>2</sub>–CH<sub>2</sub> fragment.<sup>55,138</sup> Thus, the C<sub>10</sub> (4 → 1) hydrogen bonded structures widely observed in  $\beta$ -turns formed by  $\alpha\alpha$  segments can be mimicked by a  $\delta$  amino acid residue flanked by two peptide bonds. Figure 11 illustrates three types of

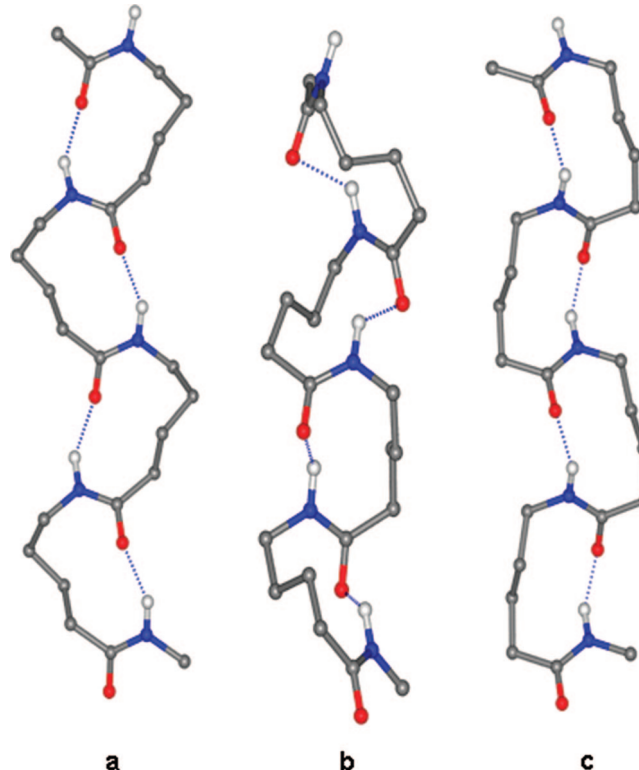


**Figure 11.** Three different types of C<sub>10</sub> hydrogen bonded ribbons in  $\delta$ -peptides generated by using the dihedral angles given by Baldauf et al.<sup>138</sup> (a) The H<sub>10</sub><sup>1</sup> Helix, which is proposed as the most stable helix and (b) a ribbon in which the  $\delta$ -residues are in C<sub>10</sub><sup>VII</sup> conformation and (c) ribbon with the  $\delta$ -residues in C<sub>10</sub><sup>VIII</sup> conformation. The latter conformations (b) and (c) are described only for the monomer.

ribbon structures formed by C<sub>10</sub> hydrogen bonded rings in  $\delta_n$  sequences. In conformer A, the dihedral angles correspond to the lowest energy conformer H<sub>10</sub><sup>1</sup> computed by Hofmann and co-workers.<sup>138</sup> Conformers B and C are generated using the C<sub>10</sub><sup>VII</sup> and C<sub>10</sub><sup>VIII</sup> structures,<sup>138</sup> which are mimetics of the canonical type I  $\beta$  turn and type II  $\beta$ -turn in  $\alpha\alpha$  sequences. Conformer B is an analog of the  $\alpha$  polypeptide 3<sub>10</sub> helix in which alternate peptide units have been replaced by ethylene (CH<sub>2</sub>–CH<sub>2</sub>) groups. In this structure, alternate 4 → 1 hydrogen bond in the 3<sub>10</sub> helix are replaced by a nonbonded contact between methylene units on adjacent residues. The closest interhydrogen distances observed for the model C<sub>10</sub><sup>VIII</sup> of Hofmann and co-workers is approximately 2.03 Å, suggesting that an optimally close packed 3-fold helical structure may indeed be accessible for  $\delta$  amino acid oligomers. The accommodation of guest  $\delta$  residues into host  $\alpha$  peptide 3<sub>10</sub> helical structures without disruption of the folding pattern, has been suggested from the NMR studies of a model heptapeptide Boc-Leu-Aib-Val- $\delta$ Ava-Leu-Aib-Val-OMe in organic solvents.<sup>53</sup>

The higher  $\omega$  amino acids may also provide an opportunity to characterize hydrogen bonded rings of the  $1 \rightarrow 1$  type, which result in  $C_8$  structures for  $\delta$  residues<sup>138</sup> and  $C_9$  structures for the  $\epsilon$  residues.<sup>139</sup> It may be noted that the  $C_{11}$  structures for the  $\epsilon$  residues may be considered as equivalent to the expanded turns formed by hybrid  $\alpha\beta$  sequences, which are considered in the next section.

### 4.3. Two Residue Hydrogen Bonds ( $4 \rightarrow 1$ , $1 \rightarrow 2$ )

Two residue hydrogen bonded rings can be formed in the case of both homodipeptide and heterodipeptide segments. In the case of hybrid peptides, it is also useful to recall the formal equivalence of the nature of the hydrogen bonded rings formed in hybrid sequences.<sup>55,53</sup> Figure 12 illustrates the  $C_{12}$  hydrogen-bonded rings in  $\alpha\gamma$  and  $\beta\beta$  segments and  $C_{13}$  hydrogen bonded rings, which may be formed in a three residue  $\alpha\alpha\alpha$  segment and the equivalent structures that can be generated in  $\beta\gamma$  and  $\alpha\delta$  units.

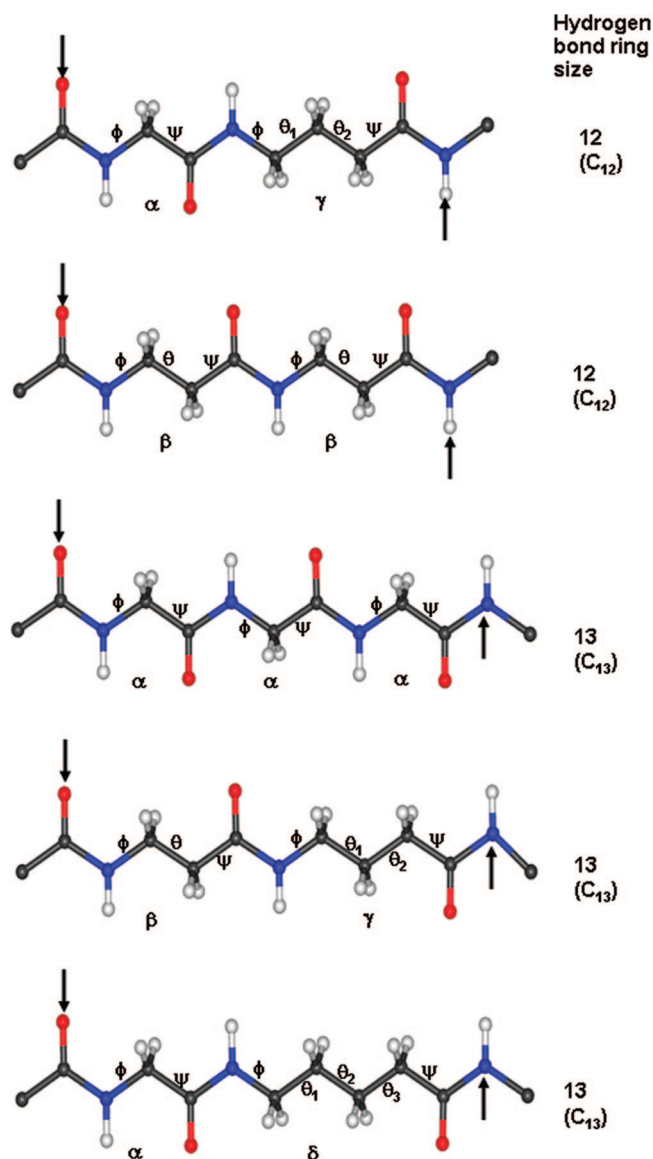


**Figure 12.** Formal equivalence of backbone atoms in polypeptides. Acceptor atoms and donor atoms in the 12 and 13-atom hydrogen bonded rings are indicated by down and up arrows, respectively. For example, a three residue  $\alpha\alpha\alpha$   $C_{13}$  hydrogen bonded turn will be equivalent to two residue  $C_{13}$  turns formed by  $\beta\gamma$  and  $\alpha\delta$  segments.

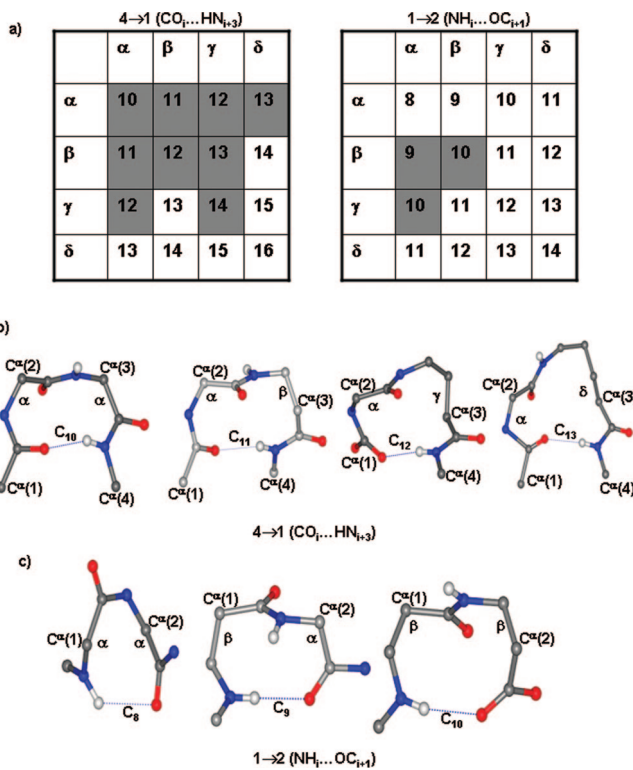


**Figure 13.** (a) Schematic diagram showing the number of atoms in the two-residue hydrogen-bonded turns ( $4 \rightarrow 1$  and  $1 \rightarrow 2$ ) in homo oligopeptides and hybrid peptides. Shaded squares correspond to crystallographically characterized examples. (b) Some examples of  $4 \rightarrow 1$  hydrogen-bonded turns in hybrid peptides. A  $C_{10}$  turn ( $\beta$ -turn) formed in an  $\alpha\alpha$  segment is also shown. (c) Examples of two-residue hydrogen bonds formed with a reversed hydrogen bond directionality ( $1 \rightarrow 2$ ). All the examples, except the  $\alpha\alpha$   $C_8$  turn (this structure required a *cis* amide conformation for the central peptide unit) in (c) are from crystal structures (type, sequence (entry number in Table S1)):  $\alpha\beta$   $C_{11}$ , Piv-Pro- $\beta^{3,3}Ac_6c-NHMe^{121}$  (48),  $\alpha\gamma$   $C_{12}$ , Boc-Ac<sub>6</sub>c-Gpn-Ac<sub>6</sub>c-OMe<sup>121</sup> (160),  $\alpha\delta$   $C_{13}$ , Boc-Leu-Val-Val-DPro- $\delta$ Ava-Leu-Val-Val-OMe,<sup>121</sup>  $\beta\alpha$   $C_9$ , iodobenzoyl-Ala- $\alpha$ , $\alpha$ -dimethyl-D- $\beta$ Ala-Phe-OMe<sup>92</sup> (89), and  $\beta\beta$   $C_{10}$ , Boc- $\beta^{2,2}Ac_6c-\beta^{2,2}Ac_6c-OMe^{97}$  (40, residues 2 and 3).

The  $4 \rightarrow 1$  hydrogen-bonded two residue structure in  $\alpha\alpha$  segments is the extremely well studied  $\beta$  turn.<sup>129,130</sup>  $\beta$  turn variants that differ in the backbone conformational angles ( $\phi, \psi$ ) at the two residues ( $i + 1, i + 2$ ) yield turns with distinctive influences on polypeptide chain folding. The type I/III structures ( $\phi_{(i+1)} = -30^\circ, \psi_{(i+1)} = -60^\circ, \phi_{(i+2)} = -60^\circ/-90^\circ$ , and  $\psi_{(i+2)} = -30^\circ/0^\circ$ ) upon repetition form helices, while the type II structures ( $\phi_{(i+1)} = -60^\circ, \psi_{(i+1)} = 120^\circ, \phi_{(i+2)} = 80^\circ$ , and  $\psi_{(i+2)} = 0^\circ$ ) facilitate reversal of chain direction. In sequences that contain all L amino acids, insertion of a type II' turn (enantiomer of type II) forming segment promotes antiparallel registry of the flanking strands, thereby stabilizing  $\beta$  hairpins.<sup>159,160</sup> Figure 13 summarizes the hydrogen bond ring sizes in two residue turns in hybrid sequences with hydrogen bond directionalities that run in normal direction ( $4 \rightarrow 1$ ) and reversed direction ( $1 \rightarrow 2$ ). Crystallographically characterized examples of  $4 \rightarrow 1$  hybrid turns in  $\alpha\beta$ ,  $\alpha\gamma$ , and  $\alpha\delta$  sequences and  $1 \rightarrow 2$  turns in  $\beta\alpha$  and  $\beta\beta$  sequences are illustrated. The  $C_8$  turn, which has been considered in the spectroscopic studies of short peptides in an  $\alpha\alpha$  sequence requires a *cis* geometry at the linking peptide unit.<sup>161</sup> Thus far no examples of the  $C_8$   $\alpha\alpha$  turn have been established in crystals. Table 2 summarizes backbone torsion angles for the various types of two-residue  $4 \rightarrow 1$  hydrogen-bonded turns in both homo and hybrid sequences.

**Table 2. Backbone Torsion Angles (deg) for Hydrogen-Bonded Turns in Hybrid Peptides and Comparison with  $\alpha$ -Peptides<sup>a</sup>**

turns	Type I/III						type II					
	$\phi$	$\theta_1$	$\theta_2$	$\psi$	$\phi$	$\theta_1$	$\theta_2$	$\psi$	$\phi$	$\theta_1$	$\theta_2$	$\psi$
$\alpha\alpha$ ( $C_{10}$ )	-60				-30	-90			0	-60		
$\beta\beta$ ( $C_{12}$ )	96.4 (13.7)	-91.8 (11.9)			101.1 (13.7)	96.4 (13.7)	-91.8 (11.9)		101.1 (13.7)	104.4 (9.7)	-176.7 (2.4)	
$\gamma\gamma$ ( $C_{14}$ )	140.4 (22.8)	-67.1 (4.8)	-54.7 (5.6)		140.4 (22.8)	-67.1 (4.8)	-54.7 (5.6)		133.7 (15.3)	151.3 (8.3)	-168.5 (2.6)	71.5 (11.5)
$\alpha\beta$ ( $C_{11}$ )	-54.4 (4.9)				-34.8 (13.4)	-94.5 (8.3)	87.9 (8.3)		-89.9 (11.7)	-51.9 (8.9)		135.7 (5.4)
$\alpha\gamma$ ( $C_{12}$ )	-61.3 (7.7)				-35.5 (13.1)	-132.9 (7.8)	53.5 (2.4)		59.9 (2.5)	-111.7 (5.5)	-47	
$\beta\gamma$ ( $C_{13}$ )	-106.1 (5.0)	79.7 (1.8)	-113.6 (9.5)	-117.7 (4.7)	62.8 (0.3)	122.2 (1.3)	-138.6	61.5	62.2 (7.4)	50.8	100.4	

<sup>a</sup> When more than one observation is available, averaged values are shown, and the corresponding esds are given in parentheses. The number of observations are  $\beta\beta$  (type I) 12, (type II) 3;  $\gamma\gamma$  (type I) 3, (type II) 3;  $\alpha\beta$  (type I) 31 ( $\alpha$ -residue), 23 ( $\beta$ -residue), 18 ( $\alpha$ -residue), 12 ( $\beta$ -residue);  $\beta\gamma$  (type I) 6.

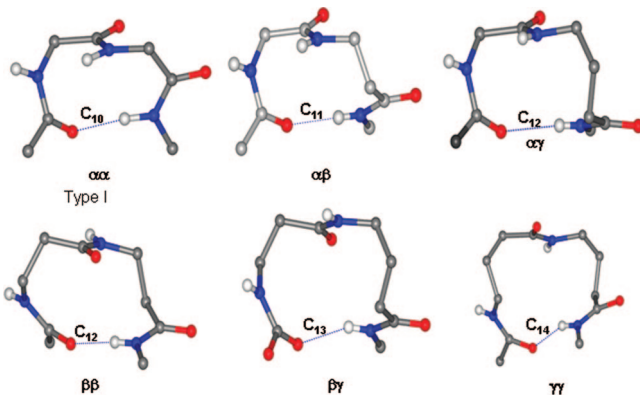


**Figure 14.** The type I  $\beta$ -turn in an  $\alpha$ -peptide sequence and analogs in  $\beta$ -,  $\gamma$ - and hybrid peptides. The backbone torsion angles are listed in Table 2. These turn types can be continuously repeated in  $(\alpha\beta)_n$ ,  $(\alpha\gamma)_n$ ,  $(\beta\gamma)_n$  and  $(\beta)_n$ , and  $(\gamma)_n$  sequences and referred to as “helical turns.”

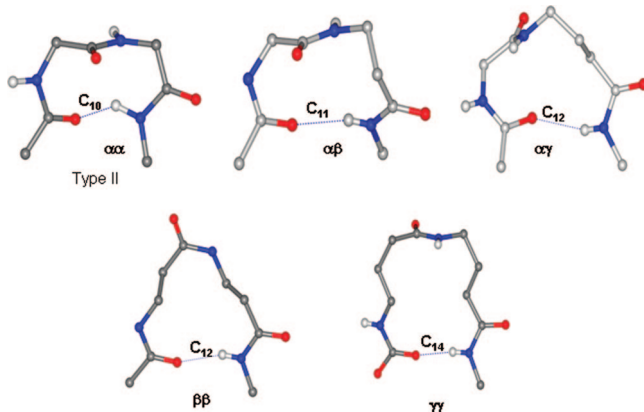


**Figure 15.** Nonrepeatable (non-helical) 4  $\rightarrow$  1 hydrogen-bonded turns. Such turns occur as isolated structural features or facilitate hairpin formation. The backbone torsion angles are listed in Table 2. The figure shows nonhelical turns in the following crystal structures:  $\alpha\beta$ , Piv-Pro- $\beta$ Ac<sub>2</sub>c-NHMe<sup>121</sup> (no. 48 in Table S1),  $\alpha\gamma$ , Boc-Leu-Phe-Val-Alb-Gpn-Leu-Phe-Val-OMe<sup>103</sup> (no. 170 in Table S1),  $\beta\beta$ , Ac- $\beta$ Gly-Nip-Nip- $\beta$ Gly-NHMe (mol. 1)<sup>109</sup> (no. 28 in Table S1), and  $\gamma\gamma$ , Boc-(4-amino-2-benzyl-4-methylbutanoyl)-(4-amino-2-methyl-4-(2-methyl-1-propyl) butanoyl)-NHMe<sup>226</sup> (no. 134 in Table S1).

Figure 14 illustrates the backbone expanded analogs of the type I  $\beta$  turn that has been widely characterized in  $\alpha\alpha$  sequences. These turns can be repeated in longer sequences resulting in the formation of successive 4  $\rightarrow$  1 hydrogen bonds generating helical structures containing a two residue hybrid repeating unit. Figure 15 provides examples of expanded analogs of the type II  $\beta$  turn widely observed in the  $\alpha\alpha$  sequences. Such turns may also be described as “non helical” turns since they cannot be repeated to generate successive 4  $\rightarrow$  1 hydrogen bonds. These structural features generate chain reversals.

#### 4.4. $3_{10}$ Helix Expanded Analogs

Helical structures stabilized by 4  $\rightarrow$  1 hydrogen bonds are observed in oligo  $\beta$  and  $\gamma$  peptides and in hybrid sequences containing  $\alpha$ ,  $\beta$ , and  $\gamma$  residues. Figure 16 illustrates 4  $\rightarrow$  1 hydrogen-bonded helices in synthetic model peptides for  $(\beta)_n$ ,<sup>45–48</sup>  $(\gamma)_n$ ,<sup>52,124</sup>  $(\alpha\beta)_n$ ,<sup>162–165</sup>  $(\alpha\gamma)_n$ ,<sup>90,100,102,103,166</sup> and  $(\beta\gamma)_n$ <sup>110</sup> sequences, characterized experimentally by X-ray diffraction. Several studies have also provided NMR evidence for formation of helical structures in solution.<sup>50,51,167–183</sup> For the

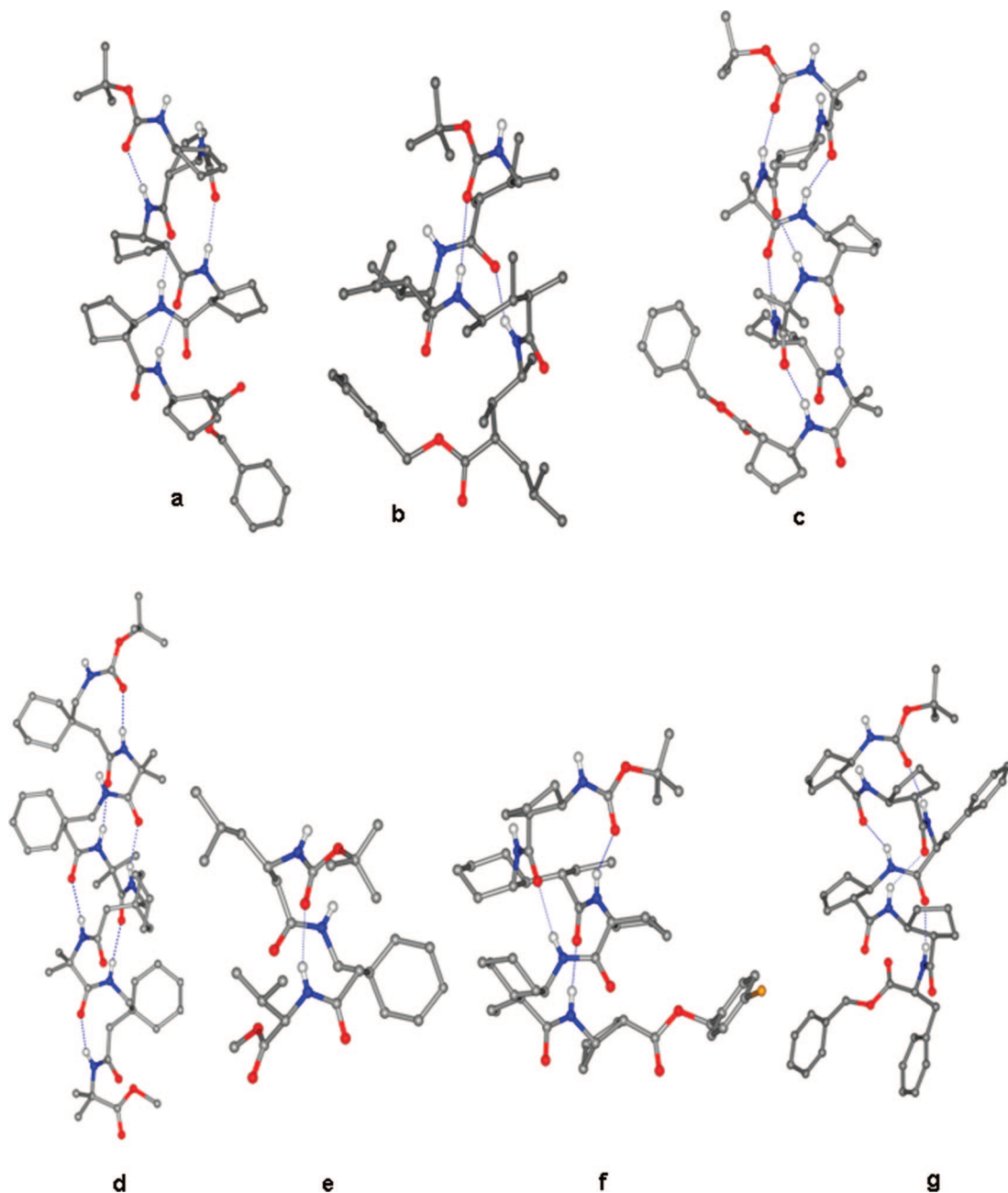


**Figure 16.** Examples of experimentally characterized helices with  $4 \rightarrow 1$  hydrogen-bonded turns in  $\beta$ ,  $\gamma$ , and hybrid peptides. (a) 12-helix formed by  $\beta$ -peptide Boc-ACPC-ACPC-ACPC-ACPC-ACPC-OBn<sup>49</sup> (no. 123 in Table S1) and (b) 14-helix formed in the  $\gamma$ -peptide Boc-(4-amino-2,3,4-trimethylbutanoyl-4-amino-3,4-dimethyl-2(2-methyl-1-propyl) butanoyl)<sub>2</sub>-OBn<sup>124</sup> (no. 136 in Table S1). (c)  $\alpha\beta$  C<sub>11</sub>-helix, Boc-Aib-ACPC-Aib-ACPC-Aib-ACPC-Aib-ACPC-OBn<sup>162</sup> (no. 110 in Table S1), (d)  $\alpha\gamma$  C<sub>12</sub>-helix, Boc-Gpn-Aib-Gpn-Aib-Gpn-Aib-Ome<sup>103</sup> (no. 169, Table S1), (e)  $\beta\gamma$  C<sub>13</sub> turn, Boc-βLeu-Gpn-Val-Ome<sup>100</sup> (no. 61 in Table S1), (f)  $\beta\gamma$  C<sub>13</sub> Helix, Boc-ACPC-(S,S,S)(2-ethyl)3ACHC-ACPC-(S,S,S)(2-ethyl)3ACHC-ACPC-OBn<sup>110</sup> (no. 96 in Table S1), and (g) 12/11/11 helix, Boc-ACPC-ACPC-Phe-OBn<sup>163</sup> (no. 100 in Table S1).

$\beta\gamma$  sequence, a single example of a  $4 \rightarrow 1$  hydrogen bonded C<sub>13</sub> helical turn has been observed in a tripeptide sequence Boc-βLeu-Gpn-Val-OMe (No:61, Table S1).<sup>100</sup> The backbone conformational angles observed for the  $\beta\gamma$  segment in this tripeptide can be repeated to generate the regular  $\beta\gamma$  C<sub>13</sub> helix (Figure 16e).<sup>102</sup> A recent report that appeared subsequent to the submission of this review revealed the crystal structure of a pentapeptide, Boc-ACPC-(S,S,S)(2-ethyl)3ACHC-ACPC-(S,S,S)(2-ethyl)3ACHC-ACPC-Obn (No: 96, Table S1), with three successive C<sub>13</sub> hydrogen bonds (Figure 16f).<sup>110</sup> Successful substitution of an entire heptad repeat in an  $\alpha$ -helical coiled-coil protein by a non-natural fragment constituting five alternating  $\beta$  and  $\gamma$  residues, with

the retention of global conformation has also been proved in solution.<sup>184</sup> Figure 17 compares the ideal backbone expanded helical structures with the idealized 3<sub>10</sub> helix of  $\alpha$  peptides. The parameters used to generate these idealized structures have been derived from crystallographic observations and are listed in Table 3.

Helices with variable  $4 \rightarrow 1$  hydrogen-bonded ring sizes have also been characterized in hybrid sequences that lack a regular  $(\alpha\omega)_n$  repeat. Mixed  $4 \rightarrow 1$  hydrogen-bond patterns of the C<sub>12</sub>/C<sub>11</sub> type have been observed in  $(\beta\beta\alpha)_n$  peptide sequences (1:2  $\alpha/\beta$  peptides)<sup>163,164</sup> (Figure 17), C<sub>10</sub>/C<sub>11</sub> mixed hydrogen bonds in  $(\alpha\alpha\beta)_n$  sequences (2:1  $\alpha/\beta$  peptides)<sup>163,164</sup> (see Table S1), while the C<sub>12</sub>/C<sub>10</sub> hydrogen-bond pattern has

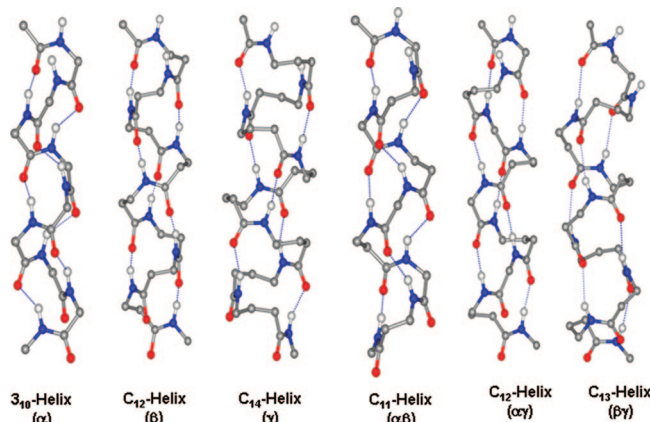


**Figure 17.** Helices with  $4 \rightarrow 1$  hydrogen-bond patterns in  $\alpha$ ,  $\beta$ ,  $\gamma$ , and hybrid peptides. The models for  $\beta$ ,  $\gamma$ , and hybrid peptide helices are constructed using the average values of torsion angles observed in crystals and then minimizing the resulting model in INSIGHT II to relieve any short contacts. The average values of torsion angles in the minimized models provided in Table 3 are used to build the final models shown in the figure.

been observed in the  $(\alpha\gamma\alpha)_n$  sequence Boc-(Leu-Gpn-Aib)<sub>2</sub>-OMe (no. 168 in Table S1).<sup>166</sup> Theoretical calculations by the group of Hofmann have resulted in energetically favorable models for  $4 \rightarrow 1$  hydrogen bonded  $C_{11}$  ( $\alpha\beta$ ),<sup>185</sup>  $C_{12}$  ( $\beta\beta/\alpha\gamma$ ),<sup>150,186</sup> and  $C_{13}$  ( $\beta\gamma$ )<sup>186</sup> helices, whose conformational parameters are in good agreement to those determined from crystal structures. The helix types in  $(\beta\delta)_n$  peptide have recently been predicted theoretically.<sup>187</sup>

#### 4.5. Three-Residue Hydrogen-Bonded Turns ( $5 \rightarrow 1$ , $1 \rightarrow 3$ )

In all  $\alpha$  peptides, three-residue hydrogen-bonded rings ( $CO(i)\cdots NH(i+4)$ ) result in a 13 atom structure ( $C_{13}$ ). Repetitive turns with successive  $5 \rightarrow 1$  hydrogen bonds along the backbone yield a classical Pauling  $\alpha$  ( $3.6_{13}$ ) helix.<sup>32,128</sup> In such a structure, the Ramachandran angles at each residue

lie in approximately the same region of  $\phi$ ,  $\psi$  space ( $\alpha_R$ :  $\phi \approx -57^\circ$ ,  $\psi \approx -47^\circ$ ). Isolated  $C_{13}$  hydrogen bonded turns in which the  $\phi$ ,  $\psi$  angles of the three residues are quite different have also been characterized in proteins and are referred to as  $\alpha$  turns (*nonhelical turns*).<sup>188,189</sup>

In three-residue segments containing  $\omega$  amino acids, expanded hydrogen bond ring sizes are obtained for  $5 \rightarrow 1$  hydrogen-bonded turns as summarized in Figure 18. Thus far, crystal structures have provided several examples of expanded three residue turns, as exemplified in Figure 18, which shows experimentally established hydrogen-bonded ring sizes of 14 ( $\alpha\alpha\beta$ ),<sup>102</sup> 15 ( $\alpha\beta\beta$ ),<sup>190</sup> and 17 ( $\gamma\alpha\gamma$ )<sup>191</sup> atoms. Of these  $C_{14}$  ( $\alpha\alpha\beta$ )<sup>102</sup> and  $C_{15}$  ( $\alpha\beta\beta$ )<sup>190</sup> turns can be repeated to yield continuous helices and may be classified as helical turns. In contrast,  $\gamma\alpha\gamma$  ( $C_{17}$ )<sup>191</sup> structure illustrated in Figure 18 is a nonhelical three-residue turn. In the case of expanded polypeptide backbones, structures in which hydrogen bond directionality is reversed  $NH(i)\cdots CO(i+n)$  must also be considered. Indeed, for a  $\beta\beta\beta$  segment, such a  $1 \rightarrow 3$  ( $NH(i)\cdots CO(i+2)$ ) hydrogen bond has been characterized in all  $\beta$  sequences<sup>46–48</sup> (Figure 18c). Repetition of this structure is indeed possible resulting in  $C_{14}$  helix.

In the case of  $\alpha$  peptide sequences, considerable conformational variability has been established within the overall framework of two residue ( $4 \rightarrow 1$ ) and three residue ( $5 \rightarrow 1$ ) hydrogen-bonded turns, which have been termed as  $\beta$  turns<sup>2,129,130,192</sup> and  $\alpha$  turns,<sup>188,189</sup> respectively. Expansion of the polypeptide backbones in sequences containing  $\omega$  amino acids must necessarily result in a variety of conformational classes within the framework of a specific hydrogen bonded ring size. These will undoubtedly be experimentally characterized, as the database of crystal structures expands to encompass hybrid sequences with greater residue diversity.

#### 4.6. $\alpha$ Helix Expanded Analogs

The  $\alpha$  helix formed by repetitive three residue ( $\alpha\alpha\alpha$ )  $5 \rightarrow 1$  hydrogen-bonded turns can be readily expanded by

**Table 3. Torsion Angles (deg) for Helices Shown in Figures 17, 20, and 21<sup>a</sup>**

helix type ( <i>n</i> , <i>h</i> )	residue repeat	atoms in hydrogen bond ring	$\phi$	$\psi$	$\phi$	$\theta_1$	$\theta_2$	$\psi$	method <sup>b</sup>
helices with normal directionality									
$4 \rightarrow 1$									
3 <sub>10</sub> -helix (3.0, 1.8)	$\alpha\alpha$	10	-49.3	-25.7					C
C <sub>12</sub> (2.6, 2.0)	$\beta\beta$	12		-96.2	91.5			-101.6	C/T
C <sub>14</sub> (2.4, 1.8)	$\gamma\gamma$	14		-153.5	66.3	-55.7	124.9		C/T
C <sub>11</sub> (3.1, 3.6)	$\alpha\beta$	11	-62.0	-44.0	-105.0	80.0		-73.0	C/T
C <sub>12</sub> (4.3, 4.1)	$\alpha\gamma$	12	-57.0	-53.0	-126.0	59.0	57.0	-99.0	C/T
C <sub>13</sub> (2.1, 2.0)	$\beta\gamma$	13		-106.0	75.0			-115.0	C/T
				-117.0	66.0	62.0		-120.0	
$5 \rightarrow 1$									
α-helix (3.6, 1.6)	$\alpha\alpha\alpha$	13	-57.8	-47.0					C
C <sub>14</sub> (8.2, 3.9)	$\alpha\alpha\beta$	14	-61.0	-50.0	-114.0	74.0		-91.0	C
			-66.0	-48.0					
C <sub>15</sub> (9.7, 3.3)	$\alpha\beta\beta$	15	-72.0	-70.0	-101.0	71.0		-128.0	C <sup>c</sup>
				-83.0	84.0			-100.0	
helices with reversed directionality									
$1 \rightarrow 3$									
C <sub>14</sub> (3.1, 1.5)	$\beta\beta\beta$	14	-136.9	55.9				-131.1	C/T
helices with mixed directionality									
C <sub>11</sub> /C <sub>9</sub> (2.8, 4.8)	$\alpha\beta$	11 and 9	-69.5	129.6	97.9	61.7		-83.4	C/T
C <sub>12</sub> /C <sub>10</sub> (3.9, 4.3)	$\alpha\gamma$	12 and 10	-66.5	125.6	84.9	37.9	40.1	-117.8	C/T

<sup>a</sup> The torsion angles listed are for idealized helices generated based on the crystal state conformations in the case of  $\beta$ ,  $\gamma$ , and hybrid peptides. <sup>b</sup> C and T indicate crystallographic and theoretical studies, respectively. <sup>c</sup> A single hydrogen bonded turn has been determined in crystals.

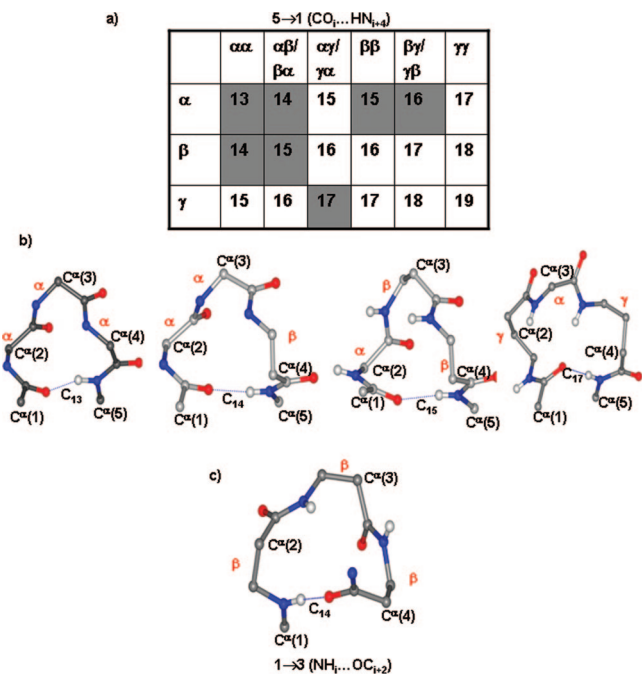


**Figure 18.** (a) Schematic diagram showing the number of atoms in the three-residue hydrogen bonded turns ( $5 \rightarrow 1$ ) in  $\alpha$ ,  $\beta$ ,  $\gamma$ , and hybrid peptides. Shaded squares correspond to turns characterized in crystal structures. (b) Examples of  $5 \rightarrow 1$  hydrogen bonded turns in hybrid peptides. A  $C_{13}$  turn of an  $\alpha$ -helix is shown for comparison. The  $\alpha\alpha\beta$   $C_{14}$  turn shown is from the crystal structure of Boc-Leu-Phe-Val-Aib- $\beta$ Phe-Leu-Phe-Val-OMe<sup>102</sup> (no. 70 in Table S1), the  $\alpha\beta\beta$   $C_{15}$  turn is observed in the peptide Boc-Val-Ala-Phe-Aib- $\beta$ Val- $\beta$ Phe-Aib-Val-Ala-Phe-Aib-OMe<sup>190</sup> (no. 60 in Table S1) and the  $\gamma\alpha\gamma$   $C_{17}$  turn is observed in the tetrapeptide Boc-Aib-Gpn-Aib-Gpn-NHMe<sup>191</sup> (no. 165 in Table S1). (c) The three residue hydrogen bond formed with reversed directionality ( $1 \rightarrow 3$ ) in  $\beta$ -peptides (14-helix).<sup>46–58</sup>

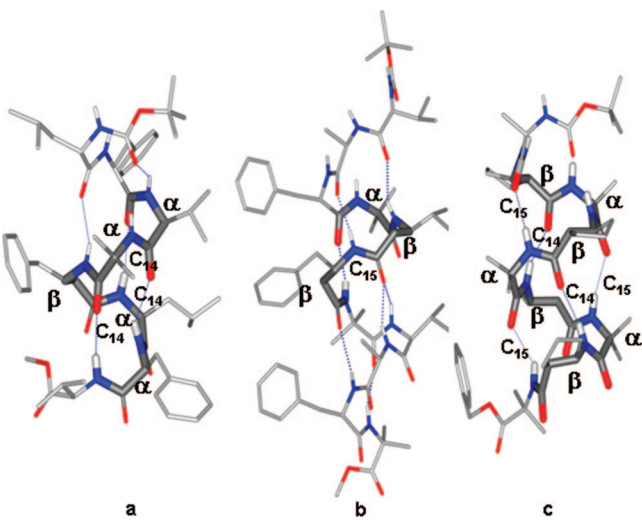


**Figure 19.** Examples of experimentally characterized  $5 \rightarrow 1$  hydrogen bonded turns in hybrid peptide helices. (a) 14 atom ( $\beta\alpha\alpha/\alpha\beta\alpha$ ) turns in Boc-Leu-Phe-Val-Aib- $\beta$ Phe-Leu-Phe-Val-OMe,<sup>102</sup> (b) 15 atom ( $\beta\beta\beta$ ) turn in Boc-Val-Ala-Phe-Aib- $\beta$ Phe-Aib-Val-Ala-Phe-Aib-OMe,<sup>190</sup> and (c) 14/15 mixed helix with alternating 14 atom ( $\alpha\beta\alpha$ ) and 15 atom ( $\beta\alpha\beta$ ) hydrogen bonds in Boc-Ala-ACPA-Aib-ACPC-Aib-ACPA-Aib-ACPC-Aib-OBn.<sup>193</sup> The backbone segment containing the  $5 \rightarrow 1$  hydrogen bonds are shown as thick lines.

insertion of  $\beta$  and  $\gamma$  residues into predominantly  $\alpha$  peptide sequences. Figure 19 illustrates three examples of crystalline hybrid peptides in which expansion of the  $C_{13}$  hydrogen

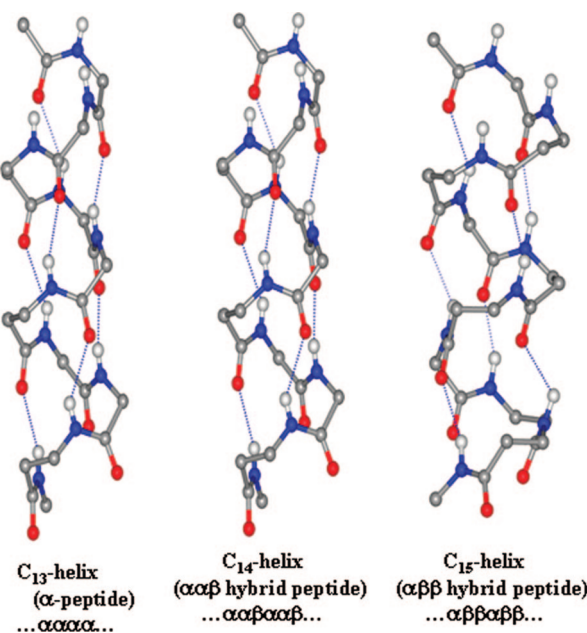


**Figure 20.** An ideal  $\alpha$ -helix and model helices with  $5 \rightarrow 1$  hydrogen bonding pattern in  $\dots\alpha\alpha\beta\alpha\alpha\beta\dots$  and  $\dots\alpha\beta\beta\alpha\beta\beta\dots$  sequences, constructed using the average values of torsion angles observed in crystals and then minimizing the resulting model in INSIGHT II to relieve any short contacts. The average values of torsion angles in the minimized models are provided in Table 3, which are used to build the final models shown in the figure.

bonded ring to 14 and 15 atoms has been realized. In the octapeptide Boc-Leu-Phe-Val-Aib- $\beta$ Phe-Leu-Phe-Val-OMe,<sup>102</sup> the central Val-Aib- $\beta$ Phe-Leu-Phe ( $\alpha\alpha\beta\alpha\alpha$ ) segment folds into a short helix stabilized by three successive  $C_{14}$  ( $5 \rightarrow 1$ ) hydrogen bonds. This example illustrates the possibility of realizing an expanded analog of the  $\alpha$  helix in an  $(\alpha\alpha\beta)_n$  sequence as shown in Figure 20. The crystal structure of the undecapeptide Boc-Val-Ala-Phe-Aib- $\beta$ Val- $\beta$ Phe-Aib-Val-Ala-Phe-Aib-OMe,<sup>190</sup> which possesses two centrally positioned contiguous  $\beta^3$  residues provides an example of a further expansion of the hydrogen bonded ring size to 15 atoms. In this peptide the central peptide segment Aib- $\beta$ Val- $\beta$ Phe-Aib reveals  $C_{15}$  hydrogen bond across a  $\alpha\beta\beta$  segment. The backbone conformation of this three residue segment may be used to generate the idealized  $C_{15}$  helix formed by continuous  $(\alpha\beta\beta)_n$  sequence as illustrated in Figure 20. The eleven residue peptide also illustrates the heterogeneity of hydrogen bonding patterns which may be encountered in hybrid sequences. The conformation of this peptide is characterized by a succession of backbone hydrogen bonds of the type  $C_{13}$  ( $\alpha\alpha\alpha$ ,  $5 \rightarrow 1$ )/ $C_{14}$  ( $\alpha\beta\beta/\beta\alpha\alpha$ ,  $5 \rightarrow 1$ )/ $C_{15}$  ( $\alpha\beta\beta$ ,  $5 \rightarrow 1$ ). An interesting example of a regular repeat of a mixed  $C_{14}/C_{15}$  hydrogen bonding pattern is provided in the crystal structure of peptide Boc-Ala-ACPC-Ala-ACPC-Ala-ACPC-Ala-ACPC-OBz (ACPC = *trans*-2-aminocyclopentanecarboxylic acid) (Figure 19c).<sup>193,194</sup>

#### 4.7. Helices with Reverse Directionality Hydrogen Bonds

In  $\alpha$  peptides and proteins, the  $3_{10}$  ( $4 \rightarrow 1$ ) and  $\alpha$  ( $5 \rightarrow 1$ ) helices have hydrogen bonds of the type  $CO(i)\cdots\text{HN}(i+n)$ , where  $n = 3, 4$ . Helices with reversal of hydrogen bond polarity of the type  $\text{NH}(i)\cdots\text{CO}(i+n)$  are not observed. Interestingly, such hydrogen bonded structures were indeed considered in a paper published by Bragg, Kendrew, and

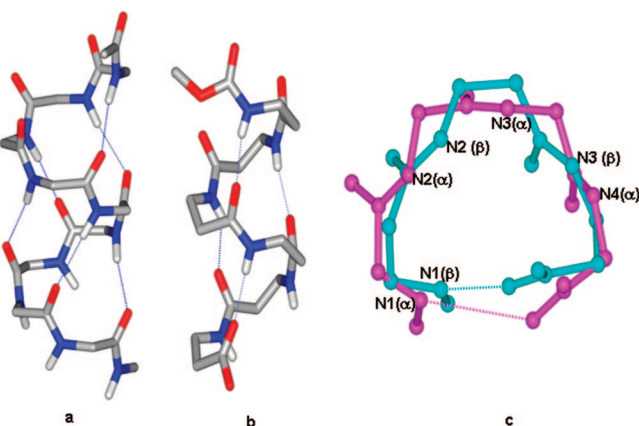


**Figure 21.** Helices with reversed hydrogen bond directionality. (a) A model of the  $\alpha$ -peptide 4.3<sub>14</sub> helix ( $\delta$ -helix) proposed by Chandrasekaran et al., for the N-terminus of the Lac repressor protein ( $\phi = -98^\circ$ ,  $\psi = -80^\circ$ ,  $\omega = 170^\circ$ ).<sup>195</sup> (b) Backbone of the  $\beta$ -peptide 14-helix Boc-(ACHC)<sub>6</sub>-OBn.<sup>46</sup> (c) Superposition of the  $\alpha\alpha\alpha\alpha$  C<sub>14</sub> hydrogen-bonded ring with the  $\beta\beta\beta$  C<sub>14</sub> hydrogen-bonded ring (rmsd = 0.75 Å).

Perutz<sup>31</sup> in 1950, before Pauling advanced the structure of the  $\alpha$  helix.<sup>32,128</sup> A helix with reversed hydrogen bond directionality was also considered for a short segment at the N-terminus of lac-repressor, to explain the NMR observations.<sup>195</sup> This structure, called the  $\delta$  helix, described in 1979 has acceptable stereochemistry and has hydrogen bonds of the type NH(*i*) $\cdots$ CO(*i* + 3) (C<sub>14</sub>, 1 $\rightarrow$ 4). The idealized  $\delta$  helix for an  $(\alpha)_n$  sequence, shown in Figure 21, was not observed when the crystal structure of the lac-repressor was determined in 1996.<sup>196</sup> The first example of a crystallographically characterized peptide helix with reversed hydrogen bond directionality was the structure of the oligo  $\beta$  peptide determined by Gellman and co-workers in 1996 (C<sub>14</sub>, 1 $\rightarrow$ 3) (no. 126 in Table S1) (Figure 21b).<sup>46</sup> The superposition of the C<sub>14</sub> hydrogen bonded rings formed in the  $\beta_n$  peptide and the proposed  $\delta$  helix in the  $\alpha_n$  sequence reveals an rmsd of 0.75 Å for a superposition of 13 atoms in the hydrogen bonded ring, suggesting an overall similarity between the two structures.

In  $\beta_n$  sequences, two types of helices C<sub>12</sub> (4 $\rightarrow$ 1)<sup>49</sup> and C<sub>14</sub> (1 $\rightarrow$ 3)<sup>46</sup> were originally characterized. While the former is an expanded analog of the 3<sub>10</sub> helix, the latter does not have well characterized precedent in the  $\alpha$  peptide structures. Interestingly, recent studies on large, designed all  $\beta$  sequences have yielded well characterized examples of C<sub>14</sub> helices,<sup>197,198</sup> suggesting that this structure may indeed be favored for  $\beta$  peptides. This has been dealt in detail later in the text under the subheading Revisiting Hydrogen-Bonded Rings in Peptide Helices. Notably, the value of the C <sup>$\alpha$</sup> –C <sup>$\beta$</sup>  torsion angle is  $\theta \approx 60^\circ$  in the C<sub>14</sub> helix and  $\sim 90^\circ$  in the C<sub>12</sub> helix.

## 5. Helices with Alternate Hydrogen Bond Directionalities

The crystal structure of the tetrapeptide Boc-Leu-Gpn-Leu-Aib-OMe,<sup>101</sup> which contains an  $\alpha\gamma\alpha$  sequence, reveals two consecutive hydrogen bonded turns with opposite directionality (Figure 22a). The observed C<sub>12</sub> (4 $\rightarrow$ 1)/C<sub>10</sub> (1 $\rightarrow$ 2) hydrogen-bonding pattern may be repeated to generate the mixed 12/10 helix for an  $(\alpha\gamma)_n$  series (Figure 22c).<sup>101</sup> In this structure, the  $\alpha$  residue adopts a polyproline (P<sup>II</sup>) conformation. The mixed 12/10 helix presents an interesting issue in

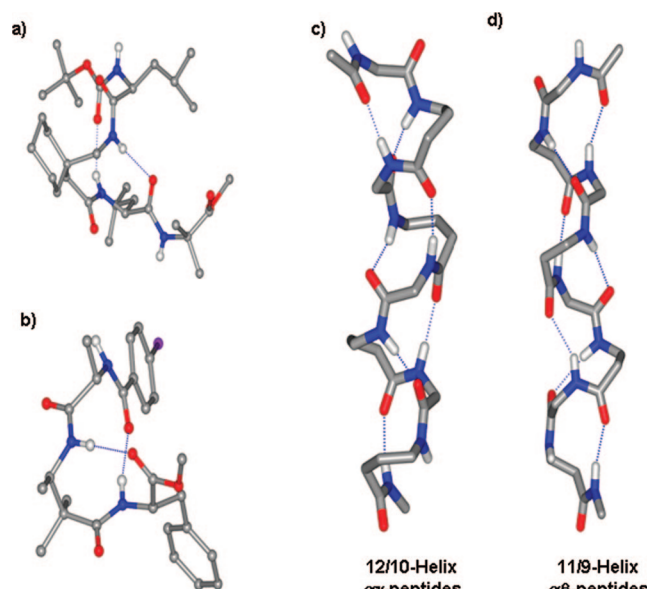


**Figure 22.** Helices with alternating hydrogen bond directionalities. (a) An  $\alpha\gamma$  hybrid peptide, Boc-Leu-Gpn-Leu-Aib-OMe<sup>101</sup> (no. 166 in Table S1) in which an  $\alpha\gamma$  C<sub>12</sub> hydrogen bond in the normal direction is followed by a  $\gamma\alpha$  C<sub>10</sub> hydrogen bond in the reverse direction. (b) Molecular conformation of a protected tripeptide, iodobenzoyl-Ala- $\alpha,\alpha$ -dimethyl-D- $\beta$ -homoalanine-Phe-OMe<sup>92</sup> (no. 89 in Table S1), with alternating  $\alpha$  and  $\beta$  residues, featuring consecutive C<sub>11</sub> ( $\alpha\beta$ , normal hydrogen bond direction) and C<sub>9</sub> ( $\beta\alpha$ , reversed hydrogen bond direction) turns in crystals. (c, d) Models of C<sub>12</sub>/C<sub>10</sub> and C<sub>11</sub>/C<sub>9</sub> helices with alternating hydrogen bond directionalities in  $\alpha\gamma$  and  $\alpha\beta$  hybrid peptides, respectively.

the description of helical structures. When considered in terms of repetition of torsion angles, the C<sub>12</sub> turn formed by the  $\alpha\gamma$  unit can be repeated to generate the 12/10 helix. However, the helix so generated consists of a mixed hydrogen bonding pattern with the result that if the hydrogen bonding scheme is viewed as a repeat motif, then the elementary unit would be an  $\alpha\gamma\alpha$  segment. In the earlier section of this review, we have classified this  $\alpha\gamma$  C<sub>12</sub> turn as a *nonhelical turn* to signify that the repetition of this unit does not yield a continuous C<sub>12</sub> helix stabilized by 12 atom hydrogen bonded rings.<sup>101</sup>

A recent report describes crystal structures of model peptides containing the trisubstituted  $\beta$  residues,  $\alpha,\alpha$ -dimethyl-D- $\beta$ -homoalanine,  $\alpha,\alpha$ -dimethyl-D- $\beta$ -homo phenylalanine,  $\alpha,\alpha$ -dimethyl-D- $\beta$ -homoleucine, and their L-enantiomers.<sup>92</sup> Although the authors do not comment on the folded structures obtained, these examples provide novel intramolecular hydrogen bonding pattern. The molecular conformation in crystals of the two  $\alpha\beta\alpha$  peptides containing these trisubstituted residues reveals two consecutive hydrogen bonded turns of the C<sub>11</sub> type ( $\alpha\beta$ , 4 $\rightarrow$ 1, normal direction) and C<sub>9</sub> type ( $\beta\alpha$ , 1 $\rightarrow$ 2, reverse direction) (Figure 22b).<sup>92</sup> This C<sub>11</sub>/C<sub>9</sub> consecutive turn structure can be repeated to generate the 11/9 helix with mixed hydrogen bond directionality in  $(\alpha\beta)_n$  sequences (Figure 22d). In this case also the  $\alpha$  residue adopts a P<sup>II</sup> conformation while the C<sub>11</sub>  $\alpha\beta$  turn may be characterized as a *nonhelical* turn since a repetitive C<sub>11</sub> structure cannot be generated.

Helices with mixed hydrogen bond directionalities have also been proposed in solution from NMR studies of oligo- $\beta$  peptides in which  $\beta^2$  and  $\beta^3$  residues alternate along the sequence.<sup>27,199–201</sup> Studies of the peptide Boc- $\beta^2$ Val- $\beta^3$ Ala- $\beta^2$ Lys- $\beta^3$ Val- $\beta^2$ Ala- $\beta^3$ Lys-OBn suggests a mixed 10/12 helix in solution.<sup>201</sup>

## 6. $\omega$ Amino Acids in Hairpins

### 6.1. Insertion into Turn Segments

In  $\alpha$  peptides and proteins, short polypeptide segments that form chain reversals facilitate registry of antiparallel strands stabilized by cross strand hydrogen bonds.  $\beta$  hairpin structures formed using tight two residue turns are commonly formed in proteins.<sup>202</sup> In the case of two residue  $\alpha\alpha$  segments, hairpins are nucleated by type I' and II' (prime) turns, a feature recognized by an analysis of protein structures by Thornton and co-workers.<sup>130</sup> The use of *prime turns* in the design of synthetic  $\beta$  hairpins and multistranded  $\beta$  sheets has relied on the use of <sup>D</sup>Pro-Xxx segments for facilitating type I'/II' turn formation<sup>19,93,203–217</sup> and to a lesser extent on the use of Asn-Gly segments.<sup>217–224</sup> The prime turns require positive  $\phi$  values at the residue ( $i + 1$ ) (type I'/II':  $\phi_{(i+1)} = 60^\circ$ ); conformations which can be readily achieved with D-amino acids or achiral residues. Among the L-amino acids, Asn has the greatest propensity to adopt the positive  $\phi$  values.<sup>93,225</sup> As in the case of  $\alpha\alpha$  segments, hybrid dipeptide segments containing backbone homologated residues can also form a variety of  $4 \rightarrow 1$  hydrogen bonded turns. Here also, turns may be classified into those that can be repeated to generate helices as described in the previous section or promote chain reversal with the possibility of generating

hairpin structures. Figure 23 shows examples of three crystalline  $\beta$ -hairpins, in which  $\beta$ ,  $\gamma$ , and  $\delta$  residues are present in the turn segment. In the case of the tetrapeptide containing a central  $\beta\beta$  segment composed of (*R*)-Nip-(*S*)-Nip (Nip = Nipecotic acid), nascent hairpin formation is observed with two cross-strand hydrogen bonds.<sup>109</sup> The nipecotic acid residue is constrained by cyclization to adopt  $\theta \approx 180^\circ$ . This  $4 \rightarrow 1$  C<sub>12</sub> hydrogen bonded turn ( $\phi_{(i+1)} = 115.6^\circ$ ,  $\theta_{(i+1)} = -175.2^\circ$ ,  $\psi_{(i+1)} = 81.7^\circ$ ;  $\phi_{(i+2)} = -117.4^\circ$ ,  $\theta_{(i+2)} = -176.6^\circ$ ,  $\psi_{(i+2)} = -71.2^\circ$ ) is distinct from the C<sub>12</sub>  $\beta\beta$  turns, which occurs in the repetitive C<sub>12</sub> helical structures.<sup>49</sup> Notably, the linking peptide unit between the residues at ( $i + 1$ ) and ( $i + 2$ ) positions adopts a cis geometry ( $\omega \approx 0^\circ$ ). This  $\beta\beta$  C<sub>12</sub> hydrogen bonded turn can be considered as a backbone expanded analog of the type VI  $\beta$  turn in  $\alpha\alpha$  sequences.<sup>2</sup> In the case of  $\gamma$  peptides, no crystal structures are available for  $\beta$ -hairpins with  $\gamma\gamma$  turns. However, an N-acyl- $\gamma$ -dipeptide amide, reveals a 14-atom hydrogen bond in crystals, with distinctly different backbone torsion angles from the helical C<sub>14</sub> hydrogen bond.<sup>226</sup> This can be considered as a  $\gamma$  analogue of the type II  $\beta$ -turns formed by  $\alpha$  peptides (see Figure 15). Hairpin nucleation by centrally positioned  $\alpha\gamma$  (Aib-Gpn)<sup>103</sup> and  $\alpha\delta$  (<sup>D</sup>Pro- $\delta$ Ava)<sup>121</sup> segments are also demonstrated in the synthetic octapeptides Boc-Leu-Phe-Val-Aib-Gpn-Leu-Phe-Val-OMe<sup>103</sup> and Boc-Leu-Val-Val-<sup>D</sup>Pro- $\delta$ Ava-Leu-Val-

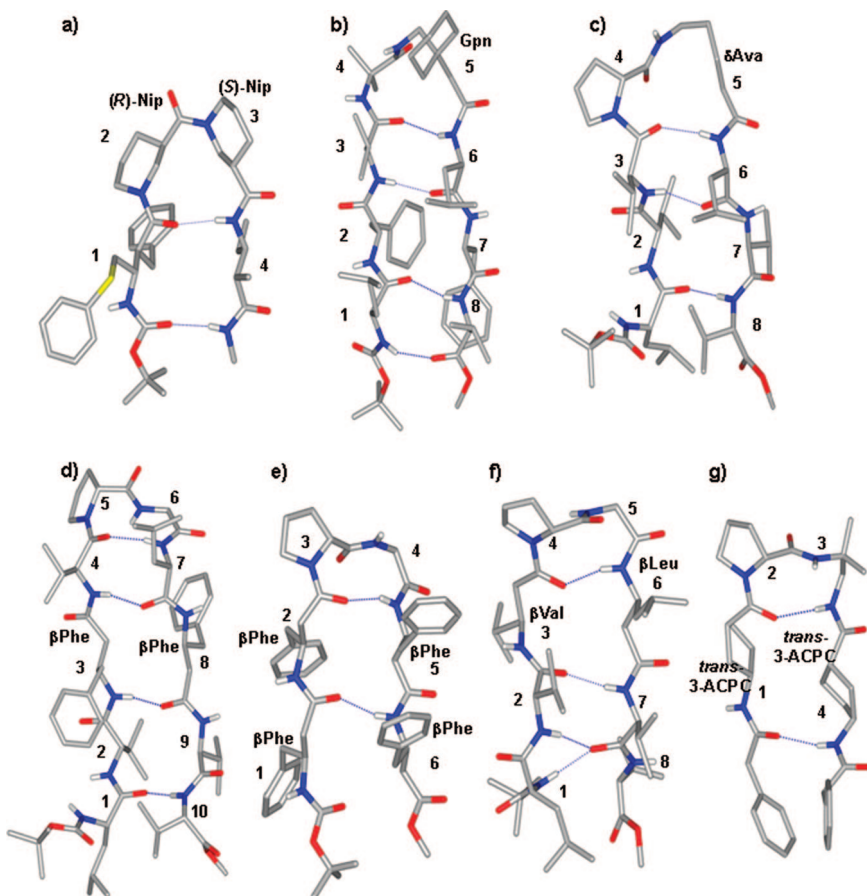


**Figure 23.** Examples of  $\beta$  and  $\gamma$  residues in the turn and strand regions of peptide  $\beta$ -hairpins. (a) The hairpin structures of a  $\beta$ -peptide, with (*R*)-nipecotic acid and (*S*)-nipecotic acid residues in the turn segment<sup>108</sup> (no. 74 in Table S1). This peptide also has vicinally disubstituted  $\beta$ -residues as the strand residues. (b) An octapeptide  $\beta$ -hairpin with a Gpn residue at the ( $i + 2$ ) position of the backbone expanded  $\beta$ -turn, in Boc-Leu-Phe-Val-Aib-Gpn-Leu-Phe-Val-OMe<sup>103</sup> (no. 170 in Table S1) (c) The unsubstituted  $\delta$ -amino acid ( $\delta$ Ava) at the ( $i + 2$ ) position of the octapeptide hairpin Boc-Leu-Val-Val-<sup>D</sup>Pro- $\delta$ Ava-Leu-Val-Val-OMe<sup>121</sup> (bottom) Examples of  $\beta$  and  $\gamma$  residues in the strand region of  $\beta$ -hairpins. (d) Boc-Leu-Val- $\beta$ Phe-Val-<sup>D</sup>Pro-Gly-Leu- $\beta$ Phe-Val-Val-OMe<sup>207</sup> (no. 72 in Table S1), (e) Boc- $\beta$ Phe- $\beta$ Phe-<sup>D</sup>Pro-Gly- $\beta$ Phe- $\beta$ Phe-OMe<sup>208</sup> (no. 69 in Table S1), (f) Boc-Leu-Val- $\beta$ Val-Val-<sup>D</sup>Pro-Gly- $\beta$ Leu-Val-OMe<sup>209</sup> (no. 59, Table S1), and (g) PhCH<sub>2</sub>-trans-3-ACPC-<sup>D</sup>Pro-((1,1-dimethyl)-1,2-diaminoethyl)-trans-3-ACPC-OtBu<sup>230</sup> (no. 138 in Table S1). The residue numbers and the  $\omega$ -residues are marked in each example.

Val-OMe.<sup>121</sup> In these cases, the strand registry is determined by four and three cross strand hydrogen bonds, respectively. The C<sub>13</sub> hydrogen bond in the  $\alpha\delta$  turn can be considered as formally equivalent to a hairpin nucleating three residue  $\alpha\alpha\alpha$  segment. Such hairpins with centrally positioned three residue turns have been characterized in solution by NMR studies of designed  $\alpha$  peptide sequences.<sup>227</sup>

## 6.2. Extended Strands

The accommodation of  $\omega$  amino acids in extended strand structures is favored when the backbone torsion angles adopt values close to 180° (trans conformation). The homologation of the backbone of extended strands in designed peptide  $\beta$  hairpins has been demonstrated in several peptide crystal structures.<sup>108,120,207–209</sup> Figure 23 provides representative examples. Strand registry can be achieved by placing the  $\omega$  amino acids in facing positions across the antiparallel chains. The structure of the decapeptide Boc-Leu-Val- $\beta$ Phe-Val-<sup>D</sup>Pro-Gly-Leu- $\beta$ Phe-Val-Val-OMe<sup>207</sup> (Figure 23d), provides a good example of facing  $\beta$ Phe residues across antiparallel strands. In this case, the  $\beta$  residue was inserted at a position which corresponds to the non-hydrogen bonded segment in the hairpins. The structure of the  $\beta$  hairpin hexapeptide Boc- $\beta$ Phe- $\beta$ Phe-<sup>D</sup>Pro-Gly- $\beta$ Phe- $\beta$ Phe-OMe (Figure 23e)<sup>209</sup> illustrates a feature of the extended strands composed of linked  $\beta$  residues. In this case, polar strands are formed in which one face presents acceptor CO groups, while the other face presents donor NH groups. Inspection of the hairpin reveals that the cross-strand hydrogen bonds are formed by interaction between antiparallel strands of opposite polarity. Polar sheet formation<sup>228–230</sup> is a property of  $\omega$  amino acids with an even number of backbone atoms between the NH and CO groups. In the case of  $\omega$  amino acids, cross strand hydrogen bonding patterns across the hairpin can be maintained even in the case of conformations, which accommodate gauche values for one of the torsion angles.<sup>229</sup> The structure of the octapeptide Boc-Leu-Val- $\beta$ Val-<sup>D</sup>Pro-Gly- $\beta$ Leu-Val-Val-OMe<sup>207</sup> (Figure 23f) provides an example of the accommodation of a gauche conformation ( $\theta \approx 65^\circ$ ) at the  $\beta$ Val(3) residue. A cross strand hydrogen bonding pattern is preserved despite the backbone distortion. A similar example in the case of  $\gamma$  residues is observed in the decapeptide Boc-Leu-Val- $\gamma$ Abu-Val-<sup>D</sup>Pro-Gly-Leu- $\gamma$ Abu-Val-Val-OMe (Figure 7),<sup>120</sup> where the  $\gamma$  residue adopts a  $\theta_2$  value of  $-65^\circ$ , without disruption of the hydrogen bonds involving the peptide units which flank the facing  $\gamma$  residues at the positions 3 and 8. The accommodation of gauche conformations in facing pairs of  $\beta\beta$  and  $\gamma\gamma$  residues across antiparallel strands is illustrated in Figure 24. Good hydrogen

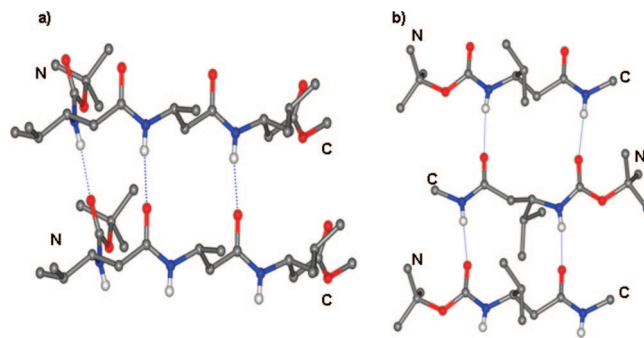


**Figure 25.** Examples of parallel and antiparallel sheet formation in short  $\beta$ -peptides: (a) parallel sheet<sup>229</sup> and (b) antiparallel sheet.<sup>228</sup>

bond geometries are possible despite the local distortion in extended strands. Constrained  $\gamma$  amino acids can also be incorporated into the strands, with the example of *trans*-3-ACPC (*trans*-3-aminocyclopentane carboxylic acid),<sup>230</sup> illustrated in Figure 23g. In this residue, the geometry of the 1,3-disubstituted cyclopentane ring results in an appropriately extended arrangement of the backbone atoms. The structure of the molecule shown in Figure 23g has a parallel strand arrangement generated by the use of a (1,1-dimethyl)-1,2-diaminoethyl unit at the ( $i + 2$ ) position of the nucleating turn.<sup>230</sup> Examples of both polar and apolar sheet formation has been demonstrated in the crystal structures of several short acyclic  $\omega$  amino acid containing peptides (Figure 25).<sup>229,231</sup>

## 7. Conformational Representations

Discussions of the backbone folding patterns of  $\alpha$  polypeptides and proteins have been greatly simplified by the use of the two-dimensional Ramachandran map.<sup>11,12</sup> In the Ramachandran representation, the two backbone torsion variables  $\phi$  (N-C $^{\alpha}$ ) and  $\psi$  (C $^{\alpha}$ -CO) define a two-dimensional conformational space. The use of dihedral angles permits reduction of an analytical problem in three dimensions to a problem in two-dimensional space. The peptide bonds flanking a given residue are restricted to the trans conformation ( $\omega \approx 180^\circ$ ), a feature overwhelmingly present in peptides and proteins. The  $\phi$ - $\psi$  space can then be partitioned into stereochemically allowed and disallowed regions using the elementary principles of hard sphere contacts between atoms. Each residue in a polypeptide chain is then represented as a point in two-dimensional  $\phi$ - $\psi$  space. Regular structures like the  $\alpha$  helix ( $\phi = -57^\circ$ ,  $\psi = -47^\circ$ ),  $\beta$  sheet ( $\phi \approx -120^\circ$  to  $140^\circ$ ,  $\psi \approx 113^\circ$  to  $135^\circ$ ), and polyproline P<sub>II</sub> ( $\phi = -78^\circ$ ,  $\psi = 149^\circ$ ) conformations are formed by successive residues which cluster in a limited domain of  $\phi$ - $\psi$  space. Ramachandran  $\phi$ - $\psi$  space has provided an important conceptual basis for the understanding of polypeptide chain folding. The original hard sphere approach, which uses van der Waals contact limits between atoms as a steric filter, have been replaced by conformational energy calculations using semiempirical force fields. Experimental observations from protein structures establish that the contours of the hard sphere map are largely in agreement with experimentally observed  $\phi$ - $\psi$  distribution.<sup>13,14</sup> In the case of backbone homologated  $\omega$  amino acids, the introduction of additional torsional variables (Figure 3) adds a further dimension of complexity to the problems of representing observed conformations. The growing body of crystallographically determined backbone conformations in synthetic peptides

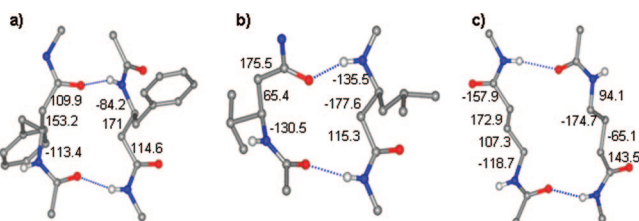


**Figure 24.** Examples of  $\beta$  and  $\gamma$  residues with gauche and trans conformations about the C-C bonds accommodated in the strand segment of hairpins. (a) Boc- $\beta$ Phe- **$\beta$ Phe**-<sup>D</sup>Pro-Gly- **$\beta$ Phe**- $\beta$ Phe-OMe,<sup>208</sup> (b) Boc-Leu-Val- **$\beta$ Val**-<sup>D</sup>Pro-Gly- **$\beta$ Leu**-Val-Val-OMe,<sup>209</sup> and (c) Boc-Leu-Val- $\gamma$ Abu-Val-<sup>D</sup>Pro-Gly-Leu- $\gamma$ Abu-Val-Val-OMe.<sup>120</sup> The residues highlighted in bold letters are shown in the figure.

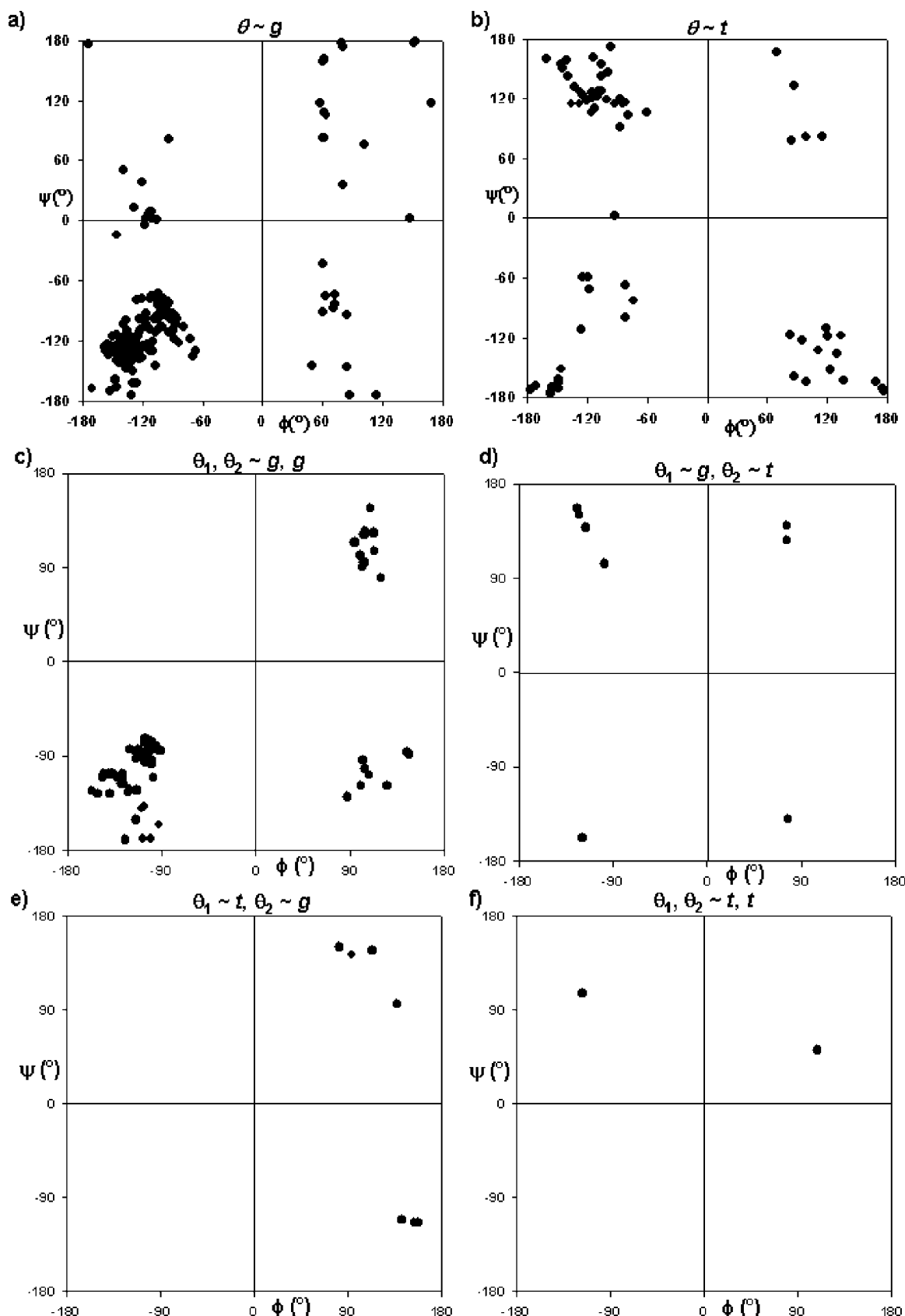


**Figure 26.** Scatter plots showing the distribution of  $\phi$ ,  $\psi$  values in crystallographically characterized  $\beta$  and  $\gamma$  residues. (a) Plot for  $\beta$ -residues with  $\theta \approx +60^\circ$  and (b) plot for  $\beta$ -residues with  $\theta \approx 180^\circ$ . (c, d, e, f) Plots for  $\gamma$ -residues with  $\theta_1, \theta_2 \approx +60^\circ$ ;  $\theta_1 \approx +60^\circ$  and  $\theta_2 \approx 180^\circ$ ;  $\theta_1 \approx 180^\circ$  and  $\theta_2 \approx +60^\circ$ ;  $\theta_1, \theta_2 \approx 180^\circ$ , respectively. The values plotted are provided in Table S1 of Supporting Information.

containing  $\omega$  amino acids suggests, that folded structures invariably require gauche conformations about the additional rotatable bonds. It is therefore useful to separate representations of the experimental data for  $\beta$  and  $\gamma$  residues into  $\phi$ ,  $\psi$

scatter plots for specific conformations (gauche (g), trans (t)) for the additional degrees of freedom. Figure 26 illustrates  $\phi$ ,  $\psi$  scatter plots that show the distribution of crystallographically characterized conformations for  $\beta$  and  $\gamma$  residues.

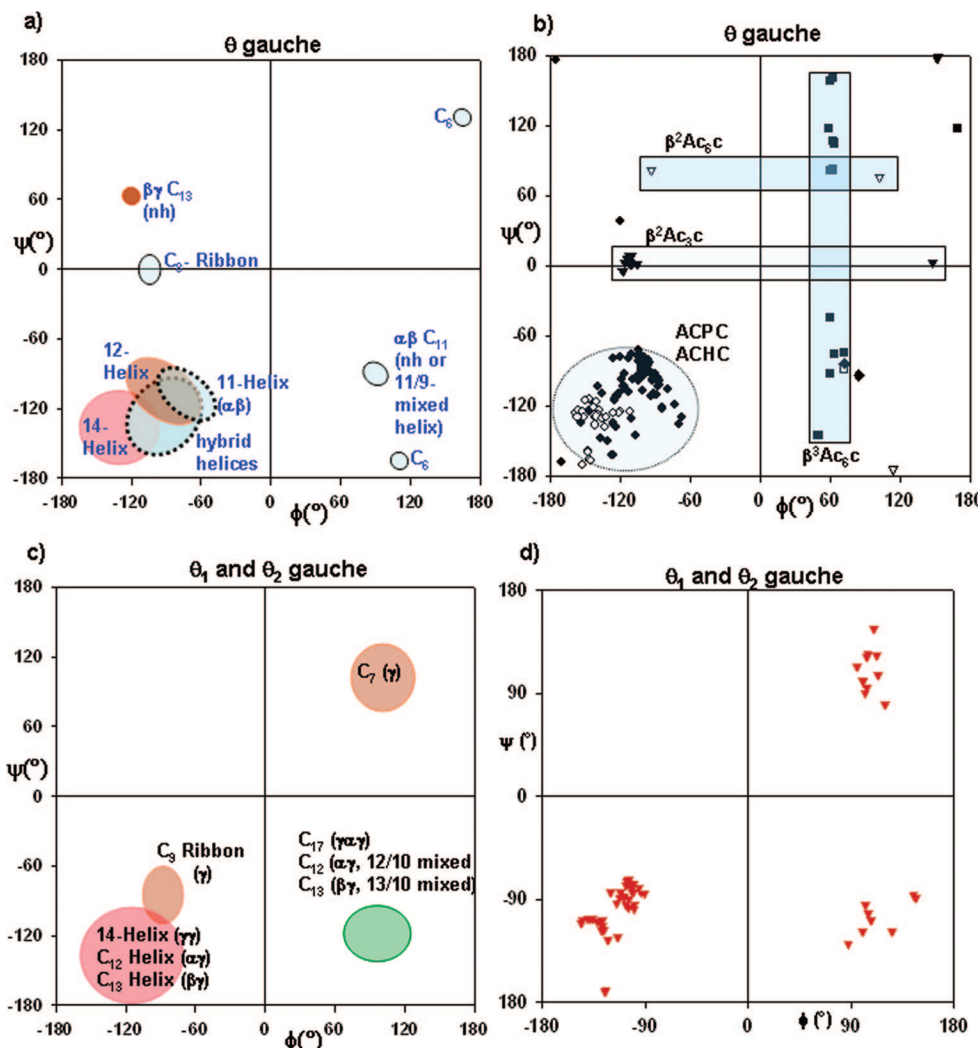


**Figure 27.** Conformational space representation. Specific regions where the regular secondary structures of  $\beta$ ,  $\gamma$ , and hybrid peptides are observed in the  $\phi$ - $\psi$  space of  $\beta$ - and  $\gamma$ -residues. (a)  $\beta$ -residues with  $\theta$  in *gauche* conformation, observed in all the helical structures and hybrid nonhelical turns. (b) Comparison of the conformational space for cyclic constrained  $\beta$ -residues ACPC, ACHC which populate the helical conformations, with geminally disubstituted  $\beta^{2,2}\text{Ac}_6\text{c}$  and  $\beta^{3,3}\text{Ac}_6\text{c}$  residues. (c) Conformational space for  $\gamma$ -residues with both  $\theta_1$  and  $\theta_2$  adopting *gauche* conformation, observed in helix and ribbon structures of  $\gamma$ -peptides and hybrid peptides. (d) Scatter plot for the experimentally observed conformations of Gpn residue, with  $\theta_1 \approx \theta_2 \approx 60^\circ$ .<sup>105</sup>

The experimental data consists of both multiply substituted, constrained residues and unsubstituted, unconstrained residues. In comparison to the  $\alpha$  amino acid residues, there is only limited data available for  $\omega$  amino acid residues. The explosive growth of protein crystal structures has provided a wealth of information on the backbone conformational preferences of the genetically coded amino acids. In contrast, conformational information on the noncoded amino acids must largely be derived from studies of synthetic peptides. The accumulated data on  $\beta$  and  $\gamma$  residues is thus biased by the nature of residues chosen in the studies of model peptides. It is clearly observed that the majority of the crystal structure observations correspond to *gauche* (*g*) conformations about the  $\text{C}^\alpha-\text{C}^\beta$  ( $\theta$ ) bond in  $\beta$  residues and a *gauche-gauche* (*gg*) conformation about the  $\text{C}^\gamma-\text{C}^\beta$  ( $\theta_1$ ) and  $\text{C}^\beta-\text{C}^\alpha$  ( $\theta_2$ ) bonds in  $\gamma$  residues. Figure 27a and c provides  $\phi$ ,  $\psi$  representations for all the observed hydrogen bonded turns and helices in oligo  $\beta$  and  $\gamma$  peptides and in hybrid peptides containing  $\alpha$ ,  $\beta$ , and  $\gamma$  residues. It is once again evident that turn formation, stabilized by intramolecular hydrogen bonds are largely observed where the additional torsional angles are localized in *gauche* conformations.

## 7.1. Conformationally Constrained Residues

The design of folded structures (foldamers)<sup>21,22,24,27,59</sup> containing  $\omega$  amino acid residues is facilitated by the use of stereochemically constrained amino acids. Conformational constraints on backbone torsional freedom can be introduced by substitution and backbone-side chain cyclization (Figure 4). Figure 27b summarizes the observed conformational distribution for constrained  $\beta$  residues. ACHC (*trans*-2-aminocyclohexane carboxylic acid)<sup>46</sup> and ACPC (*trans*-2-aminocyclopentane carboxylic acid)<sup>49</sup> provide examples of the covalent restriction on the dihedral angle  $\theta$ , while the  $\beta^{2,2}\text{Ac}_6\text{c}$  (1-aminomethylcyclopropane carboxylic acid),<sup>97</sup>  $\beta^{2,2}\text{Ac}_6\text{c}$  (1-aminomethylcyclohexane carboxylic acid),<sup>98</sup> and  $\beta^{3,3}\text{Ac}_6\text{c}$  (1-aminocyclohexane acetic acid)<sup>142</sup> are examples where gem dialkyl substitution limits the flanking torsional variables. A comparison of Figure 27a and b reveals that the amino acids ACPC and ACHC largely supports helical conformations and can also be readily accommodated into hybrid helical structures. In contrast, the  $\beta^{3,3}\text{Ac}_6\text{c}$  residue is almost entirely restricted to nonhelical conformations.<sup>142</sup> For  $\gamma$  residues, the most extensively used residue is gabapentin

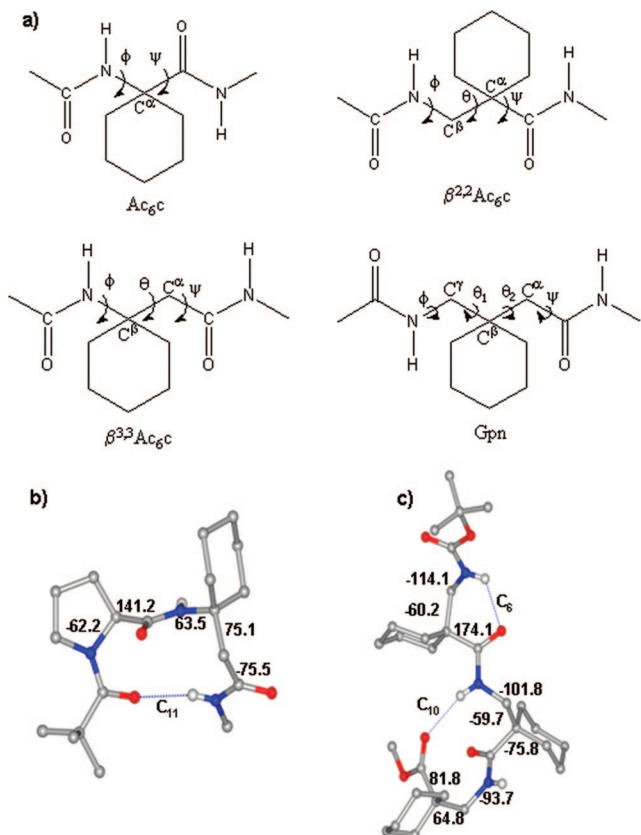


**Figure 28.** (a) Stereochemically restricted C<sup>α,α</sup>-dialkylated α-residue Ac<sub>6</sub>c (1-amino cyclohexane-1-carboxylic acid) and its backbone homologated analogs β<sup>2,2</sup>Ac<sub>6</sub>c, β<sup>3,3</sup>Ac<sub>6</sub>c and Gpn. (b) Molecular conformation of the dipeptide Piv-Pro-β<sup>3,3</sup>Ac<sub>6</sub>c-NHMe<sup>121</sup> (no. 48, Table S1) in crystals, in which the β-residue is involved in an αβ nonhelical C<sub>11</sub> hydrogen bond. (c) Molecular conformation of the tripeptide Boc-β<sup>2,2</sup>Ac<sub>6</sub>c-β<sup>2,2</sup>Ac<sub>6</sub>c-β<sup>2,2</sup>Ac<sub>6</sub>c-OMe<sup>97</sup> (no. 40 in Table S1), which has a C<sub>6</sub> hydrogen bond at β<sup>2,2</sup>Ac<sub>6</sub>c (1) and a nonhelical ββ C<sub>10</sub> hydrogen bond with reversed directionality, at the β<sup>2,2</sup>Ac<sub>6</sub>c (2)-β<sup>2,2</sup>Ac<sub>6</sub>c (3) segment. The backbone dihedral angles are marked.

(Gpn).<sup>99–107</sup> Figure 27d summarizes the observed conformational distribution of Gpn peptides, in  $\phi$ – $\psi$  space, with  $\theta_1 \approx \theta_2 \approx 60^\circ$ .<sup>105,106</sup> Only one example of a Gpn residue adopting a gt conformation for  $\theta_1$ ,  $\theta_2$  is observed in crystals of the octapeptide Boc-Leu-Phe-Val-Aib-Gpn-Leu-Phe-Val-OMe (Figures 5 and 23).<sup>103</sup>

The presence of gem dialkyl substituents on a carbon atom results in a restriction of the flanking torsional angles. In the case of α residues, α aminoisobutyric acid (Aib) has been the most widely investigated residue. A large number of experimental and theoretical studies have established that Aib is almost exclusively constrained to the right- and left-handed helical regions of  $\phi$ – $\psi$  space,<sup>17,93–96</sup> with a very few exceptions, most of which are observed in short peptides.<sup>232–234</sup> The related residue 1-aminocyclohexane-1-carboxylic acid Ac<sub>6</sub>c, has been shown to almost exclusively favor local helical conformations ( $\phi = \pm 60^\circ$ ,  $\psi = 30 \pm 5^\circ$ ).<sup>235–240</sup> Figure 28 illustrates the structure of β and γ residues that can be formally considered as Ac<sub>6</sub>c analogs, all of which are achiral. Of these, the γ amino acid residue gabapentin (Gpn) is readily available as a bulk drug, while both β<sup>2,2</sup>Ac<sub>6</sub>c and β<sup>3,3</sup>Ac<sub>6</sub>c are accessible synthetically. A large number of crystallographic examples of short peptides containing β<sup>3,3</sup>Ac<sub>6</sub>c reveal a limited range of  $\phi$ ,  $\psi$  values as shown in Figure 27b.<sup>142</sup> These conformations do not lie in the regions that support helical folding in hybrid sequences. Interestingly,

the only example of a 4 → 1 hydrogen-bonded conformation involving β<sup>3,3</sup>Ac<sub>6</sub>c is in the peptide Piv-Pro-β<sup>3,3</sup>Ac<sub>6</sub>c-NHMe (Figure 28b).<sup>121</sup> This conformation may be formally considered as an αβ expanded analog of the conventional αα type II β-turn and may be classified as a *nonhelical* turn. The structure of the tetrapeptide Boc-(β<sup>2,2</sup>Ac<sub>6</sub>c)<sub>3</sub>-OMe reveals a reverse directionality 1 → 2 (C<sub>10</sub>) hydrogen bond and also the C<sub>6</sub> hydrogen bonded conformation of an isolated β residue (Figure 28c).<sup>98</sup> As shown in the Figure 27d, the Gpn residue is an excellent building block for the design of folded peptides with hybrid backbones. In the Gpn residue, geminal disubstitution at the β carbon atom, limits the flanking torsion angles  $\theta_1$  and  $\theta_2$  almost exclusively to gauche conformations (Figure 5).<sup>105,106</sup> A fully extended conformation results in steric overlap between methylene groups and backbone atoms, while for the axial substituents, a θ value of 180° results in unfavorable 1–3 diaxial interactions.<sup>106</sup> Conformational energy calculations using semiempirical force fields establish that Gpn residues can be accommodated in a relatively limited region of conformational space.<sup>105,106</sup> In the design of folded hybrid peptides, the use of stereochemically constrained ω amino acids permits a biasing of the local conformational choices along the polypeptide backbone. The area of hybrid peptides must undoubtedly benefit from the explosive development of synthetic methodologies directed toward preparation of a wide variety of substituted β and γ amino acids together with methodologies for backbone homologation at the C-terminus residues of α peptides.<sup>63–92</sup>

The design of hybrid helices, which are backbone expanded analogs of the canonical helices formed by α polypeptides, is aided by the availability of amino acid residues, which preferentially favor backbone torsion angles that lie in the *helical* region of conformational space. Figure 29 provides a representation that enables an understanding of the relationship between the helical conformation of α, β, and γ residues. In the conformational diagram shown in Figure 29, the αβ/βα helical turn is represented as a double edged arrow. This corresponds to a repetition of the torsion angles in an (αβ)<sub>n</sub> sequence resulting in the generation of a 4 → 1 hydrogen bonded C<sub>11</sub> helix, which is the backbone expanded analog of the C<sub>10</sub> helix in all α sequences (see also Figures 16a and 17). Similarly the αγ/γα C<sub>12</sub> helix and the βγ/βα C<sub>13</sub> helix are also represented on the diagram (see Figures 16b, c and 17). Inspection of Figure 29 suggests the possibility of designing hybrid helices that contain α, β, and γ residues such that several variations of the hydrogen bonded rings may be generated. For example, an –αβγαβγ– sequence could result in a C<sub>11</sub>/C<sub>13</sub>/C<sub>12</sub>/C<sub>11</sub>/C<sub>13</sub> hydrogen bonding pattern. An –αββγαβ– pattern would give a C<sub>11</sub>/C<sub>12</sub>/C<sub>13</sub>/C<sub>12</sub>/C<sub>11</sub> hydrogen bonding patterns. The ability to systematically vary the number of atoms in hydrogen bonded helical turns may be used to modify spatial relationships between projecting side chains on a helical scaffold. The use of α, β, and γ residues in conjunction with functional side chains may be of significance in the design of analogs of biologically active α peptide sequences. The construction of large structures composed of homologated amino acids has progressed rapidly in the area of all β peptides and hybrid αβ sequences. The Schepartz group has reported the crystal structures of β dodecapeptides (H<sub>2</sub>N-β<sup>3</sup>Glu-β<sup>3</sup>Leu-β<sup>3</sup>Orn-β<sup>3</sup>Phe-β<sup>3</sup>Leu-β<sup>3</sup>Asp-β<sup>3</sup>Phe-β<sup>3</sup>Leu-β<sup>3</sup>Orn-β<sup>3</sup>Leu-β<sup>3</sup>Asp-OH and H<sub>2</sub>N-β<sup>3</sup>Glu-β<sup>3</sup>Leu-β<sup>3</sup>Orn-β<sup>3</sup>Phe\*-β<sup>3</sup>Leu-β<sup>3</sup>Asp-β<sup>3</sup>Tyr-β<sup>3</sup>Leu-β<sup>3</sup>Orn-β<sup>3</sup>Glu-β<sup>3</sup>Leu-β<sup>3</sup>Asp-OH, where β<sup>3</sup>Phe\* stands for β<sup>3</sup>-4-iodohomophenylalanine), which adopt 14

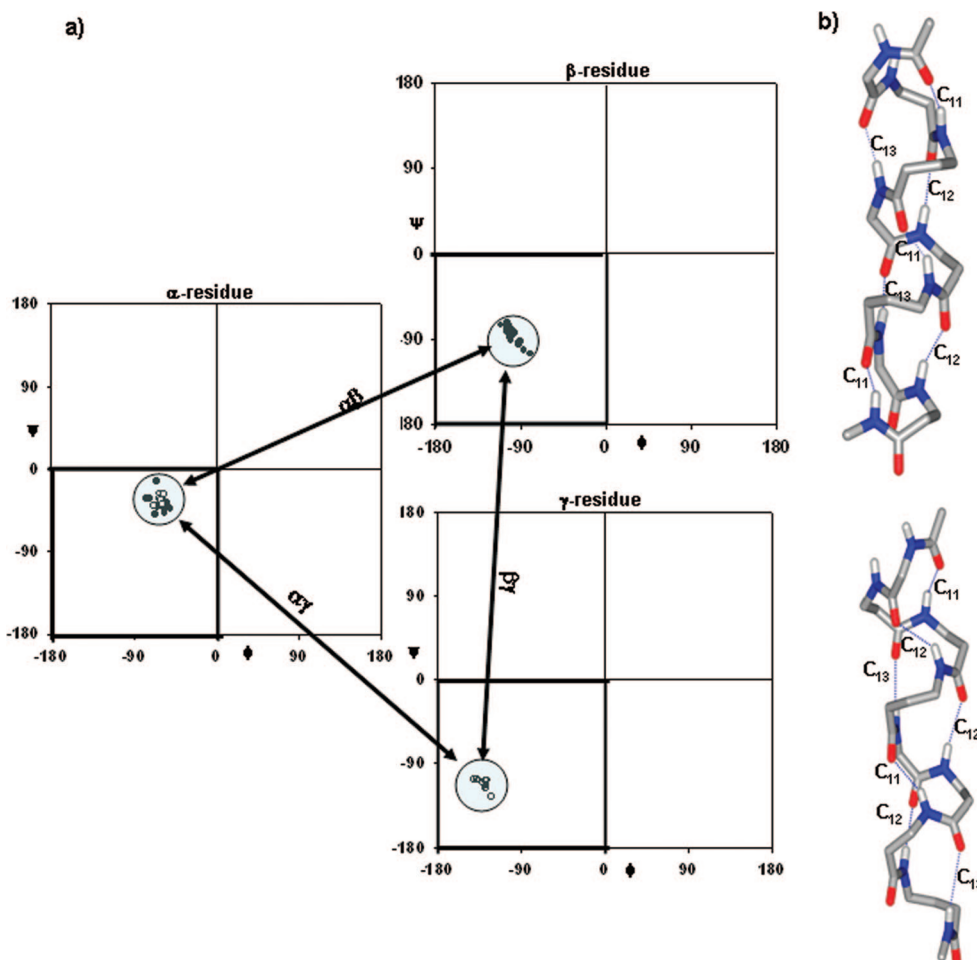


**Figure 29.** (a) Schematic diagram illustrating the relationship between helical conformations of  $\alpha$ ,  $\beta$ , and  $\gamma$  residues. The double edged arrows indicate that the residues can occupy the central position of a consecutive hydrogen bonded turn structure (incipient helix), leading to the formation of helical structures. The experimental points plotted are extracted from the crystal structures of hybrid  $\beta\alpha$  and  $\gamma\alpha$  helices (see Table S1). (b) (top) Model of hybrid peptide helix containing  $\alpha$ ,  $\beta$ , and  $\gamma$  residues (... $\alpha\beta\gamma\alpha\beta\gamma\ldots$ ) with varying hydrogen bonded ring size resulting from 4  $\rightarrow$  1 hydrogen bonds. The helix can be described as a 11/13/12 mixed helix (top). (bottom) A model helix with the sequence repeat - $\alpha\beta\beta\gamma/\alpha\beta\beta\gamma-$ . 4 $\rightarrow$ 1 hydrogen bonds in this sequence results in a mixed helix with 11/12/13/12/11/12/13 hydrogen bond pattern (bottom).

helix ( $3_{14}$ ) conformation that assembles into helical bundles containing four crystallographically distinct molecules (Figure 30a).<sup>197,199</sup> All the amino acids in the sequence are  $\beta^3$  amino acids which are homologues of L amino acids. This 14 helix has hydrogen bond directionality opposite to that observed in conventional  $\alpha$  peptides (Figure 21).<sup>46</sup> The average backbone dihedral angle for the  $\beta$  residues are  $\phi = -135.5^\circ$ ,  $\theta = 55.6^\circ$ , and  $\psi = -126.4^\circ$ . The Gellman group has characterized hybrid analogs of the yeast transcription factors GCN4,<sup>241,242</sup> in which specific positions along the heptad repeat sequence is replaced by  $\beta$  residues. The structure thus obtained fold into helix bundles, with the successful crystallographic demonstration of a  $\beta$  amino acid core (Figure 30b). The hybrid helix is characterized by successive 14 atom hydrogen bonds.

## 8. Conformational Variability and Biological Activity

### 8.1. Conformational Variability in Solution

Despite the many successes in characterizing folded structures in peptides containing backbone homologated amino acids, it must be recognized that even for conformationally constrained residues, several distinct regions of

conformational space are energetically accessible. For example, inspection of crystallographically characterized conformations for the  $\gamma$  amino acid residue gabapentin (Gpn) reveal three distinct clusters in  $\phi-\psi$  space with  $\theta_1$  and  $\theta_2$  restricted to gauche conformations.<sup>166,191</sup> Conformational heterogeneity can lead to polymorphic crystal forms that reveal distinct conformations. An example is provided by the determination of crystal structure of the tetrapeptide Boc-Aib-Gpn-Aib-Gpn-NHMe in three polymorphic forms,<sup>191</sup> all of which yield conformations distinct from the anticipated  $C_{12}$  helical structure. Evidence for multiple conformations is obtained by selective line broadening of NH resonances in solution NMR spectra (Figure 31) and by the observation of interproton nuclear Overhauser effects (NOEs) incompatible with a single conformational species.<sup>166,191</sup> The interpretation of NOE data in solution is complicated in the case of exchanging conformations in which interproton distances vary widely between the two states (Figure 32).<sup>166</sup> In such situations minor conformations with short interproton distances can result in NOEs of significant intensities. Studies in solution of peptides containing backbone homologated amino acids have thus far been largely restricted to relatively short sequences. It is likely that in longer sequences, the energetics of helix formation may indeed favor a more

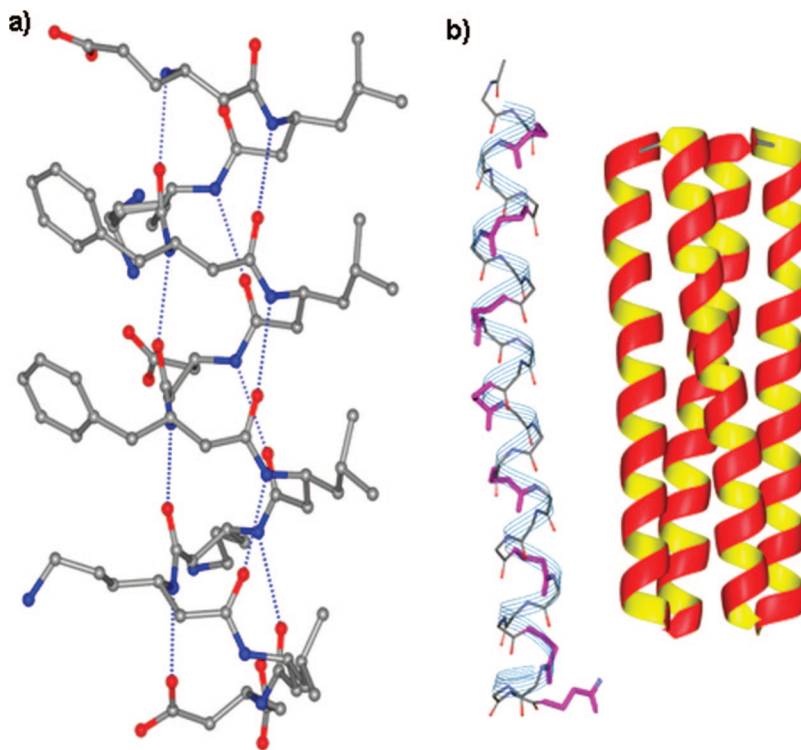


**Figure 30.** Crystallographic examples of helix bundles in  $\beta$ -peptides and  $\alpha\beta$ -hybrid peptides. (a) Molecular conformation of a  $\beta^3$ -dodecapeptide 14-helix in  $\text{H}_2\text{N}-\beta\text{Glu}-\beta\text{Leu}-\beta\text{Orn}-\beta\text{Phe}-\beta\text{Leu}-\beta\text{Asp}-\beta\text{Phe}-\beta\text{Leu}-\beta\text{Orn}-\beta\text{Leu}-\beta\text{Asp}-\text{OH}$  (no. 64 in Table S1), in crystals. Four molecules in the asymmetric unit of this peptide in the space group  $P4_12_12$  form a helix bundle.<sup>197</sup> (b) Conformation of the  $\alpha\beta$  hybrid peptide with the sequence repeat  $\alpha\alpha\beta$ , which is derived from a 33 residue  $\alpha$ -peptide of the dimerization domain of yeast transcriptional regulator.<sup>241</sup> The figure (left) shows the conformation of molecule-A of the peptide which has four molecules in the crystallographic asymmetric unit, resulting in a four helix bundle (right). Only backbone atoms are shown for clarity, with the  $\beta$ -residues highlighted in pink color. The  $\beta$ -residues present in this sequence are  $\beta^3\text{Lys}$  (residues 4, 16, 28),  $\beta^3\text{Asp}$  (residue 8),  $\beta^3\text{Glu}$  (residue 12),  $\beta^3\text{Ile}$  (residue 20),  $\beta^3\text{Leu}$  (residue 24), and  $\beta\text{Gly}$  (residue 32). The  $5 \rightarrow 1$  hydrogen bonded helix has a hydrogen bond pattern 14/14/14/13, with the 14 atom hydrogen bonds corresponding to  $\alpha\alpha\beta/\alpha\beta\alpha/\beta\alpha\alpha$  turns and the 13 atom turn corresponding to an  $\alpha\alpha\alpha$  turn. For the sequence and backbone torsion angles of  $\beta$ -residues see Table S1, entry number 32. Panels a and b are generated using the coordinates available for the peptides in the crystallographic databases CSD and PDB.

homogeneous conformational distribution. Structures in solution of a  $\beta^3$ -icosapeptide containing all the 20 proteino-*genic* side chains have been reported using NMR methods.<sup>243</sup> Circular dichroism (CD) has been reported only for relatively few examples of backbone expanded peptides, in particular, oligomeric  $\beta$  peptides.<sup>22,24</sup> Systematic circular dichroism studies of backbone homologated peptides which address issues of chain length dependence of helix formation remain to be done.

## 8.2. Biological Activity of Synthetic Peptides

Structure function studies of peptides containing backbone homologated residues have been stimulated by the demonstration of a wide spectrum of biological activity in synthetic sequences. Table 4 lists representative examples of peptides exhibiting biological activity. The overwhelming majority of examples reported to date have involved  $\beta$  peptides. An important feature of  $\beta$  peptide sequences is their established resistance to proteolytic degradation,<sup>244–255</sup> although reports of specific enzymes that hydrolyze  $\omega$  peptide bonds are available.<sup>256–263</sup>

## 9. Revisiting Hydrogen-Bonded Rings and Polypeptide Helices

The insertion of additional atoms into polypeptide backbone results in an expansion of the size of the hydrogen-bonded rings that are formed upon local folding.

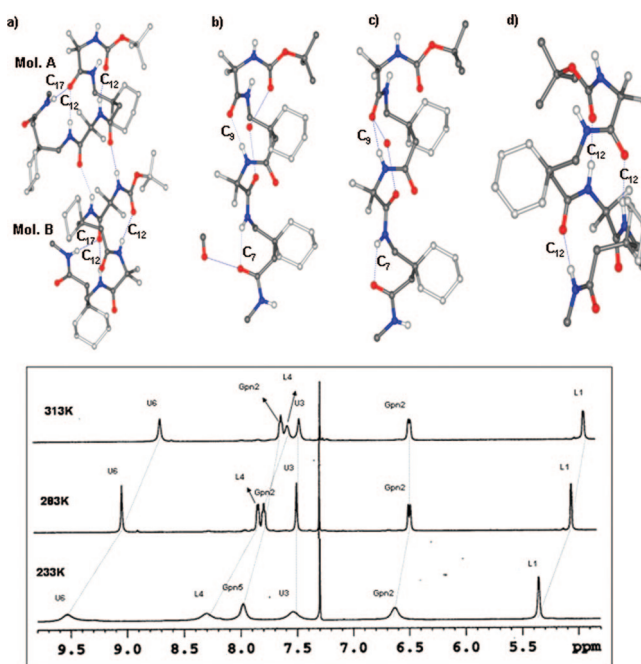


**Figure 31.** (Top) (a, b, c) Conformations in polymorphic crystals of Boc-Aib-Gpn-Aib-Gpn-NHMe<sup>191</sup> and (d) anticipated  $\text{C}_{12}$  helix in Boc-Aib-Gpn-Aib-Gpn-NHMe evidenced in solution. (Bottom) Temperature dependence of line widths of NMR resonances characteristic of presence of conformational exchange processes in solution.

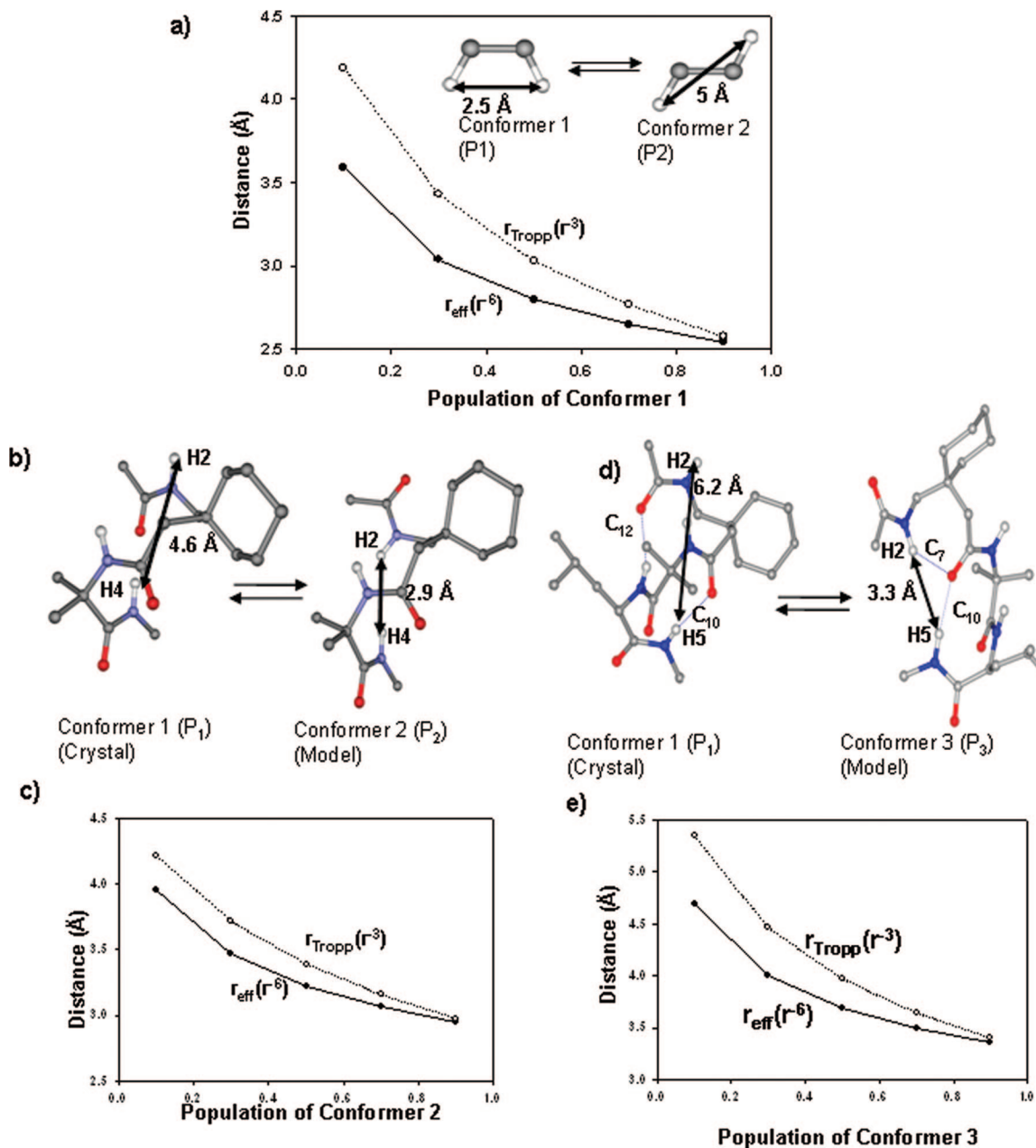


**Figure 32.** Averaging of NOE when two conformations with populations  $P_1$  and  $P_2$  ( $P_1 + P_2 = 1$ ) equilibrate in solution. (a) An ideal case of two protons equilibrating between distinct conformations with interproton distances of 2.5 and 5.0 Å. (b) Two distinct conformations across Gpn-Aib segment wherein  $d_{2,4}$  are 4.5 and 2.9 Å, respectively. (c) Effective internuclear distances at different populations of the two conformers shown in b. (d) Two distinct conformations across the Gpn-Aib-Leu segment wherein  $d_{2,5}$  are 6.2 and 3.3 Å. (e) Effective internuclear distances for different populations of the two conformers shown in (d).<sup>166</sup> Reprinted with permission from ref 166. Copyright 2005 John Wiley and Sons.

Peptide helices are generated by sequential hydrogen bonded turns. In the case of  $\alpha$  polypeptides, the  $3_{10}$  and the  $\alpha(3.6_{13})$  helices, which contain 10 and 13 atom hydrogen bonded rings, respectively are the only structures that have been well characterized. The  $\pi$  helix ( $4.4_{16}$ ), which contains repetitive 16 atom hydrogen bonds has not been observed. However, isolated 16 atom hydrogen bonded rings involving a 6 → 1 hydrogen bond have been observed in the Schellman motif which often terminates helical segments in proteins.<sup>264–267</sup> This structural feature observed at the C-terminal end requires chiral reversals ( $\alpha_L$  conformation) at the penultimate residue and possess both a 4 → 1 and a 6 → 1 hydrogen bond (Figure 33). Hydrogen bonded rings with ring sizes greater than 13 atoms can be formed in sequences containing  $\omega$  amino

acids. Illustrative examples of C<sub>15</sub>, C<sub>16</sub>, C<sub>17</sub>, and C<sub>19</sub> hydrogen bonds are shown in Figure 33. Of these, C<sub>15</sub> ( $\alpha\beta\beta/\beta\alpha\beta/\beta\beta\alpha$ ),<sup>190,193,194</sup> C<sub>16</sub> ( $\alpha\beta\gamma$ ),<sup>54</sup> and C<sub>19</sub> ( $\beta\gamma\alpha\alpha$ )<sup>54</sup> occur in structures of helical hybrid peptides. The C<sub>17</sub> hydrogen bond is a feature obtained in the structure of a protected tetrapeptide sequence.<sup>191</sup> The C<sub>19</sub> hydrogen bond characterized over the C-terminal segment  $\beta$ Gly- $\gamma$ Abu-Leu-Aib-Val ( $\beta\gamma\alpha\alpha$ ) can be considered as a backbone expanded analog of the Schellman motif.<sup>54</sup> In this case, the penultimate residue at the C-terminus (Aib(7)), adopts an  $\alpha_L$  conformation and an internal C<sub>12</sub> hydrogen bond is formed by the  $\gamma\alpha$  segment. This hydrogen bonding pattern shown in Figure 33f can be compared with the Schellman motif shown in Figure 33a. The characterization of large hydrogen-bonded rings upon backbone homologation raises the question as to

**Table 4. Biologically Active Peptides<sup>a</sup>**

peptide	$\omega$ amino acids	biological activity	reference
H-( $\beta$ Phe- $\beta$ Ala- $\beta$ Lys)- $\beta$ Phe-OH	$\beta$ Phe, $\beta$ Ala, $\beta$ Lys, $\beta$ Ser	inhibits cholesteryl oleate uptake in the brush-border membrane (small intestine)	Werder et al., 1999 <sup>275</sup>
H-( $\beta$ Phe- $\beta$ Ala- $\beta$ Lys- $\beta$ Ser)- $\beta$ Phe-OH			Karlsson et al., 2006 <sup>276</sup> 2009 <sup>277</sup>
14-helical $\beta$ -peptides			Chiba et al., 1999 <sup>278</sup>
cyclic tetrapeptide from <i>Rhodococcus</i>			Liu and DeGrado, 2001 <sup>279</sup>
H-( $\beta$ Ala- $\beta$ hAla- $\beta$ hLys- $\beta$ hVal) <sub>n</sub> NH <sub>2</sub> ; n = 4–5			Hamuro et al., 1999 <sup>280</sup>
H-( $\beta$ Ala- $\beta$ hAla- $\beta$ hLys- $\beta$ hLeu) <sub>n</sub> OH; n = 2–4;			Arvidsson, et al., 2001 <sup>281</sup>
H-( $\beta$ Ala- $\beta$ hAla- $\beta$ hLys- $\beta$ hLeu) <sub>n</sub> OH; n = 3–6;			
Fmoc-( $\beta$ Ala- $\beta$ hAla- $\beta$ hLys- $\beta$ hLeu) <sub>n</sub> OH; n = 2–4;			
H-( $\beta$ Ala- $\beta$ hAla- $\beta$ hLys- $\beta$ hLeu) <sub>n</sub> OH; n = 2–4;			
H-( $\beta$ Ala- $\beta$ hAla- $\beta$ hLys- $\beta$ hLeu)- $\beta$ hLys- $\beta$ hLeu-			
cyclic $\beta$ peptides			
C16-Lys-Gly-Gly-Lys			
C16-Lys-Ala-Ala-Lys			
C16-Lys-Lys-Lys-Lys			
C12-Lys-Leu-Lys			
Ac-ACPC-C- $\beta$ ACPC-APC-ACPC-APC-			
ACPC- $\beta$ ACPC-NH <sub>2</sub>			
Ac-ACPC-ACPC-(AP-ACPC-AP-ACPC-			
ACPC <sub>3</sub> -NH <sub>2</sub>			
Ac-ACPC-Leu-APC-(Lys-APC-Leu-ACPC)- <sub>2</sub> -			
Leu-ACPC-Leu-ACPC-NH <sub>2</sub>			
Ac-APC-Leu-APC-Leu-ACPC-Lys-ACPC-Leu-			
ACPC-Leu-APC-Leu-ACPC-Lys-ACPC-NH <sub>2</sub>			
Ac-APC-Leu-ACPC-Leu-ACPC-Ala-APC-Ala-			
ACPC-Lys-ACPC-Ala-APC-Leu-ACPC-NH <sub>2</sub>			
ACPC-Leu-ACPC-Ala-APC-Ala-ACPC-Lys-			
Ac-APC-Leu-ACPC-Ala-APC-Lys-ACPC-Ala-APC-NH <sub>2</sub>			
cyclic $\beta$ peptide			
( $\beta$ Glu- $\beta$ Glu- $\beta$ Glu)			
R-carnitine			
cyclic $\beta$ peptide			
( $\beta$ Phe- $\beta$ Thr- $\beta$ Lys- $\beta$ Trp)			
cyclo- $\beta$ -tetrapeptide			
Ac- $\beta$ hThr- $\beta$ hLys- $\beta$ hTrp- $\beta$ hPhe-NH <sub>2</sub>			
Ac- $\beta$ hPhe- $\beta$ hTrp- $\beta$ hLys- $\beta$ hThr lactone			
Ac- $\beta$ hPhe- $\beta$ hTrp- $\beta$ hLys- $\beta$ hThr lactone			
Nap- $\gamma$ Res- $\gamma$ Res B-NHMe			
Fl-( $\beta$ Arg) <sub>7</sub> NH <sub>2</sub>			
fluorescently labeled $\beta$ decaarginine			
and $\beta$ octarginine			
H-( $\beta$ Arg) <sub>n</sub> NH <sub>2</sub> ; n = 6, 8			
H-( $\beta$ Arg) <sub>n</sub> OH; n = 6, 8			
C-14 labeled $\beta$ -octarginine peptide			
cryptophycin/blue green algae			
carnosine( $\beta$ Cl- $\beta$ His) anserine, carnicine			
taxol			
$\beta$ -DAsp-Arg-Val-Tyr-Ile-His-Pro-Phe			
$\beta$ -LAsp-Arg-Val-Tyr-Ile-His-Pro-Phe			
Asp-Arg-Val-Tyr-Ile-His-Pro-Phe			
Asp-Arg-Val-Tyr- $\beta$ Ile-His-Pro-Phe			
Asp-Arg-Val-Tyr- $\beta$ Ile-His-Pro-Phe			

**Table 4.** Continued

peptide	$\omega$ amino acids	biological activity	reference
$\beta$ -Gly(4) oxytocin bradykinin analogs	$\beta$ -Gly	marked decrease in oxytocic activity	Manning et al., 1965 <sup>308</sup>
Arg-Pro-Pro-Gly-Phe-Ser-Pro-Phe- $\beta$ -Asp	$\beta$ -Asp $\beta$ -Phe	equipotent to bradykinin in vasodepressor activity	Ondetti and Engel, 1975 <sup>309</sup>
Arg-Pro-Pro-Gly-Phe-Ser-Pro-Phe- $\beta$ -Phe	$\beta$ -Leu, $\beta$ -Asp, $\beta$ -Phe	slightly less active	
Boc-Trp- $\beta$ Leu- $\beta$ Asp- $\beta$ Phe	$\beta$ -Leu, $\beta$ -Phe, $\beta$ -Phe	gastrin agonist (all $\alpha$ peptide analog) converted to gastrin antagonist	Rodríguez et al., 1989 <sup>310</sup>
analog of parent peptide H-D-Phe-Gin-Trp-Ala- Val-Gly-Ets-Leu-Leu-NH <sub>2</sub>		bombesin antagonist	Llinás et al., 1997 <sup>311</sup>
morphiceptin (Tyr-Pro-Phe-Pro-NH2)			Mierke et al., 1990 <sup>312</sup>
analog with ACPC at position 2		$\mu$ opioid receptor affinities	
endomorphin-1 (Tyr-Pro-Trp-Phe-NH2) analog with $\beta$ -(R)Pro or $\beta$ -(S)Pro at position 2	$\beta$ -Pro	Yamazaki, et al., 1997 <sup>313</sup>	
endomorphin analogs with <i>cis</i> -(I,S;2R)-ACPC / <i>cis</i> -(I,S;2R)-ACHC at position 2	<i>cis</i> -(I,S;2R)-ACPC <i>cis</i> -(I,S;2R)-ACHC	binds to MHC class I molecules	Cardillo et al., 2000 <sup>314</sup>
Gly-Arg-Ala-( $\beta$ Ala) <sub>5</sub> -Lys	$\beta$ -Ala	2-amino cyclohexane carboxylic acid	Keresztes et al., 2008 <sup>315</sup>
Ser-Ile-Ile-( $\beta$ Ala)- $\beta$ Phe-Glu-Lys-Leu	$\beta$ -Phe	proton transport activity in a liposome based assay	Poenaru et al., 1999 <sup>316</sup>
cyclol[(- $\beta$ -Ile- $\beta$ Trp) <sub>4</sub> ] cyclol[(- $\beta$ -Ile- $\beta$ Trp- $\beta$ -Ile- $\beta$ Leu)-] Fl- $\beta$ -TrpTyr- $\beta$ <sup>3HGly-<math>\beta</math><sup>3hArg-<math>\beta</math><sup>3hLys-<math>\beta</math><sup>3hArg-<math>\beta</math><sup>3hLys-<math>\beta</math><sup>3hArg-NH<sub>2</sub></sup></sup></sup></sup></sup></sup>	$\beta$ <sup>3-HTrp <math>\beta</math><sup>3</sup>-HTip <math>\beta</math><sup>3</sup>-hTyr <math>\beta</math><sup>3</sup>hGly</sup>	translocation across cell membrane	Webb et al., 2005 <sup>318</sup>
Chimeric $\beta$ peptide: ( $\beta$ Se- $\beta$ Asp- $\beta$ Tyr- $\beta$ Ile- $\beta$ Lys- $\beta$ Gln- $\beta$ Leu- $\beta$ Ala- $\beta$ Leu- $\beta$ Pro) ( $\beta$ Trp- $\beta$ Arg- $\beta$ Gln- $\beta$ Ile- $\beta$ Lys- $\beta$ Glu- $\beta$ Phe- $\beta$ Arg- $\beta$ Ala- $\beta$ Val- $\beta$ Lys- $\beta$ Glu- $\beta$ Ala- $\beta$ Asn)	$\beta$ -Ser, $\beta$ -Asp, $\beta$ -Tyr, $\beta$ -Ile, $\beta$ -Lys, $\beta$ -Gln, $\beta$ -Leu, $\beta$ -Ala, $\beta$ -Phe, $\beta$ -Pro	comparable activity to native human interleukin-8 (hIL-8)	Clark et al., 1998 <sup>319</sup>
$\beta$ Orn, $\beta$ Val, $\beta$ Ile, $\beta$ Leu, $\beta$ Glu, $\beta$ Phe $\beta$ Ala, $\beta$ Tyr, $\beta$ Trp		inhibitors of p53-hDM2 complexation	Umezawa et al., 2001 <sup>320</sup>
$\beta$ Orn, $\beta$ Val, $\beta$ Ile, $\beta$ Leu, $\beta$ Glu, $\beta$ Phe $\beta$ Ala, $\beta$ Tyr, $\beta$ Trp		inhibitors of p53-hDM2 complexation	David et al., 2008 <sup>321</sup>
$\beta$ Orn- $\beta$ Ile- $\beta$ Leu- $\beta$ Ala- $\beta$ Leu- $\beta$ Ile-Z-		ligand to the antiapoptotic protein Bcl-xL	Kritzer et al., 2004 <sup>322</sup>
amino-4-(2-trifluoromethylphenyl)butyric acid)		catalytic activity in the retroaldol cleavage of $\beta$ -hydroxyketone	Harker et al., 2009 <sup>323</sup>
bridged $\beta$ -peptides		inhibit HSV-1 infection (antiviral agent)	Bautista et al., 2010 <sup>324</sup>
Ac-ACPC- $\beta$ Ala-ACPC-Arg-ACPC-Leu-ACPC-Lys- $\beta$ Xxx-Gly-Asp- $\beta$ Ala-Phe-Asn-Arg-NH2; $\beta$ Xxx = $\beta$ Leu, $\beta$ Nle	ACPC, $\beta$ -Leu, $\beta$ Nle	HIV fusion inhibitors	Muller et al., 2009 <sup>325</sup>
CH <sub>3</sub> (CH <sub>2</sub> ) <sub>5</sub> CO- $\beta$ Tyr-(ACHC-ACHC- $\beta$ Trp- $\beta$ Leu- $\beta$ Tyr- $\beta$ Gly- $\beta$ Arg- $\beta$ Arg- $\beta$ Arg- $\beta$ NH <sub>2</sub>	$\beta$ Tyr, ACHC, ACHC, $\beta$ Lys	HIV fusion inhibitors	Akkarawongsa et al., 2008 <sup>327</sup>
$\beta$ Tyr- $\beta$ Gly- $\beta$ Arg- $\beta$ Arg- $\beta$ Arg- $\beta$ NH <sub>2</sub>	$\beta$ Tyr, $\beta$ Gly, $\beta$ Arg, $\beta$ Val, ACHC		Stephens et al., 2005 <sup>328</sup>
$\beta$ H <sub>2</sub> N- $\beta$ Orn- $\beta$ X2- $\beta$ X3- $\beta$ Glu- $\beta$ X5- $\beta$ X6- $\beta$ Orn- $\beta$ X8- $\beta$ X9- $\beta$ Glu-OH	$\beta$ Orn, $\beta$ Glu, $\beta$ Val, $\beta$ Ile, $\beta$ Trp		Home et al., 2009 <sup>329</sup>
$\beta$ , ACPC, and APC analogues of the peptide, Ac-Thr-Thr-Trp-Glu-Ala-Tip-Asp-Arg-Ala- Ile-Ala-Glu-Tyr-Ala-Ala-Arg-Ile-Glu-Ala-Leu- Ile-Arg-Ala-Ala-Gln-Glu-Gln-Gly-Lys-Asn- Glu-Ala-Ala-Ala-Leu-Alg-Glu-Leu-NH2	$\beta$ Thr, $\beta$ Ala, $\beta$ Arg, $\beta$ Glu, ACPC, APC		Giuliano et al., 2009 <sup>42</sup>
Ac-Arg- $\beta$ Met-Lys-Gln- $\beta$ Ile-Glu-Asp-Lys- $\beta$ Leu- Glu-Glu- $\beta$ Ile-Leu-Ser-Lys- $\beta$ Ile-Tyr-His- $\beta$ - Ile-Glu-Ala-Glu- $\beta$ Leu-Ala-Arg- $\beta$ Ile-Lys-Lys- Leu- $\beta$ Leu-Gly-Glu- $\beta$ Arg-OH	$\beta$ Met, $\beta$ Ile, $\beta$ Leu, $\beta$ Arg	4-helix bundle analogous to the dimerization domain of yeast transcription factor GCN4-pL1	Gademann and Seebach, 2001 <sup>330</sup>
cyclo( $\beta$ -HSer) <sub>3</sub>	$\beta$ -HSer, $\beta$ -HGlU	antiproliferative against a range of human cancers	
cyclo( $\beta$ -HGlu(OBn)) <sub>3</sub>	$\beta$ <sup>3</sup> Tyr, $\beta$ <sup>3</sup> Gly, $\beta$ <sup>3</sup> Arg, $\beta$ <sup>3</sup> Lys, $\beta$ <sup>3</sup> Gln	mimic of HIV-tat protein, bind to TAR RNA	Gelman et al., 2003 <sup>331</sup>
$\beta$ <sup>3</sup> (Tyr-Gly-Arg-Gly-OBn)3	$\beta$ <sup>3</sup> Lys, $\beta$ <sup>3</sup> Phe, $\beta$ <sup>3</sup> Ala, $\beta$ <sup>3</sup> Gln, $\beta$ <sup>3</sup> Asn	bind to 20-mer DNA	Namoto et al., 2006 <sup>332</sup>

<sup>a</sup>  $\beta$ -residues are denoted by  $\beta$ Xxx, where Xxx is the three letter code for the corresponding  $\alpha$ -residue.

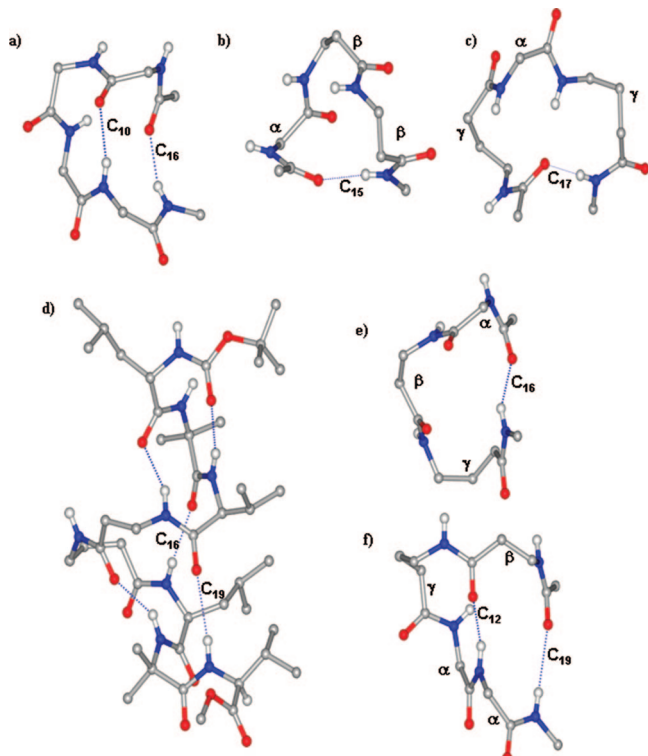


**Figure 33.** Hydrogen bonds with larger ring sizes determined in crystals. (a) Example of a Schellman motif widely characterized in  $\alpha$ -peptides. Residues 5–8 of the peptide Boc-Leu-Aib-Val-Gly-Leu-Aib-Val-D<sup>D</sup>Ala-D<sup>D</sup>Leu-Aib-OMe<sup>267</sup> are shown in the figure. (b) C<sub>15</sub> turn determined in the Boc-Val-Ala-Phe-Aib- $\beta$ Val- $\beta$ Phe-Aib-Val-Ala-Phe-Aib-OMe<sup>190</sup> (see Figure 19b), (c) C<sub>17</sub> turn in Boc-Aib-Gpn-Aib-Gpn-NHMe,<sup>191</sup> (d) Boc-Leu-Aib-Val- $\beta$ Gly- $\gamma$ Abu-Leu-Aib-Val-OMe,<sup>54</sup> (e) C<sub>16</sub> turn, and (f) C<sub>19</sub> turn (bottom) characterized in Boc-Leu-Aib-Val- $\beta$ Gly- $\gamma$ Abu-Leu-Aib-Val-OMe. Backbone torsion angles are provided in Table S1.

whether helices accommodating such expanded ring sizes can be characterized. Discussion of helices in  $\alpha$  polypeptides and protein structures have centered almost exclusively on the 3<sub>10</sub> and the 3.6<sub>13</sub> helices. Both of these structures have hydrogen bonding patterns of the type CO(i)…NH(i + n), n = 3, 4. As described earlier, the postulation of the  $\delta$  helix with a 1 → 4 hydrogen bond pattern is an isolated example of the reversal of hydrogen bond directionality in  $\alpha$  peptides. Hydrogen bonds of the type NH(i)…CO(i + n) have now been well characterized in  $\beta$  peptides and hybrid sequences. Extensive fiber diffraction studies on nylons, specifically nylon-3( $\beta$ -polypeptide) and poly- $\alpha$ -alkyl- $\beta$ -L-aspartates have suggested that larger helical structures, for example the 18 helix, (C<sub>18</sub>) may indeed be formed in these systems.<sup>40,41,268,269</sup> Such a helix would correspond to a repetitive  $\beta\beta\beta\beta$  segment, with a 1 → 4 hydrogen-bonding pattern and would be an expanded version of the well characterized C<sub>14</sub> helix of the  $\beta$  peptides. Much of the early work on poly  $\gamma$  peptides was stimulated by the production of poly- $\gamma$ -D glutamic acid by *Bacillus anthracis* and *Bacillus subtilis*.<sup>34</sup> In work published in the mid 1960s, Rydon proposed helices with hydrogen bond ring sizes of 19 atoms (normal direction, 5 → 1, CO(i)…NH(i + 4)) and 17 atoms (reverse direction, 1 → 3, NH(i)…CO(i + 2)).<sup>30</sup> The C<sub>19</sub> helix would be the expanded  $\gamma$  peptide analog of the  $\alpha$  helix. The C<sub>17</sub> helix would be the expanded analog of the C<sub>14</sub> helix of  $\beta$  peptides. Theoretical analysis of the conformational preferences of ionized poly- $\gamma$ -D-glutamic acid, using molecular dynamics and quantum chemical calculations suggests that a left

handed helix with a 19-membered hydrogen-bonding pattern (5 → 1) may indeed be the most stable.<sup>43</sup> Note that Figure 1 of ref 43 labels this hydrogen bond scheme as (i, i + 3). More recent experimental investigations of poly- $\gamma$ -glutamates have used biosynthetically derived samples (bionylons) that contain both L- and D-glutamic acid residues.<sup>270</sup> An interesting feature of naturally occurring poly- $\gamma$ -glutamates is that several organisms produce poly- $\gamma$ -D-glutamate, while others produce D, L copolymers of variable stereochemical composition.<sup>271</sup> Poly glutamate-biosynthesis has now been established in both prokaryotes and archaea and the sole example of its production in an eukaryotic organism has been reported.<sup>272</sup>

Helical structures that are optimally close packed would be anticipated to be the most energetically favorable, since hydrogen-bonding interactions and van der Waals interactions may both be maximized. Table 4 provides a summary of hydrogen-bond patterns and internal helix diameters for idealized structures formed by homopolymers of  $\alpha$ ,  $\beta$ , and  $\gamma$  residues. In  $\alpha$  peptide helices, the 3<sub>10</sub> helix and the 3.6<sub>13</sub> ( $\alpha$ ) helix have closely packed interiors as seen from the space filling representations viewed as projections down the helix axis (Figure 34). Indeed, there has been considerable discussion in the literature on the relative energetics of the 3<sub>10</sub> and  $\alpha$  helical structures for the  $\alpha$  peptides with the former having somewhat unfavorable non bonded interactions. The view shown in Figure 34 of the 4.4<sub>16</sub> ( $\pi$ ) helix reveals an internal cavity with the estimated Miyazawa diameter<sup>273</sup> of ~4.2 Å. Using a value of 2.7–2.9 Å for the sum of the van der Waals radii of C, N, O atoms lining the helix interior, the resultant cavity size may be estimated. For the  $\pi$  helix, the cavity diameter would correspond to approximately 1.3–1.5 Å. The nonoccurrence of the  $\pi$  helix in protein structures must indeed be a consequence of its loose interior packing. Figure 34 also compares helix packing for the C<sub>12</sub> ( $\beta\beta$ ) and the C<sub>16</sub> ( $\beta\beta\beta$ ) helices in  $\beta$  peptides and C<sub>14</sub> ( $\gamma\gamma$ ) and C<sub>19</sub> ( $\gamma\gamma\gamma$ ) helices in  $\gamma$  peptides. While the C<sub>12</sub>  $\beta\beta$  helix is a well packed structure, the C<sub>14</sub>  $\gamma\gamma$  helix also reveals only a very small internal cavity (diameter ≈ 0.5–0.7 Å). Both of these helices are experimentally characterized, although the C<sub>14</sub> ( $\gamma\gamma$ ) helix has thus far been established only in a short peptide (Figure 16).<sup>124</sup> In contrast, the C<sub>16</sub> helix for a  $\beta_n$  sequence and the C<sub>19</sub> helix for a  $\gamma_n$  sequence reveal somewhat larger internal cavities, which may be anticipated to be destabilizing. Figure 35 compares the helix packing in three polypeptide helices with reverse hydrogen bond directionality (NH(i)…CO(i + n)). The experimentally characterized C<sub>14</sub> helix for a  $\beta_n$  polypeptide, reveals an internal cavity diameter of ~1.2 Å, while a significantly larger cavity (~2.2 Å) is obtained for the proposed C<sub>18</sub> helix in the nylons.<sup>274</sup> Interestingly, the hypothesized 14 helix in  $\alpha$  peptides ( $\delta$  helix)<sup>195</sup> reveals a significantly large internal cavity in addition to having somewhat unfavorable  $\phi$ ,  $\psi$  angles, which should be estimated to make the structure energetically unfavorable.

## 10. Conclusions

The growing diversity of folded hydrogen-bonded structures containing  $\beta$ ,  $\gamma$ , and higher  $\omega$  amino acids suggests that hybrid sequences may provide unanticipated opportunities for the design of novel peptide structures. The  $\omega$  amino acids offer great scope for a variety of backbone substitutions. Advances in synthetic methodologies will undoubtedly rapidly enhance the number of  $\omega$  amino acid building blocks available to peptide

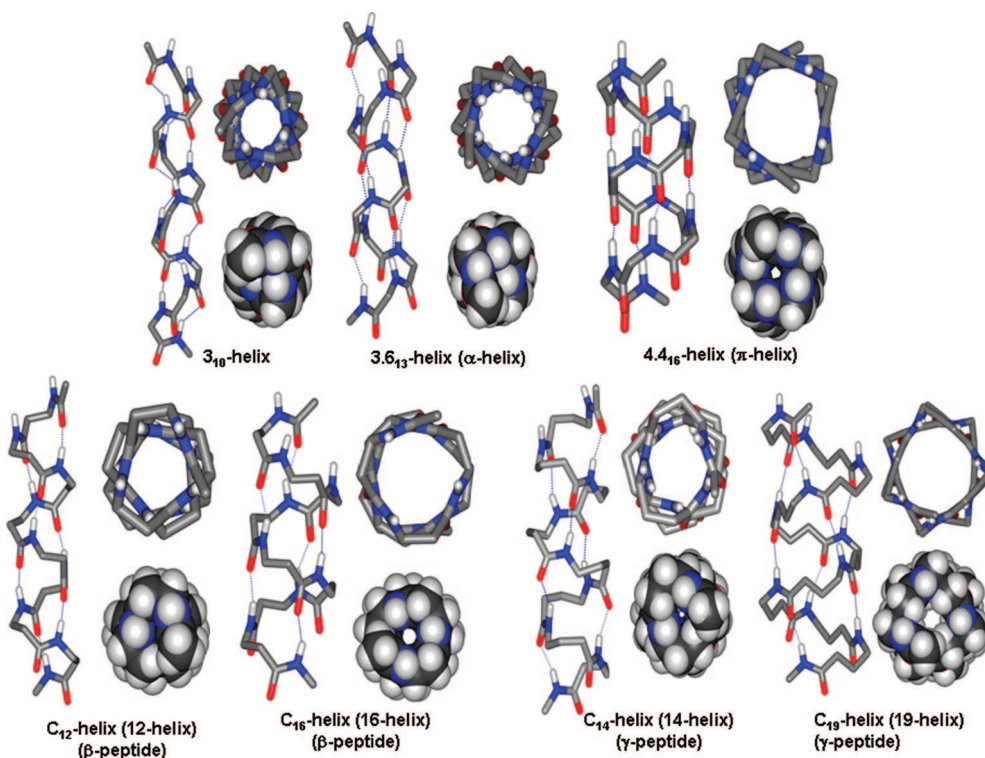


**Figure 34.** Comparison of helices formed in  $\alpha$ ,  $\beta$ , and  $\gamma$  homo oligo peptides. The top panel shows helices of  $\alpha$ -peptides formed with 4 → 1 ( $3_{10}$ -helix), 5 → 1 ( $\alpha$ -helix), and 6 → 1 ( $\pi$ -helix) hydrogen-bond patterns. The bottom panel shows helices in  $\beta$  and  $\gamma$  peptides with 4 → 1 (12-helix for  $\beta$ -peptide, 14-helix for  $\gamma$ -peptide) and 5 → 1 (16-helix for  $\beta$ -peptide, 19-helix for  $\gamma$ -peptides) hydrogen-bond patterns. The helices for  $\alpha$ -peptides are generated using ideal values of backbone torsion angles for right handed helices. The backbone dihedral angles for the 12-helix of  $\beta$ -peptide and 14-helix of  $\gamma$ -peptides are obtained by averaging the values determined in crystal structures (see Table 3, Table S1). For the 16-helix of  $\beta$ -peptide and 19 helix of  $\gamma$ -peptides, torsion angle values derived from the fiber diffraction experiments on poly-( $\alpha$ -isobutyl-L-aspartate)<sup>269</sup> and poly( $\alpha$ -benzyl- $\gamma$ -D,L-glutamate),<sup>270</sup> respectively, were used. The values are 16-helix,  $\phi = 126.6^\circ$ ,  $\theta = -103.3^\circ$ ,  $\psi = 113.6^\circ$ ; 19-helix,  $\phi = -71^\circ$ ,  $\theta_1 = -53^\circ$ ,  $\theta_2 = 171.6^\circ$  and  $\psi = -160.6^\circ$ . For the 12-helix, 14-helix, and 16-helix, which are derived from chiral structures, the helix handedness shown (left-handed) is as reported in the original publications. For the 19-helix, which is derived from a racemic crystal structure, a right-handed helix is shown. Projections perpendicular to the helix axis and down the helix axis are shown. For the projections down the helix axis, a space filling model is also shown, to permit visualization of internal cavity formation. The projections are not scaled. A comparison of the cavity dimension is provided in Table 5.

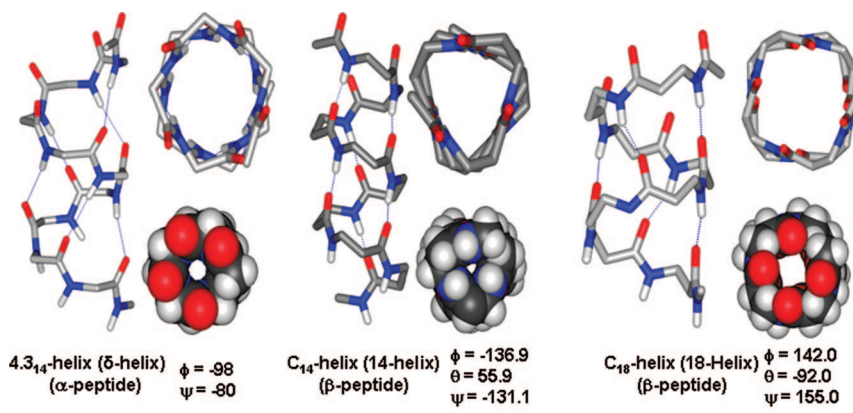


**Figure 35.** Comparison of helices with reversed directionality in  $\alpha$ - and  $\beta$ -peptides. (a) The 4.3<sub>14</sub> helix ( $\delta$ -helix) with 1 → 4 hydrogen bonds, (b) the widely characterized  $\beta$ -peptide 14-helix (3<sub>14</sub>-helix) with 1 → 3 hydrogen bonds, and (c) 18-helix formed with 1 → 4 hydrogen bonds in  $\beta$ -peptides. The left-handed 4.3<sub>14</sub> helix of  $\alpha$ -peptides is generated using the backbone torsion angles given by Chandrasekaran et al.<sup>195</sup> and the right-handed 18-helix of  $\beta$ -peptides is built using the torsion angle values given by Fernandez-Santin et al. for poly-( $\alpha$ -methyl-L-aspartate).<sup>268</sup> The backbone dihedral angles of the left handed 14-helix of  $\beta$ -peptides shown is averaged from crystal structures containing  $\beta^3$ -residues with S-configuration (as there are more number of crystallographic examples in this case; see Table S1).

chemists.<sup>63–92</sup> The ability to bias backbone conformational choices should permit the use of a variety of substituted  $\omega$  amino acids in rational peptide design. The use of stereochemically constrained residues that can occupy only limited regions of conformational space may be valuable in generating peptide sequences, which are conformationally homogeneous, permitting crystallization and definitive structural characterization. The

utility of many readily available stereochemically constrained  $\beta$  and  $\gamma$  residues to stabilize specific folded conformations remain to be fully explored. Helices with mixed hydrogen bond directionalities must be realized in long sequences and may provide a new class of helical scaffolds for arraying functional side chains.  $\beta$ ,  $\gamma$ , and higher  $\omega$  amino acids promise to expand the structural space for polypeptides. Backbone expanded

**Table 5. Ring Sizes of Normal and Reverse Direction Hydrogen Bonds in  $\alpha$ ,  $\beta$ , and  $\gamma$  Peptides<sup>a</sup>**

	4→1	5→1	6→1	1→2	1→3	1→4
$\alpha$	10 (2.8 Å)	13 (3.2 Å)	16 (4.2 Å)	8	11	14 (4.46 Å)
$\beta$	12 (3.2 Å)	16 (4.3 Å)	20 (4.2 Å)	10	14 (4.0 Å)	18 (5.8 Å)
$\gamma$	14 (3.4 Å)	19	24	12	17	22

<sup>a</sup> Inner diameter of the helix is given in parentheses. Inner diameter is reported only for helices which are experimentally observed and for helices, which are theoretically proposed. Helix parameters were calculated following the procedure of Miyazawa,<sup>273</sup> using all the backbone atoms in  $\omega$ -peptide helices. The reported radii corresponds to the shortest distance between the backbone atom lining the helix interior and the helix axis. An estimate of the cavity dimension may be obtained by subtracting the sum of van der Waals radii of the closest facing atoms from the Miyazawa diameter.

analogs of the well studied locally folded conformations of  $\alpha$  peptides will undoubtedly prove important in the area of biomimetic design. The results summarized in the review also point to the need to revisit experimentally oligomeric  $\gamma$  peptides related to the naturally occurring polypeptide poly- $\gamma$ -D-glutamate. The prospects for designing hybrid polypeptide mimics of naturally occurring proteins are bright, with recent studies providing examples of helix bundle formation.<sup>197,198,241,242</sup>

## 11. Acknowledgments

This research was supported by a grant from the Council of Scientific and Industrial Research (CSIR) and Program Support in the area of Molecular Diversity and Design, Department of Biotechnology, India. P.G.V. and S.C. thank the CSIR for Senior Research Fellowships. The contribution of many collaborators and co-workers whose name appear in the references are gratefully acknowledged.

## 12. Supporting Information Available

Table listing the crystallographically characterized peptides containing  $\beta$ - and  $\gamma$ -amino acid residues, their backbone torsion angles, and references. This information is available free of charge via the Internet at <http://pubs.acs.org/>.

## 13. References

- Kendrew, J. C.; Dickerson, R. E.; Strandberg, B. E.; Hart, R. G.; Davies, D. R.; Phillips, D. C.; Shore, V. C. *Nature* **1960**, *185*, 422.
- Richardson, J. S. *Adv. Protein Chem.* **1981**, *34*, 167.
- Thornton, J. M.; Orengo, C. A.; Todd, A. E.; Pearl, F. M. *J. Mol. Biol.* **1999**, *293*, 333.
- Branden, C.; Tooze, J. *Introduction to Protein Structure*; Garland: New York, 1991.
- Petsko, G. A.; Ringe, D. *Protein Structure and Function (Primers in Biology)*; New Science Press Ltd.: London, 2004.
- Dill, K. A. *Biochemistry* **1990**, *29*, 7133.
- Baker, E. N.; Hubbard, R. E. *Prog. Biophys. Mol. Biol.* **1984**, *44*, 97.
- Burley, S. K.; Petsko, G. A. *Science* **1985**, *239*, 23.
- Burley, S. K.; Petsko, G. A. *Adv. Protein Chem.* **1988**, *39*, 125.
- Burley, S. K.; Petsko, G. A. *Trends Biotechnol.* **1989**, *7*, 354.
- Ramachandran, G. N.; Ramakrishnan, C.; Sasisekharan, V. *J. Mol. Biol.* **1963**, *7*, 95.
- Ramachandran, G. N.; Sasisekharan, V. *Adv. Protein Chem.* **1968**, *23*, 283.
- Gunasekaran, K.; Ramakrishnan, C.; Balaram, P. *J. Mol. Biol.* **1996**, *264*, 191.
- Hovmöller, S.; Zhou, T.; Ohlson, T. *Acta Crystallogr.* **2002**, *D58*, 768.
- Pal, D.; Chakrabarti, P. *Biopolymers* **2002**, *63*, 195.
- Ho, B. K.; Brasseur, R. *BMC Struct. Biol.* **2005**, *5*, 14.
- Aravinda, S.; Shamala, N.; Roy, R. S.; Balaram, P. *Proc. Indian Acad. Sci. (Chem. Sci.)* **2003**, *115*, 373.
- Balaram, P. *Curr. Opin. Struct. Biol.* **1992**, *2*, 845.
- Xie, J.; Schultz, P. G. *Curr. Opin. Chem. Biol.* **2005**, *9*, 548.
- Ryu, Y.; Schultz, P. G. *Nat. Methods* **2006**, *3*, 263.
- Seebach, D.; Matthews, J. L. *Chem. Commun.* **1997**, *21*, 2015.
- Seebach, D.; Beck, A. K.; Bierbaum, D. *J. Chem. Biodiversity* **2004**, *1*, 1111.
- Kimmerlin, T.; Seebach, D. *J. Pept. Res.* **2005**, *65*, 229.
- Seebach, D.; Hook, D. F.; Glattli, A. *Biopolymers* **2006**, *84*, 23.
- Lelais, G.; Seebach, D. *Biopolymers* **2004**, *76*, 206.
- Gellman, S. H. *Acc. Chem. Res.* **1998**, *31*, 173.
- Cheng, R. P.; Gellman, S. H.; DeGrado, W. F. *Chem. Rev.* **2001**, *101*, 3219.
- Hanby, W. E.; Rydon, H. N. *Biochem. J.* **1946**, *40*, 297.
- Edelhoch, H.; Lippoldt, R. E. *Biochim. Biophys. Acta* **1958**, *30*, 657.
- Rydon, H. N. *J. Chem. Soc.* **1964**, 1328.
- Bragg, L.; Kendrew, J. C.; Perutz, M. F. *Proc. Roy. Soc. A* **1950**, *203*, 321.
- Pauling, L.; Corey, R. B.; Branson, H. R. *Proc. Natl. Acad. Sci. U. S. A.* **1951**, *37*, 205.
- Kovacs, J.; Ballina, R.; Rodin, R. L.; Balasubramanian, D.; Applequist, J. *J. Am. Chem. Soc.* **1965**, *87*, 119.
- Glickson, J. D.; Applequist, J. *J. Am. Chem. Soc.* **1971**, *93*, 3276.
- Lovinger, A. J. *J. Appl. Phys.* **1978**, *49*, 5014.
- Fernandez-Santin, J. M.; Aymani, J.; Rodriguez-Galan, A.; Muñoz-Guerra, S.; Subirana, J. A. *Nature* **1984**, *311*, 53.
- Muñoz-Guerra, S.; Fernandez-Santin, J. M.; Rodriguez-Galan, A.; Subirana, J. A. *J. Polym. Sci.* **1985**, *23*, 733.
- Puiggali, J.; Muñoz-Guerra, S. *Macromolecules* **1986**, *19*, 1119.
- Lopez-Carrasco, F.; Alemán, C.; Muñoz-Guerra, S. *Biopolymers* **1995**, *36*, 263.
- Navas, J. J.; Alemán, C.; Lopez-Carrasco, F.; Muñoz-Guerra, S. *Macromolecules* **1995**, *28*, 4487.
- Bella, J.; Alemán, C.; Fernandez-Santin, J.; Alegre, C.; Subirana, J. A. *Macromolecules* **1992**, *25*, 5225.
- Alemán, C.; Navas, J. J.; Muñoz-Guerra, S. *Biopolymers* **1997**, *41*, 721.
- Zanuy, D.; Alemán, C.; Muñoz-Guerra, S. *Int. J. Biol. Macromolecules* **1998**, *23*, 175.
- Seebach, D.; Overhand, M.; Kuhnle, F. M. N.; Martinoni, B.; Oberer, L.; Hommel, U.; Widmer, H. *Helv. Chim. Acta* **1996**, *79*, 913.
- Seebach, D.; Cireri, P. E.; Overhand, M.; Jaun, B.; Rigo, D.; Oberer, L.; Hommel, U.; Amstutz, R.; Widmer, H. *Helv. Chim. Acta* **1996**, *79*, 2043.
- Appella, D. H.; Christianson, L. A.; Karle, I. L.; Powell, D. R.; Gellman, S. H. *J. Am. Chem. Soc.* **1996**, *118*, 13071.
- Appella, D. H.; Christianson, L. A.; Klein, D. A.; Powell, D. R.; Huang, L.; Barchi, J. J.; Gellman, S. H. *Nature* **1997**, *387*, 381.
- Appella, D. H.; Christianson, L. A.; Karle, I. L.; Powell, D. R.; Gellman, S. H. *J. Am. Chem. Soc.* **1999**, *121*, 6206.
- Appella, D. H.; Christianson, L. A.; Klein, D. A.; Richards, M. A.; Powell, D. R.; Gellman, S. H. *J. Am. Chem. Soc.* **1999**, *121*, 7574.
- Hanessian, S.; Luo, X.; Schaum, R.; Michnick, S. *J. Am. Chem. Soc.* **1998**, *120*, 8569.
- Hanessian, S.; Luo, X.; Schaum, R. *Tetrahedron Lett.* **1999**, *40*, 4925.
- Seebach, D.; Brenner, M.; Rueping, M.; Schweizer, B.; Jaun, B. *Chem. Commun.* **2001**, *2*, 207.
- Banerjee, A.; Pramanik, A.; Bhattacharjya, S.; Balaram, P. *Biopolymers* **1996**, *39*, 769.
- Karle, I. L.; Pramanik, A.; Bannerjee, A.; Bhattacharya, S.; Balaram, P. *J. Am. Chem. Soc.* **1997**, *119*, 9087.
- Banerjee, A.; Balaram, P. *Curr. Sci.* **1997**, *73*, 1067.
- Hill, D. J.; Mio, M. J.; Prince, R. B.; Hughes, T. S.; Moore, J. S. *Chem. Rev.* **2001**, *101*, 3893.
- DeGrado, W. F.; Schneider, J. P.; Hamuro, Y. *J. Pept. Res.* **1999**, *54*, 206.
- Goodman, C. M.; Choi, S.; Shandler, S.; DeGrado, W. F. *Nat. Chem. Biol.* **2007**, *3*, 252.
- Horne, W. S.; Gellman, S. H. *Acc. Chem. Res.* **2008**, *41*, 1399.
- Seebach, D.; Gardiner, J. *Acc. Chem. Res.* **2008**, *41*, 1366.
- Roy, R. S.; Balaram, P. *J. Pept. Res.* **2004**, *61*, 274.
- Chatterjee, S.; Roy, R. S.; Balaram, P. *J. R. Soc., Interface* **2007**, *4*, 587.
- Podlech, J.; Seebach, D. *Angew. Chem., Int. Ed.* **1995**, *34*, 471.
- Podlech, J.; Seebach, D. *Liebigs Ann.* **1995**, *7*, 1217.
- Podlech, J.; Seebach, D. *Helv. Chim. Acta* **1995**, *78*, 1238.
- Juaristi, E.; Soloshonok, V. A., Eds. *Enantioselective Synthesis of  $\beta$  Amino Acids*; John Wiley & Sons, Inc.: New York, 2005.
- Gray, D.; Concellon, C.; Gallagher, T. *J. Org. Chem.* **2004**, *69*, 4849.
- Augilar, M. A.; Purcell, A. W.; Devi, R.; Lew, R.; Rossjohn, J.; Smith, A. I.; Perlmutter, P. *Org. Biomol. Chem.* **2007**, *5*, 2884.
- Fülop, F.; Martinek, T. A.; Toth, G. A. *Chem. Soc. Rev.* **2006**, *35*, 323.
- Abele, S.; Seebach, D. *Eur. J. Org. Chem.* **2000**, *1*, 1.
- Lui, M.; Sibi, M. *Tetrahedron* **2002**, *58*, 7991.
- Drey, C. N. C. *Chemistry and Biochemistry of Amino Acids, Peptides and Proteins*; Weinstein, B., Ed.; Marcel Dekker: New York, 1977; Vol. 4, p 241.
- Cardillo, G.; Tomasini, C. *Chem. Soc. Rev.* **1996**, *25*, 117.
- Sewald, N. *Amino Acids* **1996**, *11*, 397.

- (75) Sibi, M. P.; Prabhagaran, N.; Ghorpade, S. G.; Jasperse, C. P. *J. Am. Chem. Soc.* **2003**, *125*, 11796.
- (76) Ojima, I.; Delalage, F. *Chem. Soc. Rev.* **1997**, *26*, 377.
- (77) Sewald, N. *Angew. Chem., Int. Ed.* **2003**, *42*, 5794.
- (78) Cole, D. C. *Tetrahedron* **1994**, *50*, 9517.
- (79) Seebach, D.; Beck, A. K.; Capone, S.; Deniau, G.; Groselj, U.; Zass, E. *Synthesis* **2009**, *1*, 1.
- (80) Zhang, J.; Kissounko, D. A.; Lee, S. E.; Gellman, S. H.; Stahl, S. S. *J. Am. Chem. Soc.* **2009**, *131*, 1589.
- (81) Kazi, B.; Kiss, L.; Forro, E.; Filóp, F. *Tetrahedron Lett.* **2010**, *51*, 82.
- (82) Hanessian, S.; Schaum, R. *Tetrahedron Lett.* **1997**, *38*, 163.
- (83) Ordonez, M.; Cativiela, C. *Tetrahedron Asymmetry* **2007**, *18*, 3.
- (84) Chi, Y.; Guo, L.; Kopf, N. A.; Gellman, S. H. *J. Am. Chem. Soc.* **2008**, *130*, 5608.
- (85) Smreina, M.; Majer, P.; Majerova, E.; Guerassina, T. A.; Eissenstat, M. A. *Tetrahedron* **1997**, *53*, 12867.
- (86) Loukas, V.; Noula, C.; Kokotos, G. *J. Pept. Sci.* **2003**, *9*, 312.
- (87) Liljeblad, A.; Kanerva, L. T. *Tetrahedron* **2006**, *62*, 5831.
- (88) Corvo, M. C.; Pereira, M. M. *Amino Acids* **2007**, *32*, 243.
- (89) Gil, S.; Parra, M.; Rodríguez, P. *Molecules* **2008**, *13*, 716.
- (90) Guo, L.; Chi, Y.; Almeida, A. M.; Guzei, I. A.; Parker, B. K.; Gellman, S. H. *J. Am. Chem. Soc.* **2009**, *131*, 16018.
- (91) Deng, J.; Hu, X.-P.; Huang, J.-D.; Yu, S.-B.; Wang, D.-Y.; Duan, Z.-C.; Zheng, Z. *J. Org. Chem.* **2008**, *73*, 6022.
- (92) Saavedra, C.; Hernandez, R.; Boto, A.; Alvarez, E. *J. Org. Chem.* **2009**, *74*, 4655.
- (93) Venkatraman, J.; Shankaramma, S. C.; Balaram, P. *Chem. Rev.* **2001**, *101*, 3131.
- (94) Prasad, B. V. V.; Balaram, P. *CRC Crit. Rev. Biochem.* **1984**, *16*, 307.
- (95) Karle, I. L.; Balaram, P. *Biochemistry* **1990**, *29*, 6747.
- (96) Toniolo, C.; Benedetti, E. *Macromolecules* **1991**, *24*, 4004.
- (97) Abele, S.; Seiler, P.; Seebach, D. *Helv. Chim. Acta* **1999**, *82*, 1559.
- (98) Seebach, D.; Abele, S.; Sifferlen, T.; Hänggi, M.; Gruner, S.; Seiler, P. *Helv. Chim. Acta* **1998**, *81*, 2218.
- (99) Ananda, K.; Aravinda, S.; Vasudev, P. G.; Raja, K. M. P.; Sivaramakrishnan, H.; Nagarajan, K.; Shamala, N.; Balaram, P. *Curr. Sci.* **2003**, *85*, 1002.
- (100) Vasudev, P. G.; Ananda, K.; Chatterjee, S.; Aravinda, S.; Shamala, N.; Balaram, P. *J. Am. Chem. Soc.* **2007**, *129*, 4039.
- (101) Vasudev, P. G.; Chatterjee, S.; Ananda, K.; Shamala, N.; Balaram, P. *Angew. Chem., Int. Ed.* **2008**, *47*, 6430.
- (102) Ananda, K.; Vasudev, P. G.; Sengupta, A.; Raja, K. M. P.; Shamala, N.; Balaram, P. *J. Am. Chem. Soc.* **2005**, *127*, 16668.
- (103) Chatterjee, S.; Vasudev, P. G.; Ragothama, S.; Ramakrishnan, C.; Shamala, N.; Balaram, P. *J. Am. Chem. Soc.* **2009**, *131*, 5956.
- (104) Aravinda, S.; Ananda, K.; Shamala, N.; Balaram, P. *Chem.—Eur. J.* **2003**, *9*, 4789.
- (105) Vasudev, P. G.; Chatterjee, S.; Shamala, N.; Balaram, P. *Acc. Chem. Res.* **2009**, *42*, 1628.
- (106) Vasudev, P. G.; Chatterjee, S.; Ramakrishnan, C.; Shamala, N.; Balaram, P. *Biopolymers (Pept. Sci.)* **2009**, *92*, 426.
- (107) Balaram, P. *Biopolymers (Pept. Sci.)* **2010**, *92*, 426.
- (108) Chung, Y. J.; Christianson, L. A.; Stanger, H. E.; Powell, D. R.; Gellman, S. H. *J. Am. Chem. Soc.* **1998**, *120*, 10555.
- (109) Chung, Y. J.; Huck, B., R.; Christianson, L. A.; Stranger, H. E.; Krauthauer, S.; Powell, D. R.; Gellman, S. H. *J. Am. Chem. Soc.* **2000**, *122*, 3995.
- (110) Guo, L.; Almeida, A. M.; Zhang, W.; Reidenbach, A. G.; Choi, S. H.; Guzei, I. A.; Gellman, S. H. *J. Am. Chem. Soc.* **2010**, *132*, 7868.
- (111) Pavone, V.; Di Blasio, B.; Lombardi, A.; Isernia, C.; Pedone, C.; Benedetti, E.; Valle, G.; Crisma, M.; Toniolo, C.; Kishore, R. *J. Chem. Soc., Perkin Trans. 2* **1992**, 1233.
- (112) Thakur, A. K.; Venugopalan, P.; Kishore, R. *J. Pept. Res.* **2000**, *56*, 55.
- (113) Thakur, A. K.; Venugopalan, P.; Kishore, R. *Biochem. Biophys. Res. Commun.* **2000**, *273*, 492.
- (114) Halder, D.; Banerjee, A.; Drew, M. G. W.; Das, A. K.; Banerjee, A. *Chem. Commun.* **2003**, 1406.
- (115) Maji, S. K.; Malik, S.; Drew, M. G. B.; Nandi, A. K.; Banerjee, A. *Tetrahedron Lett.* **2003**, *44*, 4103.
- (116) Bhadbhade, M. M.; Kishore, R. *Biochem. Biophys. Res. Commun.* **2004**, *316*, 1029.
- (117) Thakur, A. K.; Kishore, R. *Tetrahedron Lett.* **1998**, *39*, 9553.
- (118) Sengupta, A.; Aravinda, S.; Shamala, N.; Raja, K. M. P.; Balaram, P. *Org. Biomol. Chem.* **2006**, *4*, 4214.
- (119) Maji, S. K.; Banerjee, R.; Velumurugan, D.; Razak, A.; Fun, H. K.; Banerjee, A. *J. Org. Chem.* **2002**, *67*, 633.
- (120) Roy, R. S.; Gopi, H. N.; Ragothama, S.; Karle, I. L.; Balaram, P. *Chem.—Eur. J.* **2006**, *12*, 3295.
- (121) Rai, R.; Vasudev, P. G.; Ananda, K.; Ragothama, S.; Shamala, N.; Karle, I. L.; Balaram, P. *Chem.—Eur. J.* **2007**, *12*, 3295.
- (122) Gademann, K.; Jaun, B.; Seebach, D.; Perozzo, R.; Scapozza, L.; Folkers, G. *Helv. Chim. Acta* **1999**, *82*, 1.
- (123) Etezady-Esfarjani, T.; Hilti, C.; Wüthrich, K.; Rueping, M.; Schreiber, J.; Seebach, D. *Helv. Chim. Acta* **2002**, *85*, 1197.
- (124) Seebach, D.; Brenner, M.; Rueping, M.; Jaun, B. *Chem.—Eur. J.* **2002**, *8*, 573.
- (125) Mathad, R. I.; Jaun, B.; Flögel, O.; Gardiner, J.; Löweneck, M.; Codée, J. D. C.; Seeberger, P. H.; Seebach, D.; Edmonds, M. K.; Graichen, F. H. M.; Abell, A. D. *Helv. Chim. Acta* **2007**, *90*, 2251.
- (126) Huggins, M. L. *Annu. Rev. Biochem.* **1942**, *11*, 27.
- (127) Huggins, M. L. *Chem. Rev.* **1943**, *32*, 195.
- (128) Pauling, L.; Corey, R. B. *Proc. Natl. Acad. Sci. U. S. A.* **1951**, *37*, 729.
- (129) Venkatachalam, C. M. *Biopolymers* **1968**, *6*, 1425.
- (130) Wilmot, C. M.; Thornton, J. M. *J. Mol. Biol.* **1988**, *203*, 221.
- (131) Mathews, B. W. *Macromolecules* **1972**, *5*, 818.
- (132) Milner -White, E. J.; Poet, R. *Biochem. J.* **1986**, *240*, 289.
- (133) Milner -White, E. J.; Poet, R. *Trends Biochem. Sci.* **1987**, *12*, 189.
- (134) Milner -White, E. J.; Ross, B. M.; Ismail, R.; Belhadj-Mostefa, K.; Poet, R. *J. Mol. Biol.* **1988**, *204*, 777.
- (135) Milner -White, E. J. *J. Mol. Biol.* **1990**, *216*, 385.
- (136) Bonora, G. M.; Toniolo, C.; Di Blasio, B.; Pavone, V.; Pedone, C.; Benedetti, E.; Lingham, I.; Hardy, P. *J. Am. Chem. Soc.* **1984**, *106*, 8152.
- (137) Toniolo, C.; Benedetti, E. *Molecular Conformation and Biological Interactions*, Balaram, P.; Ramaseshan, S., Eds. Indian Academy of Sciences: Bangalore, 1991, 511.
- (138) Baldauf, C.; Günther, R.; Hofmann, H. *J. J. Org. Chem.* **2004**, *69*, 6214.
- (139) Schramm, P.; Hofmann, H. *J. THEOCHEM* **2009**, *907*, 109.
- (140) Jimenez, A. I.; Ballano, G.; Cativiela, C. *Angew. Chem., Int. Ed.* **2004**, *44*, 396.
- (141) Vasudev, P. G.; Ananda, K.; Shamala, N.; Balaram, P. *Angew. Chem., Int. Ed.* **2005**, *44*, 4972.
- (142) Vasudev, P. G.; Rai, R.; Shamala, N.; Balaram, P. *Biopolymers (Pept. Sci.)* **2008**, *90*, 138.
- (143) Wu, Y.-D.; Wang, D.-P. *J. Am. Chem. Soc.* **1998**, *120*, 13485.
- (144) Lin, J.-Q.; Luo, S.-W.; Wu, Y.-D. *J. Comput. Chem.* **2002**, *23*, 1551.
- (145) Wu, Y.-D.; Han, W.; Wang, D.-P.; Gao, Y.; Zhao, Y.-L. *Acc. Chem. Res.* **2008**, *41*, 1418.
- (146) Wu, Y.-D.; Lin, J.-Q.; Zhao, Y.-L. *Helv. Chim. Acta* **2002**, *85*, 3144.
- (147) Bernado, P.; Alemán, C.; Puiggalí, J. *Macromol. Theory Simul.* **1998**, *7*, 659.
- (148) Zhu, X.; Koenig, P.; Hoffmann, M.; Yethiraj, A.; Ciu, Q. *J. Comput. Chem.* **2010**, *31*, 2063.
- (149) Keller, B.; Gattin, Z.; van Gunsteren, W. F. *Proteins Struct. Funct. Gen.* **2010**, *78*, 1677.
- (150) Mohle, K.; Gunther, R.; Thormann, M.; Sewald, N.; Hofmann, H. *J. Biopolymers* **1999**, *50*, 167.
- (151) Baldauf, C.; Günther, R.; Hofmann, H. *J. Helv. Chim. Acta* **2003**, *86*, 2573.
- (152) Daura, X.; van Gunsteren, W. F.; Rigo, D.; Jaun, B.; Seebach, D. *Chem.—Eur. J.* **1997**, *3*, 1410.
- (153) Daura, X.; Jaun, B.; Seebach, D.; van Gunsteren, W. F.; Mark, A. E. *J. Mol. Biol.* **1998**, *280*, 925.
- (154) Daura, X.; Gademann, K.; Jaun, B.; Seebach, D.; van Gunsteren, W. F.; Mark, A. E. *Angew. Chem., Int. Ed.* **1999**, *38*, 236.
- (155) Seebach, D.; Schreiber, J. V.; Abele, S.; Daura, X.; van Gunsteren, W. F. *Helv. Chim. Acta* **2000**, *83*, 34.
- (156) Daura, X.; Gademann, K.; Schafer, H.; Seebach, D.; van Gunsteren, W. F.; Mark, A. E. *Acc. Chem. Res.* **2001**, *123*, 2393.
- (157) Glatth, A.; Seebach, D.; van Gunsteren, W. F. *Helv. Chim. Acta* **2004**, *87*, 2487.
- (158) Glatth, A.; Daura, X.; Bindschadler, P.; Jaun, B.; Mahajan, Y. R.; Mathad, R. I.; Rueping, M.; seebach, D.; van Gunsteren, W. F. *Chem.—Eur. J.* **2005**, *11*, 7276.
- (159) Gunasekaran, K.; Ramakrishnan, C.; Balaram, P. *Protein Eng.* **1997**, *10*, 1131.
- (160) Sibanda, B. L.; Thornton, J. M. *Nature* **1985**, *316*, 170.
- (161) Rao, P.; Nagaraj, R.; Rao, C. N. R.; Balaram, P. *FEBS Lett.* **1979**, *100*, 244.
- (162) Schmitt, M. A.; Choi, S. H.; Guzei, I. A.; Gellman, S. H. *J. Am. Chem. Soc.* **2005**, *127*, 13130.
- (163) Schmitt, M. A.; Choi, S. H.; Guzei, I. A.; Gellman, S. H. *J. Am. Chem. Soc.* **2006**, *128*, 4538.
- (164) Choi, S. H.; Guzei, I. A.; Spencer, L. C.; Gellman, S. H. *J. Am. Chem. Soc.* **2009**, *131*, 2917.
- (165) Horne, W. S.; Price, J. L.; Keck, J. L.; Gellman, S. H. *J. Am. Chem. Soc.* **2007**, *129*, 4178.
- (166) Chatterjee, S.; Vasudev, P. G.; Ragothama, S.; Shamala, N.; Balaram, P. *Biopolymers (Pept. Sci.)* **2008**, *90*, 759.
- (167) Hayen, A.; Schmitt, M. A.; Ngassa, F. N.; Thomasson, K. A.; Gellman, S. H. *Angew. Chem., Int. Ed.* **2004**, *43*, 505.
- (168) Schmitt, M. A.; Weisblum, B.; Gellman, S. H. *J. Am. Chem. Soc.* **2004**, *126*, 6848.

- (169) Sadowsky, J. D.; Schmitt, M. A.; Lee, H.-S.; Umezawa, N.; Wang, S.; Tomita, Y.; Gellman, S. H. *J. Am. Chem. Soc.* **2005**, *127*, 11966.
- (170) Sadowsky, J. D.; Fairlie, W. D.; Hadley, E. B.; Lee, H. S.; Umezawa, N.; Nikolovska-Coleska, Z.; Wang, S. M.; Huang, D. C. S.; Tomita, Y.; Gellman, S. H. *J. Am. Chem. Soc.* **2007**, *129*, 139.
- (171) Schmitt, M. A.; Weisblum, B.; Gellman, S. H. *J. Am. Chem. Soc.* **2007**, *129*, 417.
- (172) Price, J. L.; Horne, W. S.; Gellman, S. H. *J. Am. Chem. Soc.* **2007**, *129*, 6376.
- (173) De Pol, S.; Zorn, C.; Klein, C. D.; Zerbe, O.; Reiser, O. *Angew. Chem., Int. Ed.* **2004**, *43*, 511.
- (174) Sharma, G. V. M.; Nagendar, P.; Jayaprakash, P.; Krishna, P. R.; Ramakrishna, K. V. S.; Kunwar, A. C. *Angew. Chem., Int. Ed.* **2005**, *44*, 5878.
- (175) Srinivasulu, G.; Kumar, S. K.; Sharma, G. V. M.; Kunwar, A. C. *J. Org. Chem.* **2006**, *71*, 8395.
- (176) Seebach, D.; Jaun, B.; Sebesta, R.; Mathad, R. I.; Flogel, O.; Limbach, M.; Sellner, H.; Cottens, S. *Helv. Chim. Acta* **2006**, *89*, 1801.
- (177) Sharma, G. V. M.; Jadhav, V. B.; Ramakrishna, K. V. S.; Jayaprakash, P.; Narasimulu, K.; Subash, V.; Kunwar, A. C. *J. Am. Chem. Soc.* **2006**, *128*, 14657.
- (178) Park, J. S.; Lee, H. S.; Lai, J. R.; Kim, B. M.; Gellman, S. H. *J. Am. Chem. Soc.* **2003**, *125*, 8539.
- (179) Woll, M. G.; Fisk, J. D.; LePlae, P. R.; Gellman, S. H. *J. Am. Chem. Soc.* **2002**, *124*, 12447.
- (180) Porter, E. A.; Wang, X.; Schmitt, M. A.; Gellman, S. H. *Org. Lett.* **2002**, *4*, 3317.
- (181) LePlae, P. R.; Fisk, J. D.; Porter, E. A.; Weisblum, B.; Gellman, S. H. *J. Am. Chem. Soc.* **2002**, *124*, 6820.
- (182) Hintermann, T.; Gademann, K.; Jaun, B.; Seebach, D. *Helv. Chim. Acta* **1998**, *81*, 983.
- (183) Sharma, G. V.; Chandramouli, N.; Chodhary, M.; Nagender, P.; Ramakrishna, K. V. S.; Kunwar, A. C.; Schramm, P.; Hofmann, H.-J. *J. Am. Chem. Soc.* **2009**, *131*, 17335.
- (184) Araghi, R. R.; Jäckel, C.; Cölfen, H.; Salwiczek, M.; Völkel, A.; Wagner, S. C.; Wieczorek, S.; Baldauf, C.; Koksch, B. *ChemBioChem* **2010**, *11*, 335.
- (185) Baldauf, C.; Günther, R.; Hofmann, H. *J. Biopolymers* **2006**, *84*, 408.
- (186) Baldauf, C.; Günther, R.; Hofmann, H. *J. J. Org. Chem.* **2006**, *71*, 1200.
- (187) Schramm, P.; Sharma, G. V. M.; Hofmann, H. *J. Biopolymers (Pept. Sci.)* **2010**, *94*, 279.
- (188) Pavone, V.; Gaeta, G.; Lombardi, A.; Nastri, F.; Maglio, O.; Isernia, C.; Saviano, M. *Biopolymers* **1996**, *38*, 705.
- (189) Ramakrishnan, C.; Natraj, D. V. *J. Pept. Sci.* **1998**, *4*, 269.
- (190) Roy, R. S.; Karle, I. L.; Raghothama, S.; Balaram, P. *Proc. Natl. Acad. Sci. U. S. A.* **2004**, *101*, 16478.
- (191) Chatterjee, S.; Vasudev, P. G.; Ananda, K.; Raghothama, S.; Shamala, N.; Balaram, P. *J. Org. Chem.* **2008**, *73*, 6595.
- (192) Zimmerman, S. S.; Scheraga, H. A. *Biopolymers* **1977**, *16*, 811.
- (193) Choi, S. H.; Guzei, I. A.; Gellman, S. H. *J. Am. Chem. Soc.* **2007**, *129*, 13780.
- (194) Choi, S. H.; Guzei, I. A.; Spencer, L. C.; Gellman, S. H. *J. Am. Chem. Soc.* **2008**, *130*, 6544.
- (195) Chandrasekaran, R.; Jardetzky, T. S.; Jardetzky, O. *FEBS Lett.* **1979**, *101*, 11.
- (196) Lewis, M.; Chang, G.; Horton, N. C.; Kercher, M. A.; Pace, H. C.; Schumacher, M. A.; Brennan, R. G.; Lu, P. *Science* **1996**, *271*, 1247.
- (197) Daniels, D. S.; Petersson, E. J.; Qui, J. X.; Schepartz, A. *J. Am. Chem. Soc.* **2007**, *129*, 1532.
- (198) Goodman, J. L.; Petersson, E. J.; Daniels, D. S.; Qiu, J. X.; Schepartz, A. *J. Am. Chem. Soc.* **2007**, *129*, 14746.
- (199) Seebach, D.; Gademann, K.; Schreiber, J. V.; Matthews, J. L.; Hintermann, T.; Jaun, B.; Oberer, L.; Hommel, U.; Widmer, H. *Helv. Chim. Acta* **1997**, *80*, 2033.
- (200) Seebach, D.; Abele, S.; Gademann, K.; Guichard, G.; Hintermann, T.; Jaun, B.; Matthews, J. L.; Schreiber, J. V. *Helv. Chim. Acta* **1998**, *81*, 932.
- (201) Rueping, M.; Schreiber, J. V.; Lelais, G.; Jaun, B.; Seebach, D. *Helv. Chim. Acta* **2002**, *85*, 2577.
- (202) Gunasekaran, K.; Gomathi, L.; Ramakrishnan, C.; Chandrasekhar, J.; Balaram, P. *J. Mol. Biol.* **1998**, *284*, 1505.
- (203) Awasthi, S. K.; Raghothama, S.; Balaram, P. *Biochem. Biophys. Res. Commun.* **1995**, *201*, 375.
- (204) Raghothama, S.; Awasthi, S. K.; Balaram, P. *J. Chem. Soc., Perkin Trans. 2* **1998**, *1*, 137.
- (205) Karle, I. L.; Awasthi, S. K.; Balaram, P. *Proc. Natl. Acad. Sci. U. S. A.* **1996**, *93*, 8189.
- (206) Das, C.; Nagan Gowda, G. A.; Karle, I. L.; Balaram, P. *Biopolymers* **2001**, *58*, 335.
- (207) Karle, I. L.; Gopi, H. N.; Balaram, P. *Proc. Natl. Acad. Sci. U. S. A.* **2001**, *98*, 3716.
- (208) Karle, I. L.; Gopi, H. N.; Balaram, P. *Proc. Natl. Acad. Sci. U. S. A.* **2002**, *99*, 5160.
- (209) Gopi, H. N.; Roy, R. S.; Raghothama, S.; Karle, I. L.; Balaram, P. *Helv. Chim. Acta* **2002**, *85*, 3313.
- (210) Gellman, S. H. *Curr. Opin. Chem. Biol.* **1998**, *2*, 717.
- (211) Schenck, H. L.; Gellman, S. H. *J. Am. Chem. Soc.* **1998**, *120*, 4869.
- (212) Haque, T. S.; Gellman, S. H. *J. Am. Chem. Soc.* **1997**, *119*, 2303.
- (213) Espinosa, J. F.; Gellman, S. H. *Angew. Chem., Int. Ed.* **2000**, *39*, 2330.
- (214) Aravinda, S.; Shamala, N.; Rai, R.; Gopi, H. N.; Balaram, P. *Angew. Chem., Int. Ed.* **2002**, *41*, 3863.
- (215) Harini, V. V.; Aravinda, S.; Rai, R.; Shamala, N.; Balaram, P. *Chem.—Eur. J.* **2005**, *11*, 3609.
- (216) Hughes, R. M.; Waters, M. L. *Curr. Opin. Struct. Biol.* **2006**, *16*, 514.
- (217) Robinson, J. A. *Acc. Chem. Res.* **2008**, *41*, 1278.
- (218) Ramirez-Alvarado, M.; Blanco, F. J.; Serrano, L. *Nat. Struct. Biol.* **1996**, *3*, 604.
- (219) Blanco, F. J.; Rivas, G.; Serrano, L. *Nat. Struct. Biol.* **1994**, *1*, 584.
- (220) Blanco, F. J.; Jimenez, M. A.; Herranz, J.; Rico, M.; Santoro, J.; Nieto, J. L. *J. Am. Chem. Soc.* **1993**, *115*, 5887.
- (221) Searle, M. S.; Williams, D. H.; Packman, L. C. *Nat. Struct. Biol.* **1995**, *2*, 999.
- (222) Maynard, A. J.; Searle, M. S. *Chem. Commun.* **1997**, *14*, 1297.
- (223) Sharman, G. J.; Searle, M. S. *Chem. Commun.* **1997**, *20*, 1955.
- (224) De Alba, E.; Rico, M.; Jimenez, M. A. *Protein Sci.* **1999**, *8*, 2234.
- (225) Creighton, T. E. *Proteins: Structure and Molecular Properties*, 2nd ed.; W. H. Freeman and Company: New York, 1993.
- (226) Brenner, M.; Seebach, D. *Helv. Chim. Acta* **2001**, *84*, 2155.
- (227) Rai, R.; Raghothama, S. R.; Balaram, P. *J. Am. Chem. Soc.* **2006**, *128*, 2675.
- (228) Krauthausen, S.; Christianson, L. A.; Powell, D. R.; Gellman, S. H. *J. Am. Chem. Soc.* **1997**, *119*, 11719.
- (229) Sengupta, A.; Roy, R. S.; Sabareesh, S.; Shamala, N.; Balaram, P. *Org. Biomol. Chem.* **2006**, *4*, 1166.
- (230) Woll, M. G.; Lai, J. R.; Guzei, I. A.; Taylor, S. J. C.; Smith, M. E. B.; Gellman, S. H. *J. Am. Chem. Soc.* **2001**, *123*, 11077.
- (231) Seebach, D.; Abele, S.; Gademann, K.; Jaun, B. *Angew. Chem., Int. Ed.* **1999**, *38*, 1595.
- (232) Shamala, N.; Nagaraj, R.; Balaram, P. *J. Chem. Soc. Chem. Commun.* **1978**, *22*, 996.
- (233) Aravinda, S.; Shamala, N.; Balaram, P. *Chem. Biodiversity* **2008**, *5*, 1238.
- (234) Toniolo, C.; Crisma, M.; Bonora, G. M.; Benedetti, E.; Di Blasio, B.; Pavone, V.; Pedone, C.; Santini, A. *Biopolymers* **1991**, *31*, 129.
- (235) Bardi, R.; Piazzesi, A. M.; Toniolo, C.; Sukumar, M.; Antony Raj, P.; Balaram, P. *Int. J. Pept. Protein Res.* **1985**, *25*, 628.
- (236) Paul, P. K. C.; Sukumar, M.; Bardi, R.; Piazzesi, A. M.; Valle, G.; Toniolo, C.; Balaram, P. *J. Am. Chem. Soc.* **1986**, *108*, 6363.
- (237) Mazzeo, M.; Isernia, C.; Rossi, F.; Saviano, M.; Pedone, C.; Paolillo, L.; Benedetti, E.; Pavone, V. *J. Pept. Sci.* **1995**, *1*, 330.
- (238) Di Blasio, B.; Lombardi, A.; Nastri, F.; Saviano, M.; Pedone, C.; Yamada, T.; Nakao, M.; Kuwata, S.; Pavone, V. *Biopolymers* **1992**, *32*, 1155.
- (239) Crisma, M.; Bonora, G. M.; Toniolo, C.; Barone, V.; Benedetti, E.; Di Blasio, B.; Pavone, V.; Pedone, C.; Santini, A.; Fraternali, F. *Int. J. Biol. Macromol.* **1989**, *11*, 345.
- (240) Saviano, M.; Isernia, C.; Rossi, F.; Di Blasio, B.; Iacovino, R.; Mazzeo, M.; Pedone, C.; Benedetti, E. *Biopolymers* **2000**, *53*, 189.
- (241) Horne, W. S.; Price, J. L.; Gellman, S. H. *Proc. Natl. Acad. Sci. U. S. A.* **2008**, *105*, 9151.
- (242) Giuliano, M. W.; Horne, W. S.; Gellman, S. H. *J. Am. Chem. Soc.* **2009**, *131*, 9860.
- (243) Seebach, D.; Mathad, R. I.; Kimmerlin, T.; Mahajan, Y. R.; Bindschäler, P.; Rueping, R.; Jaun, B. *Helv. Chim. Acta* **2005**, *88*, 1969.
- (244) Abdel-Magid, A.-F.; Cohen, J-H; Maryanoff, C. A. *Curr. Med. Chem.* **1999**, *6*, 955.
- (245) Juaristi, E.; Lopez-Ruiz, H. *Curr. Med. Chem.* **1999**, *6*, 983.
- (246) Hinterman, T.; Seebach, D. *Chimia* **1997**, *51*, 244.
- (247) Seebach, D.; Abele, S.; Schreiber, J. V.; Martinoni, B.; Nussbaum, A. K.; Schild, H.; Schulz, H.; Hennecke, H.; Woessner, R.; Bitsch, F. *Chimia* **1998**, *52*, 734.
- (248) Frackenpohl, J.; Arvidsson, P. I.; Schreiber, J. V.; Seebach, D. *ChemBioChem* **2001**, *2*, 445.
- (249) Seebach, D.; Rueping, M.; Arvidsson, P. I.; Kimmerlin, T.; Micuch, P.; Noti, C.; Langenegger, D.; Hoyer, D. *Helv. Chim. Acta* **2001**, *84*, 3503.
- (250) Lelais, G.; Seebach, D. *Helv. Chim. Acta* **2003**, *86*, 4152.
- (251) Hook, D.; Gessier, F.; Noti, C.; Kast, P.; Seebach, D. *ChemBioChem* **2004**, *5*, 691.
- (252) Porter, E. A.; Weisblum, B.; Gellman, S. H. *J. Am. Chem. Soc.* **2002**, *124*, 7324.
- (253) Hintermann, T.; Seebach, D. *Chimia* **1997**, *50*, 244.

- (254) Park, H. D.; Sasaki, Y.; Maruyama, T.; Yanagisawa, E.; Hiraishi, A.; Kato, K. *Environ. Toxicol.* **2001**, *16*, 337.
- (255) Saito, T.; Okano, K.; Park, H. D.; Itayama, T.; Inamori, Y.; Neilan, B. A.; Burns, B. P.; Sugiura, N. *FEBS Microbiol. Lett.* **2003**, *229*, 271.
- (256) Schreiber, J. V.; Frackenpohl, J.; Moser, F.; Fleischmann, T.; Kohler, H.-P. E.; Seebach, D. *ChemBioChem* **2002**, *3*, 424.
- (257) Geueke, B.; Namoto, K.; Seebach, D.; Kohler, H.-P. *E. J. Bacteriol.* **2005**, *187*, 5910.
- (258) Scorpio, A.; Cabot, D. J.; Day, W. A.; O'Brien, D. K.; Vietri, N. J.; Itoh, Y.; Mohamadzadeh, M.; Friedlander, A. M. *Antimicrob. Agents Chemother.* **2007**, *51*, 215.
- (259) Ashiuchi, M.; Nakamura, H.; Yamamoto, M.; Misono, H. *J. Biosci. Bioeng.* **2006**, *102*, 60.
- (260) Kimura, K.; Itoh, Y. *Appl. Environ. Microbiol.* **2003**, *69*, 2491.
- (261) Heck, T.; Limbach, M.; Geueke, B.; Zacharias, M.; Gardiner, J.; Kohler, H. P.; Seebach, D. *Chem. Biodivers.* **2006**, *3*, 1325.
- (262) Gopi, H. N.; Ravindra, G.; Pal, P. P.; Patnaik, P.; Balaram, H.; Balaram, P. *FEBS Lett.* **2003**, *535*, 175.
- (263) Kallenbach, N. R.; Gong, Y. *Bioorg. Med. Chem.* **1999**, *7*, 143.
- (264) Sukumar, M.; Giersch, L. M. *Folding Des.* **1997**, *2*, 211.
- (265) Karle, I. L.; Flippin-Anderson, J. L.; Uma, K.; Balaram, P. *Int. J. Pept. Protein Res.* **1993**, *42*, 401.
- (266) Das, C.; Shankaramma, S. C.; Balaram, P. *Chem.—Eur. J.* **2001**, *7*, 840.
- (267) Aravinda, S.; Shamala, N.; Pramanik, A.; Das, C.; Balaram, P. *Biochem. Biophys. Res. Commun.* **2000**, *273*, 933.
- (268) Fernandez-Santin, J. M.; Muñoz-Guerra, S.; Rodriguez-Galan, A.; Aymami, J.; Lloveras, J.; Subirana, J. A.; Giralt, E.; Ptak, M. *Macromolecules* **1987**, *20*, 62.
- (269) Lopez-Carrasco, F.; Alemán, C.; Garcia-Alvarez, M.; de Ilarduya, A. M.; Muñoz-Guerra, S. *Macromol. Chem. Phys.* **1995**, *196*, 253.
- (270) Melis, J.; Zanuy, D.; Alemán, C.; Garcia-Alvarez, M.; Muñoz-Guerra, S. *Macromolecules* **2002**, *35*, 8774.
- (271) Candel, T.; Fouet, A. *Mol. Microbiol.* **2006**, *60*, 1091.
- (272) Weber, J. *J. Biol. Chem.* **1990**, *265*, 9664.
- (273) Miyazawa, T. *J. Polym. Sci.* **1961**, *55*, 215.
- (274) Lopez-Carrasco, F.; Garcia-Alvarez, M.; Navas, J. J.; Alemán, C.; Muñoz-Guerra, S. *Macromolecules* **1996**, *29*, 8449.
- (275) Werder, M.; Hauser, H.; Abele, S.; Seebach, D. *Helv. Chim. Acta* **1999**, *82*, 1774.
- (276) Karlsson, A. J.; Pomerantz, W. C.; Weisblum, B.; Gellman, S. H.; Palecek, S. P. *J. Am. Chem. Soc.* **2006**, *128*, 12630.
- (277) Karlsson, A. J.; Pomerantz, W. C.; Neilsen, K. J.; Gellman, S. H.; Palecek, S. P. *ACS Chem. Biol.* **2009**, *4*, 567.
- (278) Chiba, H.; Agematu, H.; Sakai, K.; Dobashi, K.; Yoshioka, T. J. *Antibiot.* **1999**, *52*, 710.
- (279) Liu, D.; DeGrado, W. F. *J. Am. Chem. Soc.* **2001**, *123*, 7553.
- (280) Hamuro, Y.; Schneider, J. P.; DeGrado, W. F. *J. Am. Chem. Soc.* **1999**, *121*, 12200.
- (281) Arvidsson, P. I.; Frankenpol, J.; Ryder, N. S.; Liechty, B.; Peterson, F.; Zimmermann, H.; Camenisch, G. P.; Woessner, R.; Seebach, D. *ChemBioChem* **2001**, *2*, 771.
- (282) Arvidsson, P. I.; Ryder, N. S.; Weiss, H. M.; Gross, G.; Kretz, O.; Woessner, R.; Seebach, D. *ChemBioChem* **2003**, *4*, 1345.
- (283) Serrano, G. N.; Zhan, G. G.; Schweizer, F. *Antimicrob. Agents Chemother.* **2009**, *53*, 2215.
- (284) Porter, E. A.; Wang, X.; Lee, H. S.; Weisblum, B.; Gellman, S. H. *Nature* **2000**, *404*, 565.
- (285) Gademann, K.; Seebach, D. *Helv. Chim. Acta* **1999**, *82*, 957.
- (286) De Simone, C.; Famularo, G. *Carnitine Today*; Springer: Heidelberg Germany, 1997.
- (287) Ferrari, R.; Di Mauro, S.; Sherwood, G. L. *Carnitine and Its Role in Medicine: From Function to Therapy*; Academic Press: San Diego, CA, 1992.
- (288) Fritz, I. B. *Current Concepts in Carnitine Research*; Karter, A. L., Ed.; CRC: Boca Raton, FL, 1992; p. 107.
- (289) Gademann, K.; Ernst, M.; Seebach, D. *Helv. Chim. Acta* **2000**, *83*, 16.
- (290) Gademann, K.; Ernst, M.; Hoyer, D.; Seebach, D. *Angew. Chem., Int. Ed.* **1999**, *38*, 1223.
- (291) Gademann, K.; Kimmerlin, T.; Hoyer, D.; Seebach, D. *J. Med. Chem.* **2001**, *44*, 2460.
- (292) Seebach, D.; Schaeffer, L.; Brenner, M.; Hoyer, D. *Angew. Chem., Int. Ed.* **2003**, *42*, 776.
- (293) Wiegand, H.; Wirz, B.; Schweitzer, A.; Gross, G.; Perez, M. I. R.; Andres, H.; Kimmerlin, T.; Rueping, M.; Seebach, D. *Chem. Biodiversity* **2004**, *1*, 1812.
- (294) Seebach, D.; Dubost, E.; Mathad, R. I.; Jaun, B.; Limbach, M.; Löweneck, M.; Flögel, O.; Gardiner, J.; Capone, S.; Beck, A. K.; Widmer, H.; Langenegger, Monaa, D.; Hoyer, D. *Helv. Chim. Acta* **2008**, *91*, 1736.
- (295) Rueping, M.; Mahajan, Y.; Sauer, M.; Seebach, D. *ChemBioChem* **2002**, *3*, 257.
- (296) Seebach, D.; Namoto, K.; Mahajan, Y. R.; Bindschadler, P.; Sustmann, R.; Kirsch, M.; Ryder, N. S.; Weiss, M.; Sauer, M.; Roth, C.; Werner, S.; Beer, H.-D.; Mundig, C.; Walde, P.; Voser, M. *Chem. Biodiversity* **2004**, *1*, 65.
- (297) Geueke, B.; Namoto, K.; Agarkova, I.; Perriard, J.-C.; Kohler, H.-P.; Seebach, D. *ChemBioChem* **2005**, *6*, 982.
- (298) Hitz, T.; Iten, R.; Gardiner, J.; Namoto, K.; Walde, P.; Seebach, D. *Biochemistry* **2006**, *45*, 5817.
- (299) Weiss, H. M.; Wirz, B.; Schweitzer, A.; Amututz, R.; Perez, M. I. R.; Andres, H.; Metz, Y.; Gardiner, J.; Seebach, D. *Chem. Biodiversity* **2007**, *4*, 1413.
- (300) Shih, C. L.; Gossett, S.; Gruber, J. M.; Grossman, C. S.; Andis, S. L.; Schultz, R. M.; Worzalla, J. F.; Coebett, T. H.; Metz, J. T. *Bioorg. Med. Chem. Lett.* **1999**, *9*, 69.
- (301) Quinn, P. J.; Boldyrev, A. A.; Formazuyk, V. E. *Mol. Aspects Med.* **1992**, *13*, 379.
- (302) Wani, M. C.; Taylor, H. L.; Wall, M. E.; Coggon, P.; McPhail, A. T. *J. Am. Chem. Soc.* **1971**, *93*, 2325.
- (303) Ojima, I.; Lin, S.; Wang, T. *Curr. Med. Chem.* **1999**, *6*, 927.
- (304) Nicolaou, K. C.; Dai, W.-M.; Guy, R. K. *Angew. Chem., Int. Ed.* **1994**, *33*, 15.
- (305) Riniker, B.; Schwyz, R. *Helv. Chim. Acta* **1964**, 2357.
- (306) Chaturvedi, N. C.; Park, W. K.; Smeby, R. R.; Bumpus, F. M. *J. Med. Chem.* **1970**, *13*, 177.
- (307) Stachowiak, K.; Khosla, M. C.; Plucinska, K.; Khairallah, P. A.; Bumpus, F. M. *J. Med. Chem.* **1979**, *22*, 1128.
- (308) Manning, M.; du Vigneaud, V. *Biochemistry* **1965**, *4*, 1884.
- (309) Ondetti, M. A.; Engel, S. L. *J. Med. Chem.* **1975**, *18*, 761.
- (310) Rodriguez, M.; Fulcrand, P.; Laur, J.; Aumelas, A.; Bali, J. P.; Martinez, J. *J. Med. Chem.* **1989**, *32*, 522.
- (311) Llinares, M.; Devin, C.; Azay, J.; Berge, G. J.; Fehrentz, A.; Martinez, J. *Eur. J. Med. Chem.* **1997**, *32*, 767.
- (312) Mierke, D. F.; Nobner, G.; Schiller, P. W.; Goodman, M. *Int. J. Pept. Protein Res.* **1990**, *35*, 35.
- (313) Yamazaki, T.; Probst, A.; Schiller, P. W.; Goodman, M. *Int. J. Pept. Protein Res.* **1991**, *37*, 364.
- (314) Cardillo, G.; Gentilucci, L.; Melchiorre, P.; Spampinato, S. *Bioorg. Med. Chem. Letters* **2000**, *10*, 2755.
- (315) Cardillo, G.; Gentilucci, L.; Qasem, A. R.; Sgarzi, F.; Spampinato, S. *J. Med. Chem.* **2002**, *45*, 2571.
- (316) Keresztes, A.; Szűcs, M.; Borics, A.; Kövér, K. E.; Forró, E.; Fülpöp, F.; Tömböly, C.; Péter, A.; Páhi, A.; Fábián, G.; Murányi, M.; Tóth, G. *J. Med. Chem.* **2008**, *51*, 4270.
- (317) Poenaru, S.; Lamas, J. R.; Folkers, G.; López de Castro, J. A.; Seebach, D.; Rognan, D. *J. Med. Chem.* **1999**, *42*, 2318.
- (318) Webb, A. I.; Dunstone, M. A.; Williamson, N. A.; Price, J. D.; Kauwe, A.; Chen, W.; Oakley, A.; Perlmuter, P.; McCluskey, J.; Aguilar, M. I.; Rossjohn, J.; Purcell, A. W. *J. Immunology* **2005**, *175*, 3810.
- (319) Clark, T. D.; Buehler, L. K.; Ghadiri, M. R. *J. Am. Chem. Soc.* **1998**, *120*, 651.
- (320) Umezawa, N.; Gelman, M. A.; Haigis, M. C.; Raines, R. T.; Gellman, S. H. *J. Am. Chem. Soc.* **2002**, *124*, 368.
- (321) David, R.; Gunther, R.; Baumann, L.; Luhmann, T.; Seebach, D.; Hofmann, H. J.; Beck-Sickinger, A. G. *J. Am. Chem. Soc.* **2008**, *130*, 15311.
- (322) Kritzer, J. S.; Lear, J. D.; Hosdon, M. E.; Schepartz, A. *J. Am. Chem. Soc.* **2004**, *126*, 9468.
- (323) Harker, E. A.; Daniels, D. S.; Guaraccino, D. A.; Schepartz, A. *Bioorg. Med. Chem.* **2009**, *17*, 2038.
- (324) Bautista, A. D.; Appelbaum, J. S.; Craig, C. J.; Michel, J.; Schepartz, A. *J. Am. Chem. Soc.* **2010**, *132*, 2904.
- (325) Lee, E. F.; Sadowsky, J. D.; Smith, B. J.; Czabotar, P. E.; Peterson-Kaufman, K. J.; Colman, P. M.; Gellman, S. H.; Fairlie, W. D. *Angew. Chem., Int. Ed.* **2009**, *48*, 4318.
- (326) Muller, M. M.; Windsor, M. A.; Pomerantz, W. C.; Gellman, S. H.; Hilvert, D. *Angew. Chem., Int. Ed.* **2009**, *48*, 922.
- (327) Akkarawongs, R.; Potocky, T. B.; English, E. P.; Gellman, S. H.; Brandt, C. R. *Antimicrob. Agents Chemother.* **2008**, *52*, 2120.
- (328) Stephens, O. M.; Kim, S.; Welch, B. D.; Hodson, M. E.; Kay, M. S.; Schepartz, A. *J. Am. Chem. Soc.* **2005**, *127*, 13126.
- (329) Horne, W. S.; Johnson, L. M.; Ketas, T. J.; Klasse, P. J.; Lu, M.; Moore, J. P.; Gellman, S. H. *Proc. Natl. Acad. Sci. U. S. A.* **2009**, *106*, 14751.
- (330) Gademann, K.; Seebach, D. *Helv. Chim. Acta* **2001**, *84*, 2924.
- (331) Gelman, M. A.; Richter, S.; Cao, H.; Umezawa, N.; Gellman, S. H.; Rana, T. M. *Org. Lett.* **2003**, *5*, 3563.
- (332) Namoto, K.; Gardiner, J.; Kimmerlin, T.; Seebach, D. *Helv. Chim. Acta* **2006**, *89*, 3087.